DOCTOR OF PHILOSOPHY

The biology of reproduction in two British pulmonate slugs.

Nicholas, J.

Award date:
1984

Awarding institution:
Bangor University

THE BIOLOGY OF REPRODUCTION IN TWO BRITISH PULMONATE SLUGS

by

Jane Nicholas

A thesis submitted in partial fulfilment of the requirements for the degree of Philosophiae Doctor in the University of Wales.

In three volumes

VOLUME III

School of Animal Biology,
University College of North Wales,
Bangor, Gwynedd,
United Kingdom.

October 1984.

KEY

a	acinus	agd	albumen gland ducts
ah	anterior, slender region of hermaphrodite duct	al	ascending limb of carrefour loop
alb	albumen gland	am	apical membrane
ap	apices	at	atrium
ax	axon		
b	bursa copulatrix	BM	basement membrane
br	brain	bs	blood sinus
bv	blood vessel	bw	body wall
C	carrefour	Ca	calcium cell
cc	cell cluster	CD	common duct
cg	carrefour gland	cil	cilated cells
cl	clear vesicles	Cm	circular muscle
co	core vesicles	coll	collagen
CT	connective tissue	cy	cytoplasm
d	desmosome	div	carrefour diverticulum

dl	descending limb of carrefour loop	du	ductule
ec	cone of epiphallus	ed	electron-dense granules
Ep	epithelium	epi	epiphallus
F	fibroblast	f	lateral foot
Fd	finger-like diverticulum	fo	focus of multiplication
foll	follicle		
g	granular connective tissue cells	gl	gland
Gly	glycogen	gr	granules
hd	hemidesmosome		
iv	intercellular vacuole	IV	intracellular vacuole
j	jelly layer		
L	duct lumen	LA	lower atrium
LM	longitudinal muscle	Ly	lysosome
M	mitochondria	mc	muscle
mf	microfibrils	mt	microtubules
mu	mucocytes	mv	microvilli

MVB	multivesicular body		
N	nucleus	Ne	neuron
nt	neurotransmitter granules	nu	nucleolus
Nv	nerve		
O	oviducal gland of common duct	oo	oocyte
Ov	oviduct		
P	polysome	pap	papilla
pb	polar body	Pd	pouched diverticulum
ph	posterior, slender region of hermaphrodite	pig	pigment
PM	penial mass	po	pore cell
pr	prostate gland	Ps	penial sac
Psp	phagocytosed sperm	pvf	perivitelline fluid
r	ciliary rootlet	rER	rough endoplasmic reticulum
S	sarcobellum	sc	secretory cells
sd	septate desmosomes	sER	smooth endoplasmic reticulum
Sg	sarcobellum gland cells	Sh	shell
sn	secretion	Sp	sperm

Sph	spermatophore	SR	sarcoplasmic reticulum
SV	seminal vesicle	Syn	synapse
t	tubule	ta	trifid appendage
tER	transitional endoplasmic reticulum		
UA	upper atrium	uncil	unciliated cells
V	vacuoles	Vd	vas deferens
za	zonula adhaerens		
♀	female duct	♂	male duct
I	type I secretory cell	II	type II secretory cell

Fig. 209 D.reticulatum, the surface of the sarcobellum.

a. General view of ciliated ridges, S.E.M. (x130).
b. Detail of (a), S.E.M. (x460).
c. Detail of (b) showing the opening of a gland cell, S.E.M. (x6.5K).
d. L.S. through ridges (x375).

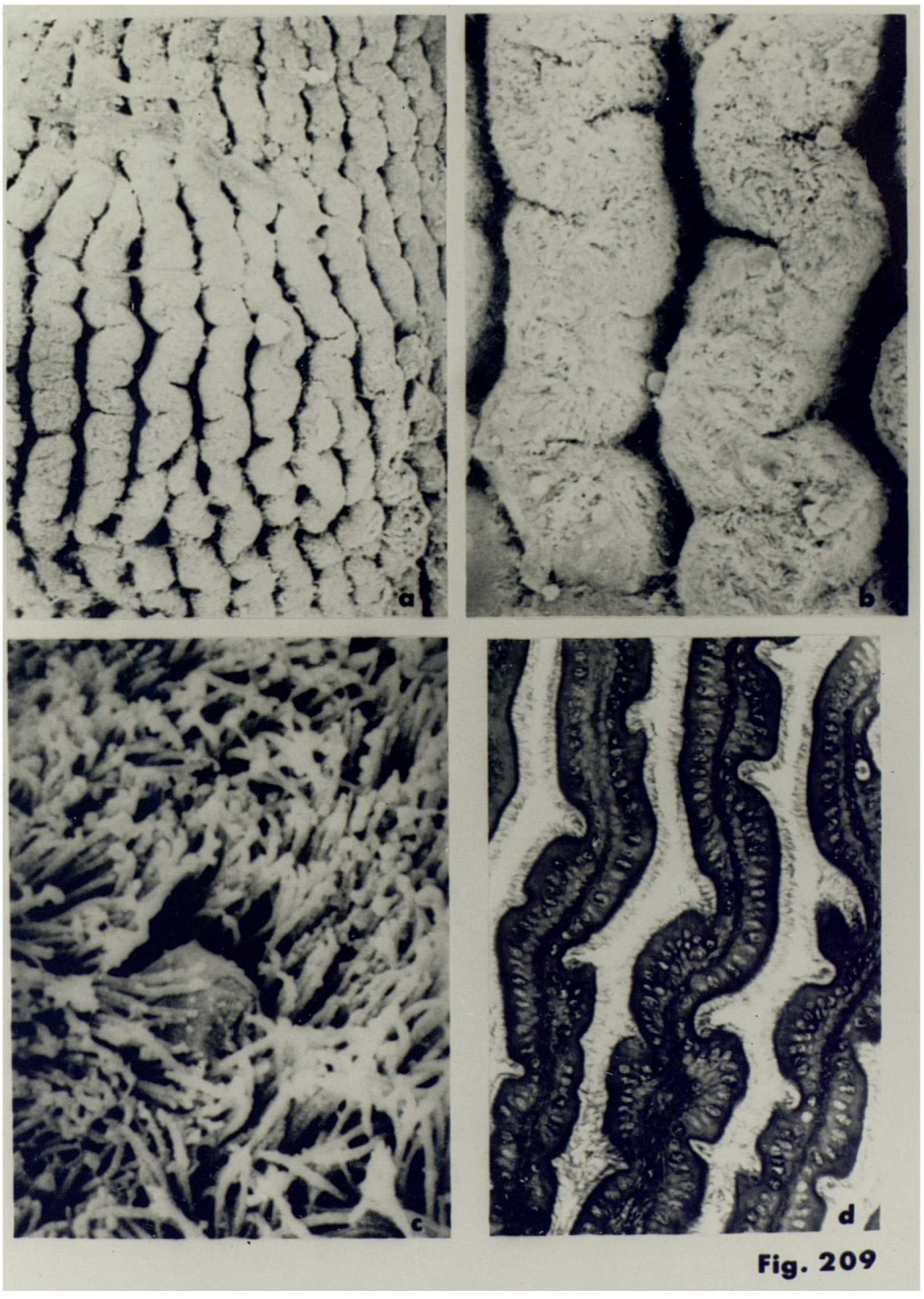

Fig. 209

D.reticulatum, sarcobellum.

Fig. 210 T.S. through the tip of the sarcobellum (x110).

Fig. 211 Detail of the ciliated ridges (x450).

Fig. 212 General view of epithelial cells (x3K).

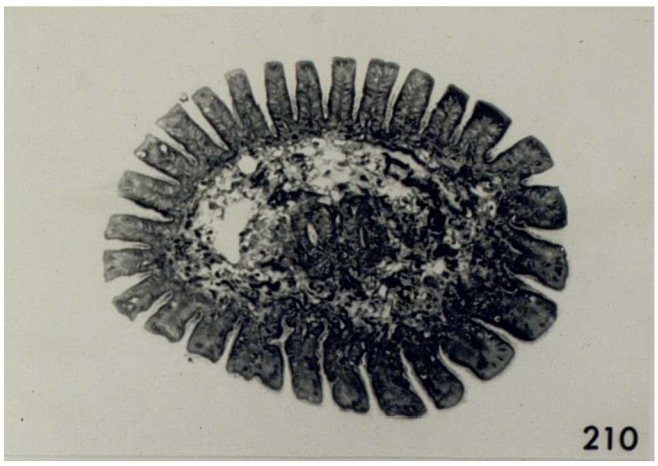

210

211

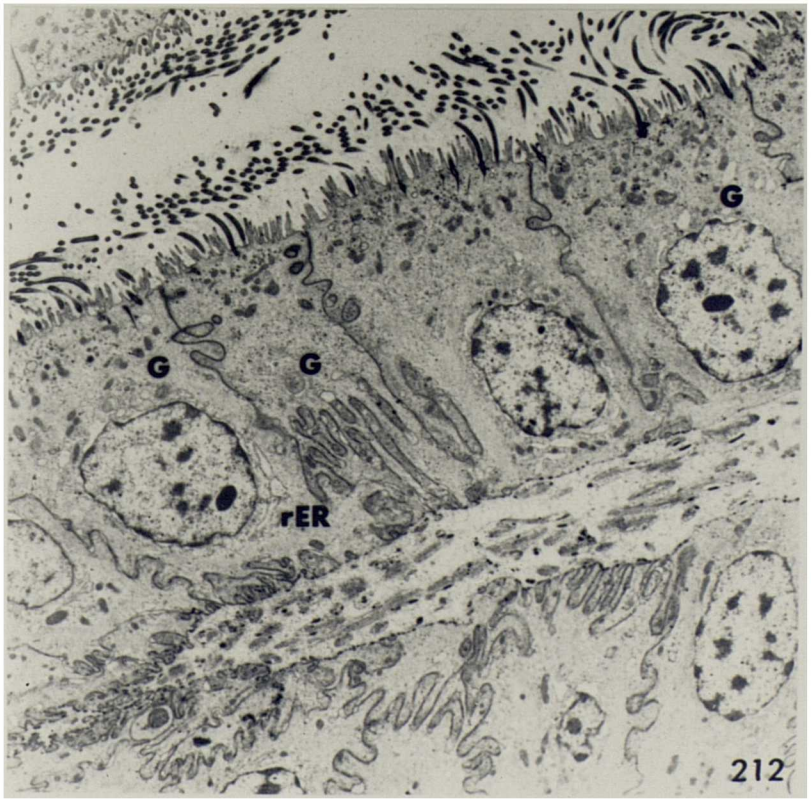

212

D.reticulatum, sarcobellum.

Fig. 213 Detail of a cell apex (x10.5K). Arrows indicate chains of vesicles.

Fig. 214 Unciliated epithelial cells (arrowed) at the bottom of the ridges (x1.5K).

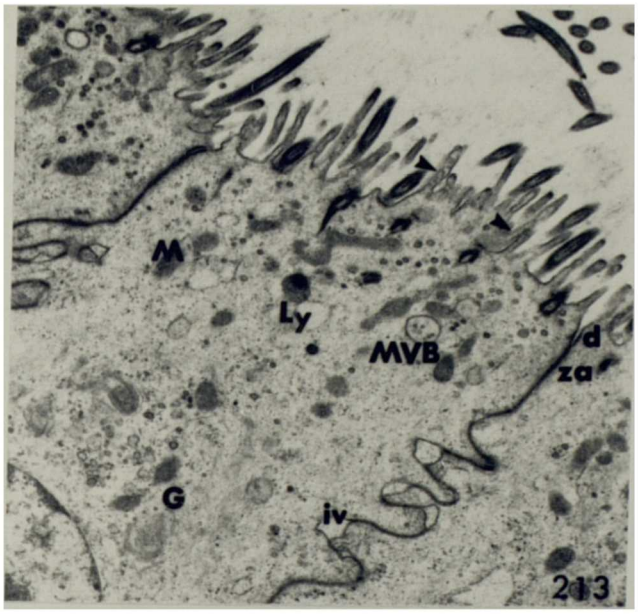
M
Ly
MVB
d
za
G
iv
213

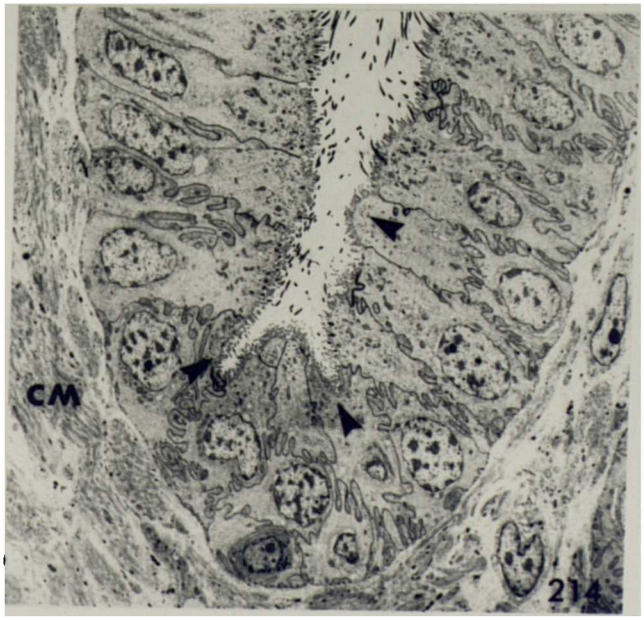
CM
214

D.reticulatum, sarcobellum.

Fig. 215 T.S. through the base of the sarcobellum (x100).

Fig. 216 General view of epithelial cells (x2.25K).

Fig. 217 Horizontal section through the epithelium in the region of the nuclei (x9K).

215

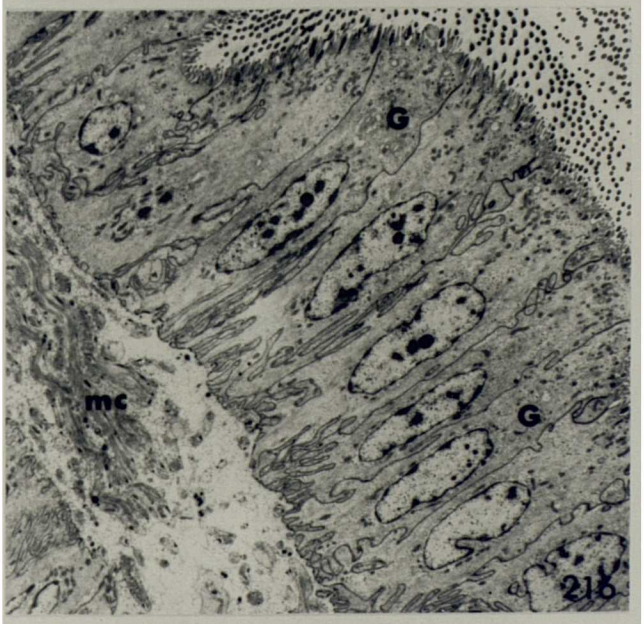

216

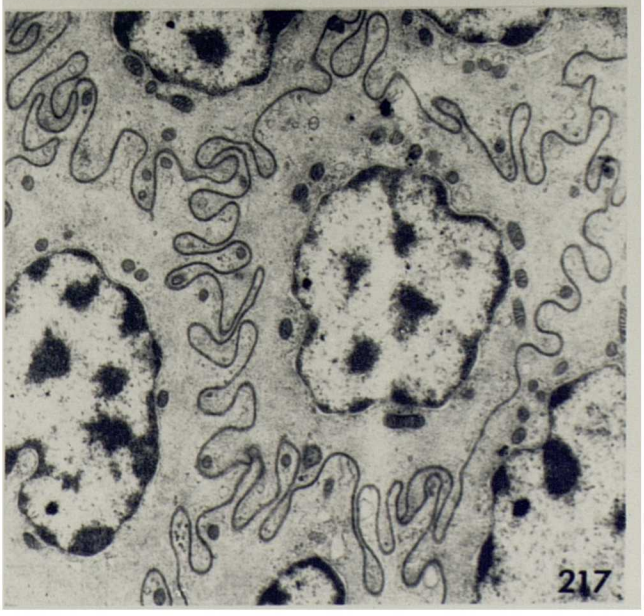

217

D.reticulatum, sarcobellum.

Fig. 218 Arrangement of the muscle within the ridges (x6K).

Fig. 219 Arrangement of the muscle in the core, at the tip of the sarcobellum (x1.5K).

Fig. 220 Arrangement of the muscle, gland and pore cells in the core, at the base of the sarcobellum (x2.25K). Arrows indicate the developing gland cells.

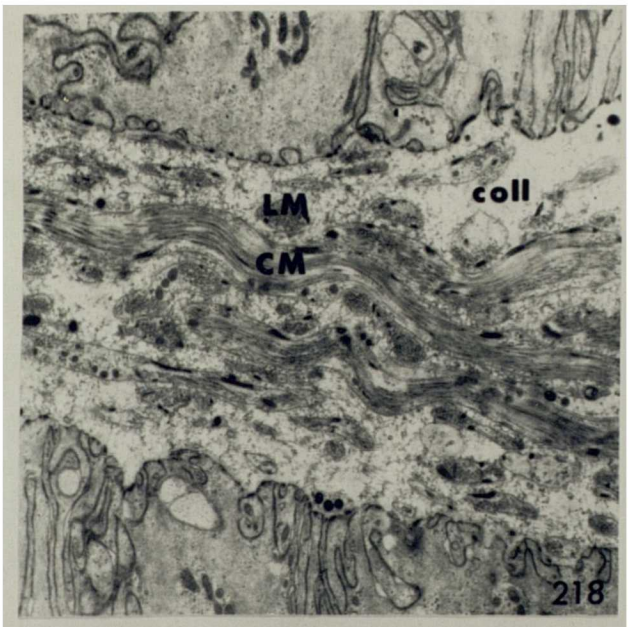
LM
CM
coll
218

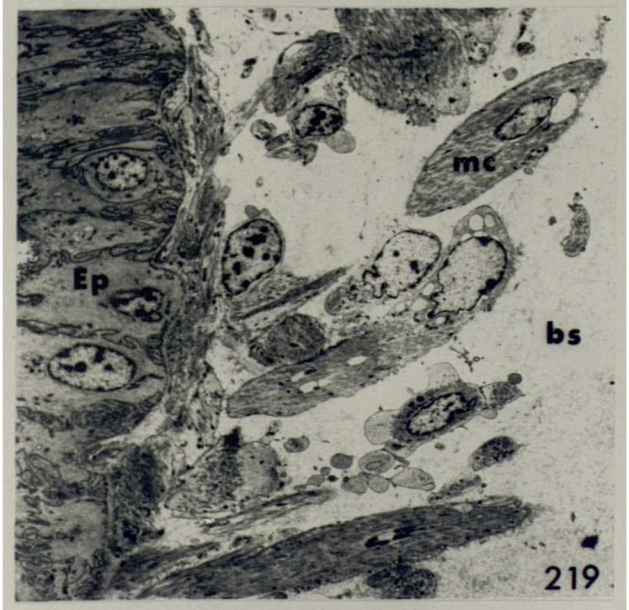
mc
Ep
bs
219

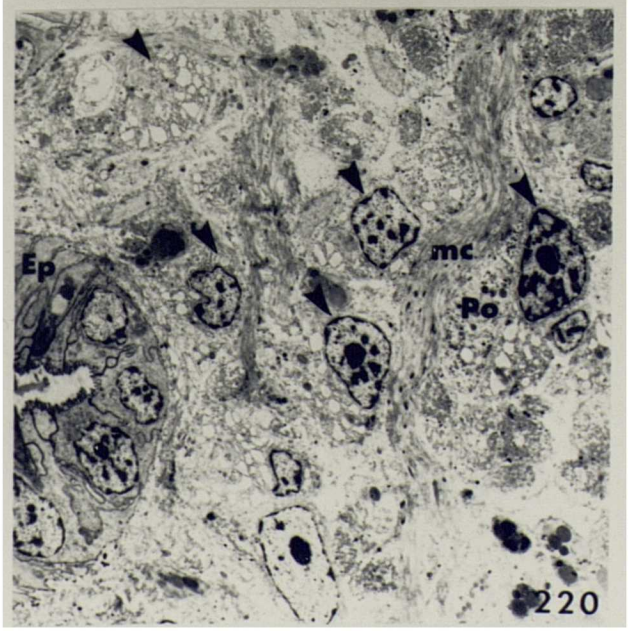
Ep
mc
Po
220

D.reticulatum, gland cells in the core of the sarcobellum.

Fig. 221 Developing gland cells, types I and II (x2.25K). Early C-stage.

Fig. 222 Type I gland cell (x4K).

Fig. 223 Type I, detail of the rER and secretion granules (x37.5K).

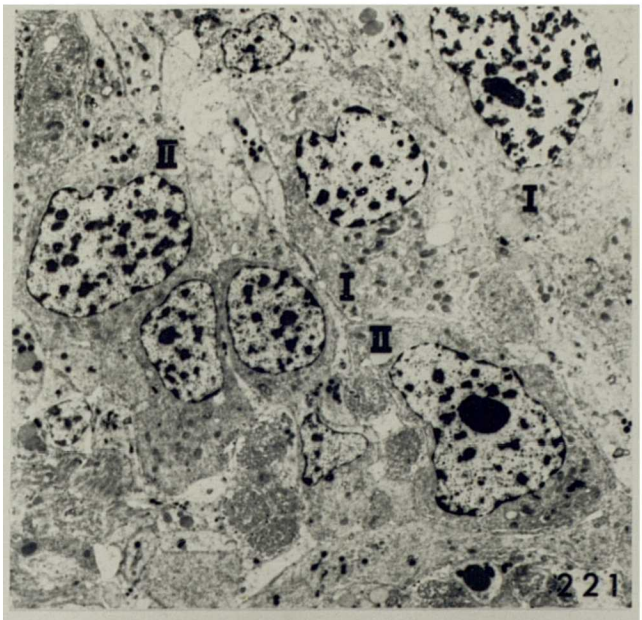

221

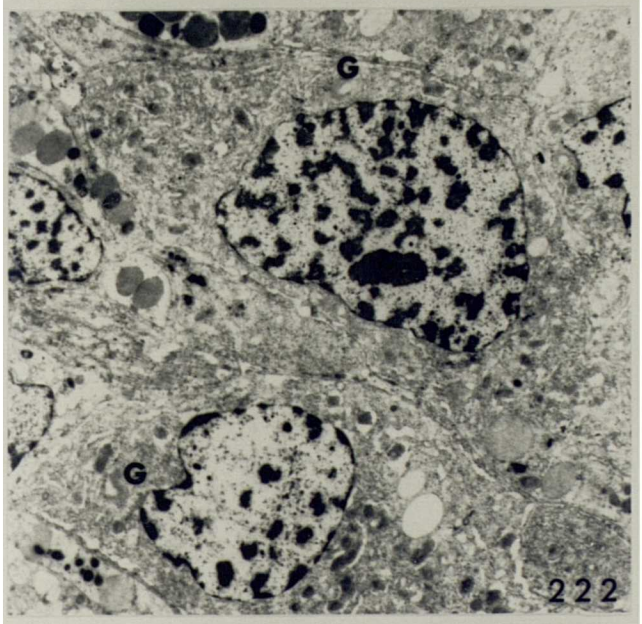

222

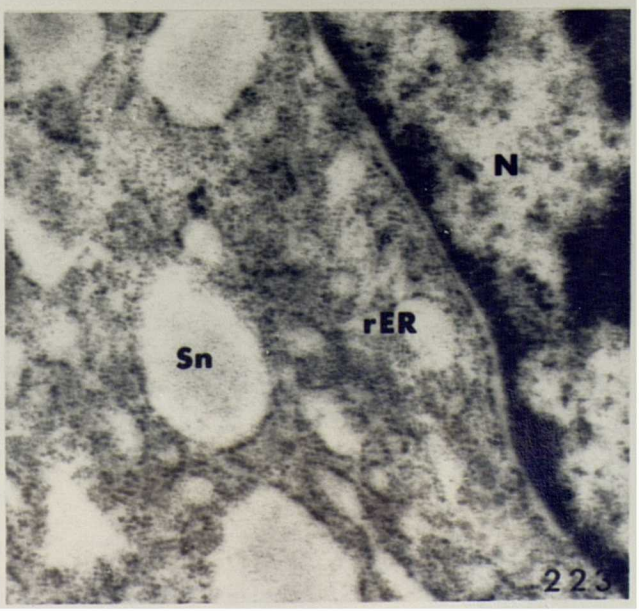

223

D.reticulatum, type I gland cells in the core of the sarcobellum.

Fig. 224 Accumulation of secretion granules in the tapering apices of the cells (x2.4K).

Fig. 225 Detail of the secretion granules and microtubules in the cell apices (x16K). The arrow indicates a chain of vesicles.

Fig. 226 Release of secretion into the unciliated region at the base of the ridges (x10K).

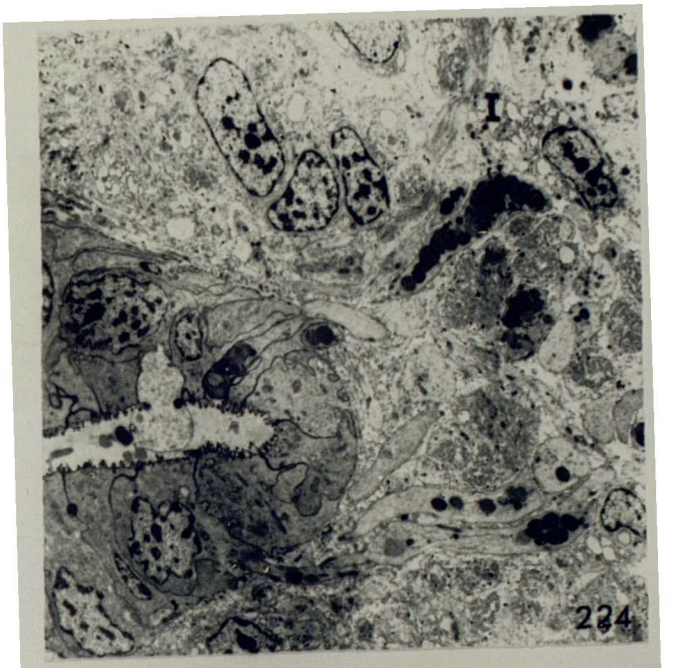
I
224


Sm
M
A
mt
225


226

D.reticulatum, gland cells in the core of the sarcobellum.

Fig. 227 Type I, cytoplasmic detail (x9K).

Fig. 228 Type II, gland cell (x9K).

Fig. 229 Type II, detail of the Golgi region (x22.5K).

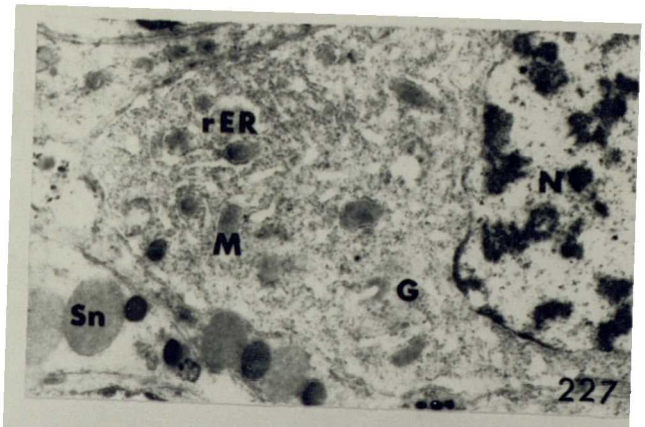

227

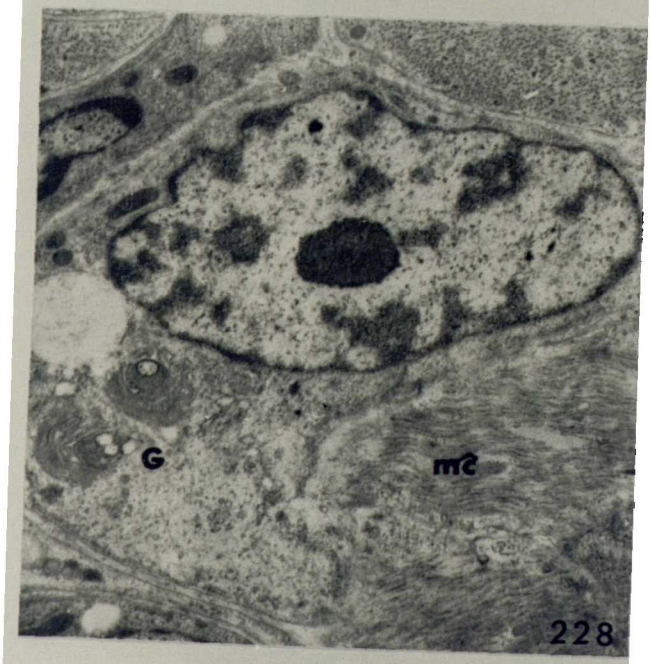

228

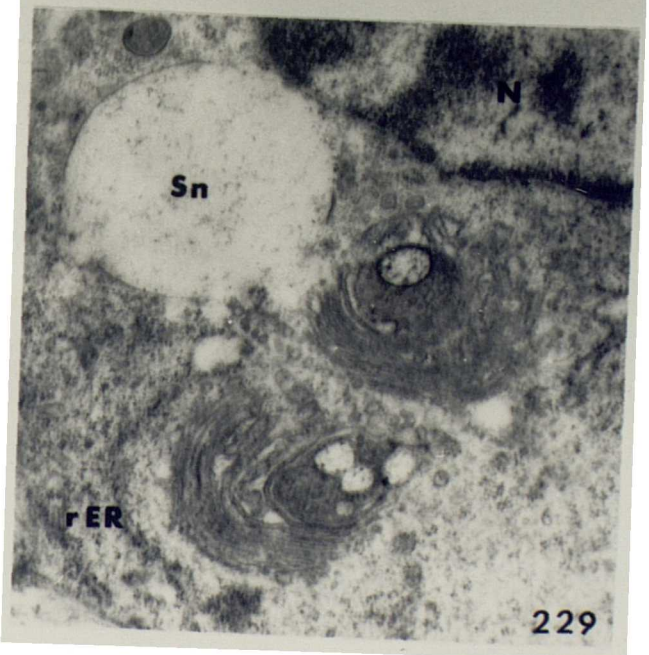

229

D.reticulatum, type II gland cells in the core of the sarcobellum.

Fig. 230 Mature gland cells (x3.8K).

Fig. 231 Release of secretion onto the surface of the sarcobellum (x6K).


Sn
230

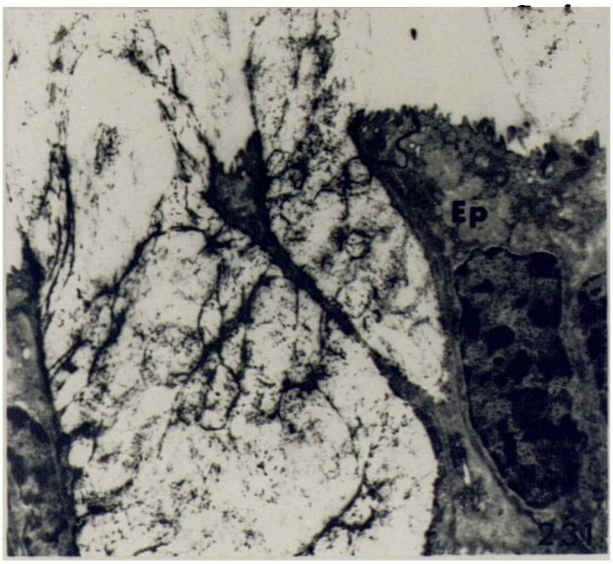
Ep

D.reticulatum, viral infection of the sarcobellum.

Fig. 232 Multiplication of viral particles in the nucleus of an epithelial cell (x3K).

Fig. 233 Breakdown of the nuclear membrane (arrowed) (x9K).

Fig. 234 Viral particles filling the cytoplasm (x9K).

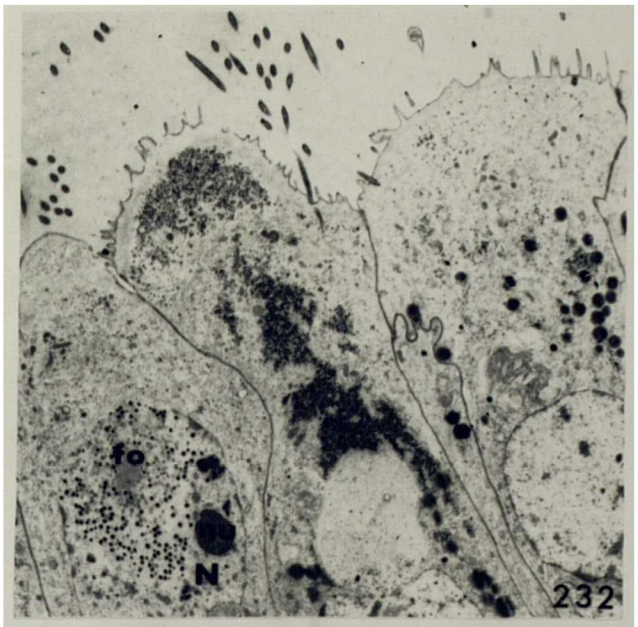
fo
N
232

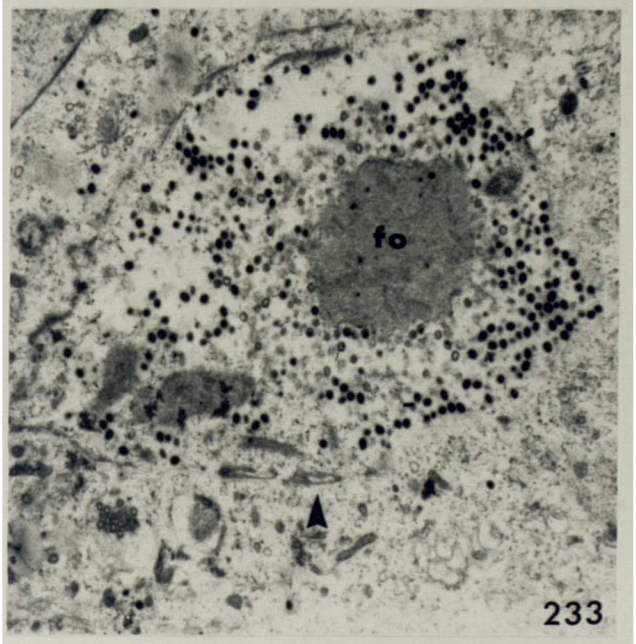
fo
233

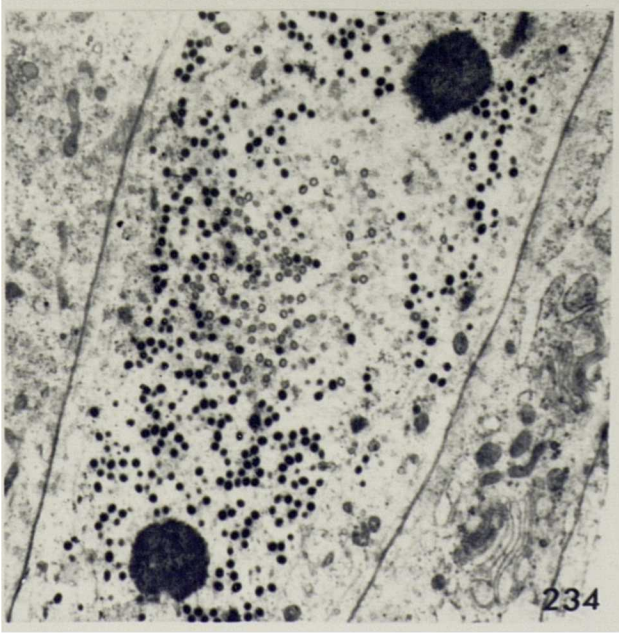
234

D.reticulatum, viral infection of the sarcobellum.

Fig. 235 Viral particles in varying stages of maturation (x35K).

Fig. 236 Mature viral particles (x40K).

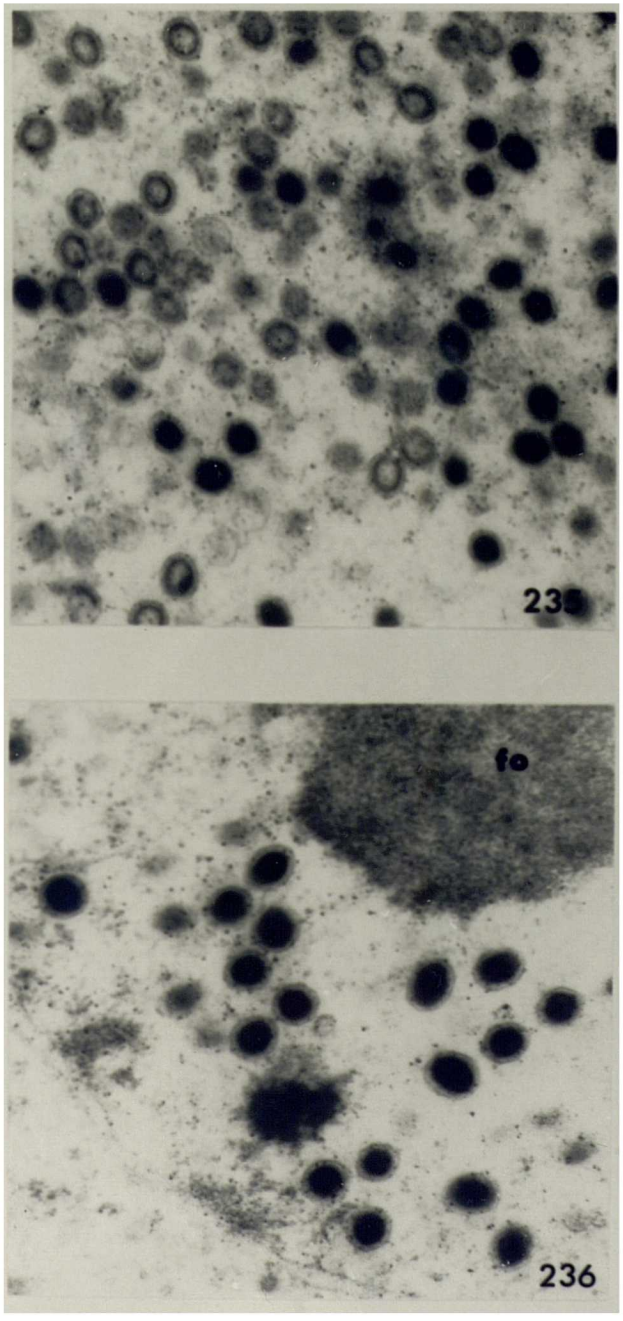
235
fo
236

D.reticulatum, viral infection of the sarcobellum.

Fig. 237 Detail of the homogeneous material which accumulates at the focus of multiplication (x9K).

Fig. 238 Bleb of cytoplasm containing viral particles, released onto the surface of the sarcobellum (x20K).

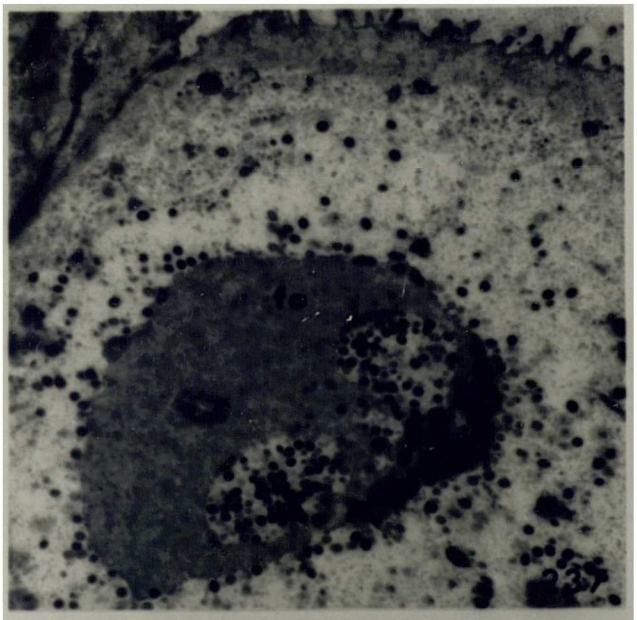
237


cil
m
238

D.reticulatum, penial sac.

Fig. 239 T.S. through the wall of the penial sac (x160).

Fig. 240 General view of epithelium with isolated type II gland cell (x2.4K).

Fig. 241 Arrangement of the muscle, nerve, gland and pore cells in the connective tissue surrounding the penial sac (x2.4K).

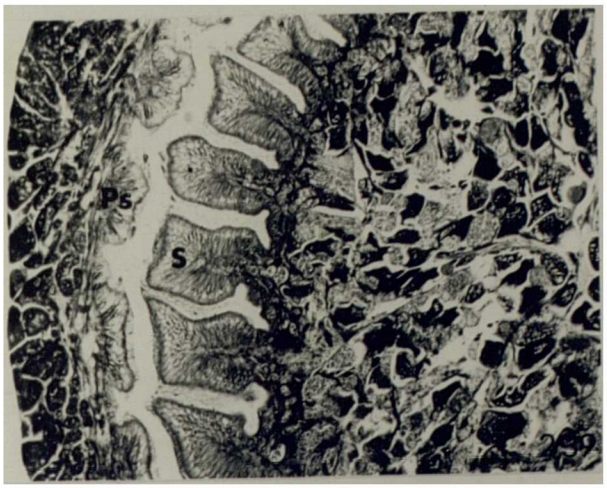
Ps
S


II
240

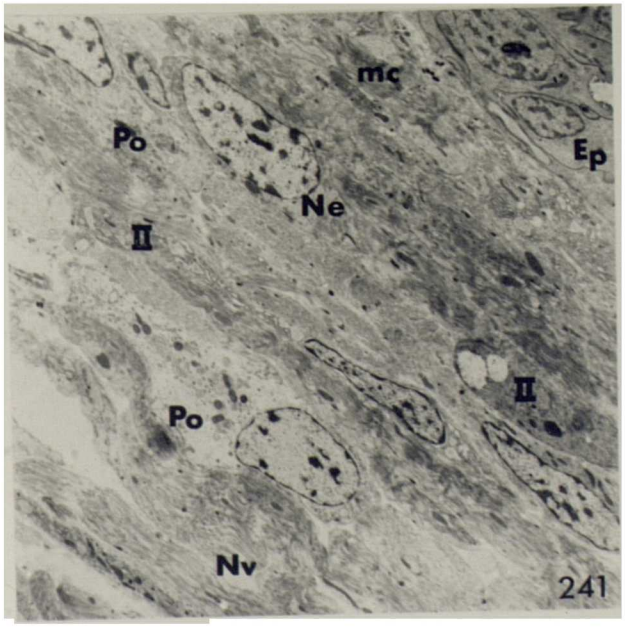
mç
Po
Ep
Ne
II
II
Po
Nv
241

D.reticulatum, trifid appendage.

Fig. 242 L.S. through the penial sac near the trifid appendage (x255).

Fig. 243 L.S. through the base of the trifid appendage (x255).

Fig. 244 L.S. through the trifid appendage (x1.5K). C-stage.

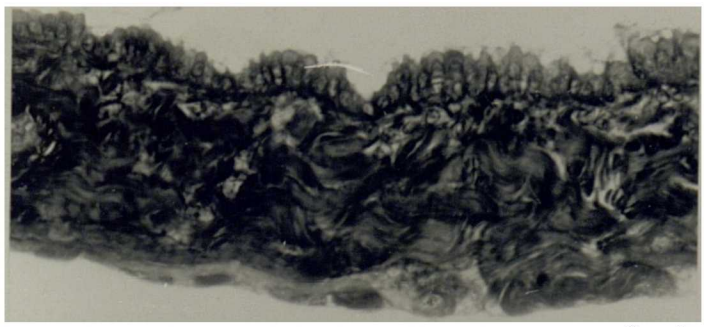

242

243

244

D.reticulatum, trifid appendage, C-stage.

Fig. 245 General view of epithelium (x6K).

Fig. 246 Detail of the Golgi region (x22.5K).

Fig. 247 Detail of the cell apices (x22.5K).

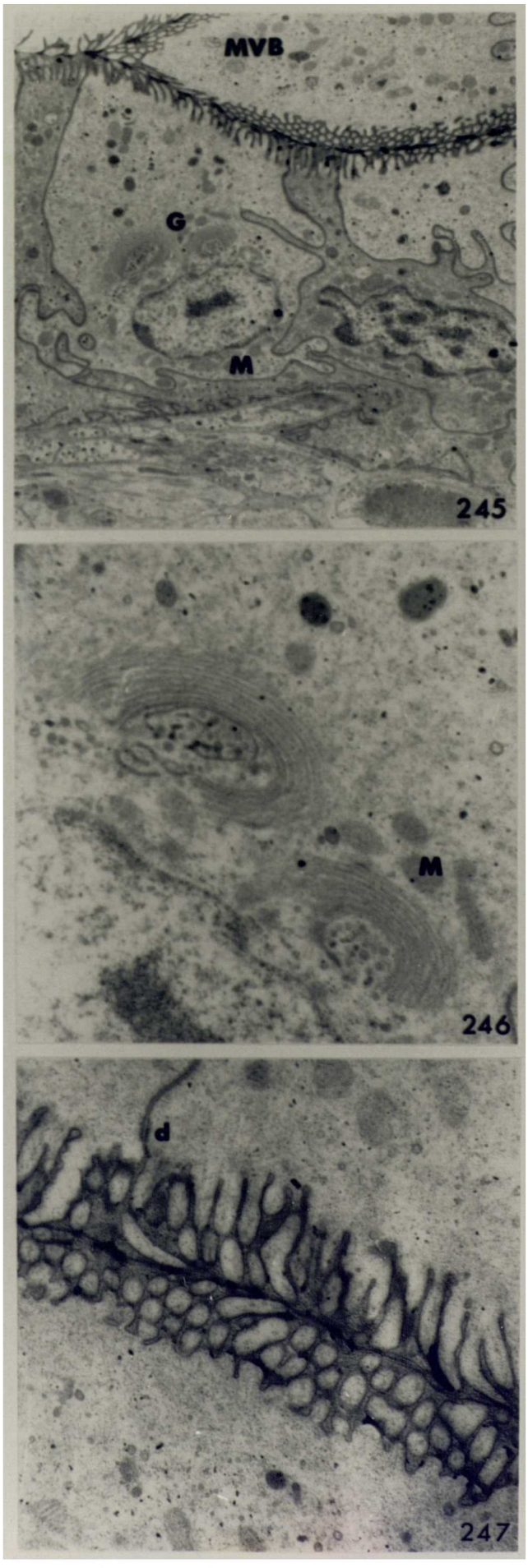
MVB
G
M
245
M
246
d
247

D.reticulatum, trifid appendage, E-stage.

Fig. 248 T.S. through the trifid appendage (x104).

Fig. 249 Detail of the Golgi region (x22.5K).

Fig. 250 General view of epithelium (x3.75K).

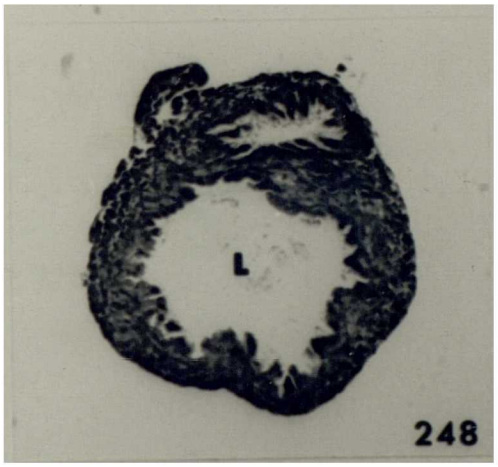
L
248

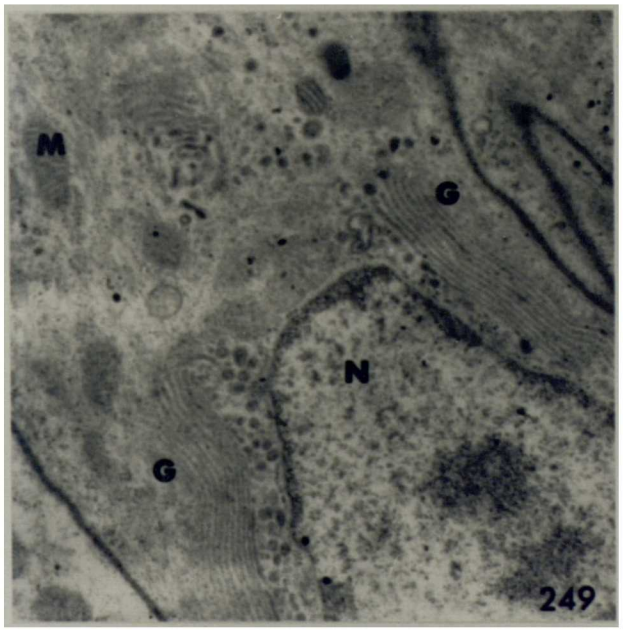
M
G
N
G
249

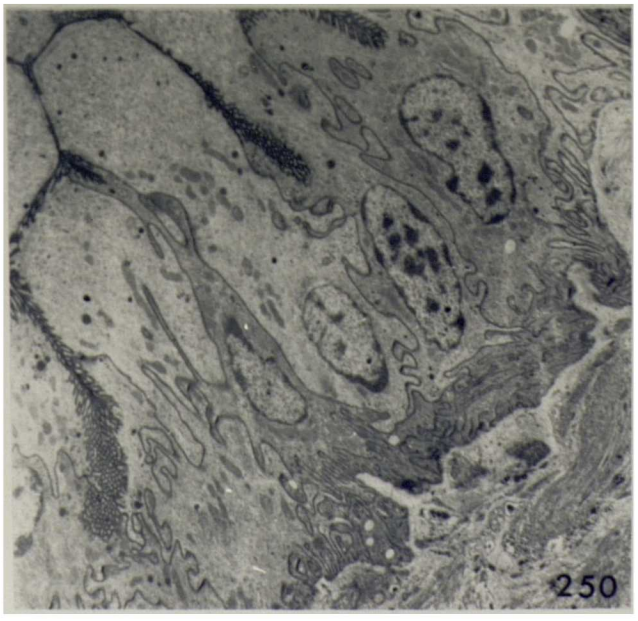
250

D.reticulatum, trifid appendage, E-stage.

Fig. 251 Detail of the cell apices (x6.5K).

Fig. 252 T.S. through a diverticulum with its lumen occluded by the swollen cell apices (x265).

Fig. 253 Arrangement of the muscle, nerve and pore cells in the connective tissue sheath (x1.5K).

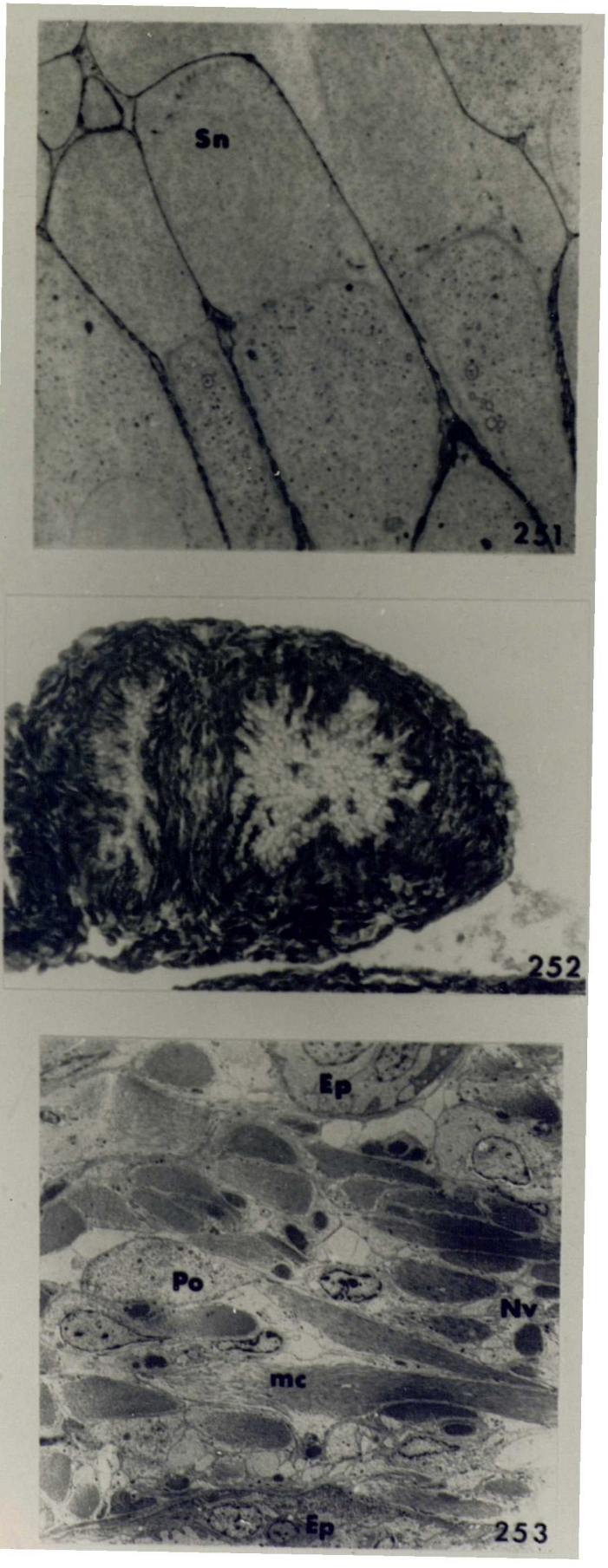
Sn
251
252
Ep
Po
Nv
mc
Ep
253

D.reticulatum, vas deferens.

Fig. 254 T.S.through the vas deferens (x260).

Fig. 255 General view of epithelium (x4.8K).

Fig. 256 General view of the Golgi region (x42K).

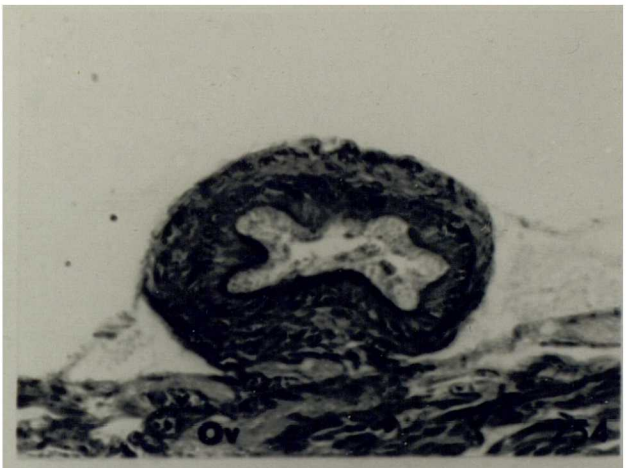
Ov

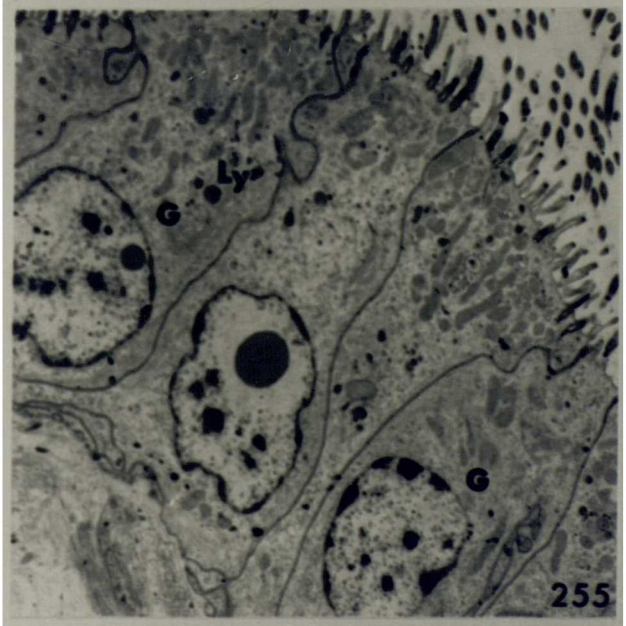
G
Lys
G
255

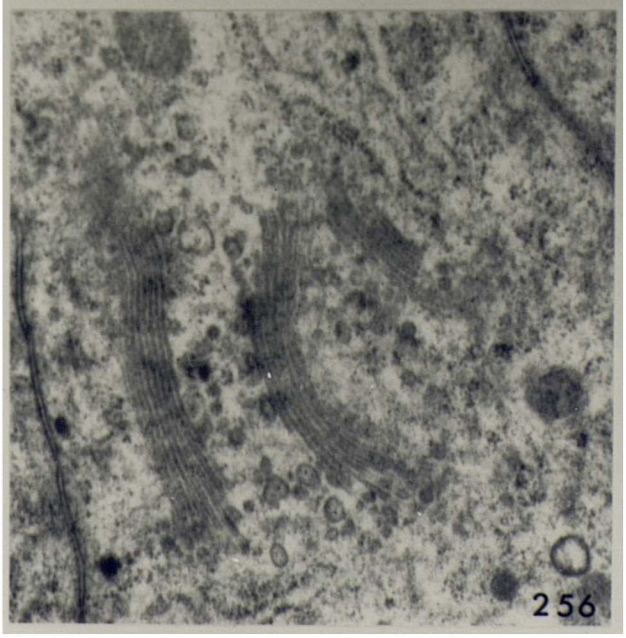
256

D.reticulatum, vas deferens.

Fig. 257 Detail of the cell apices (x22.5K). Arrows indicate vesicle chains.

Fig. 258 Arrangement of the muscle and nervous tissue in the connective tissue sheath (x1.5K).

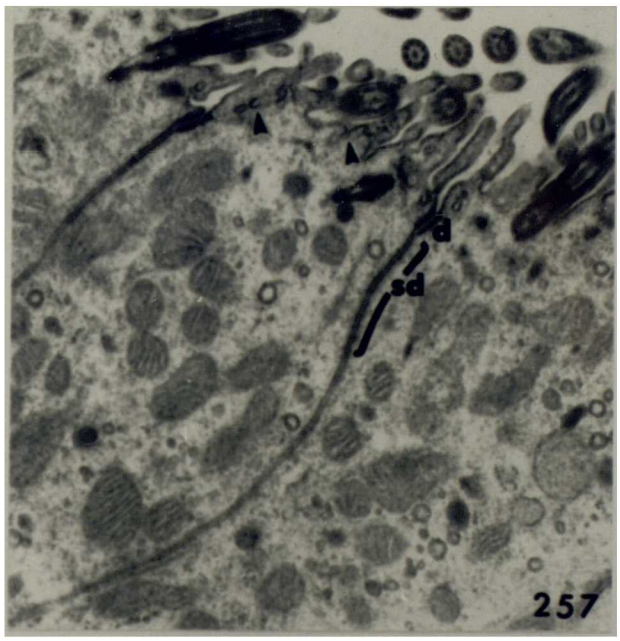
d
sd
257

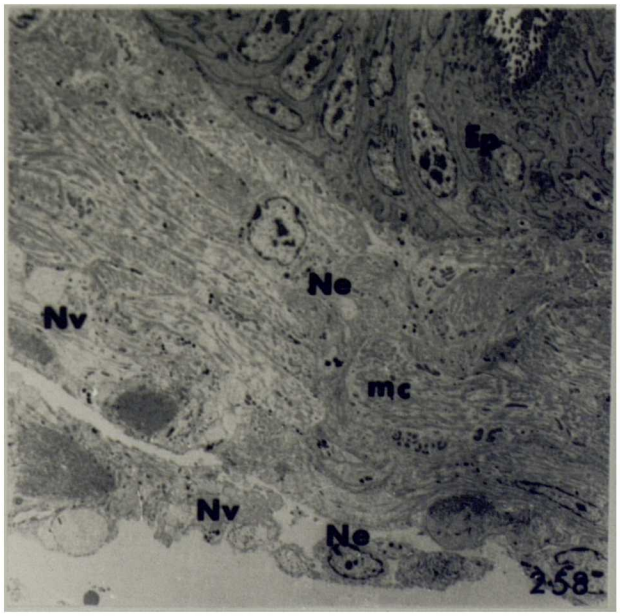
Ep
Ne
Nv
mc
Nv
Ne
258

D.reticulatum, oviduct, epithelial cells.

Fig. 259 General view of epithelium (x2.5K).

Fig. 260 Detail of the epithelial cells (x6K). Arrows indicate small, possibly pinocytotic vesicles.

Fig. 261 Detail of the Golgi region (x20K).

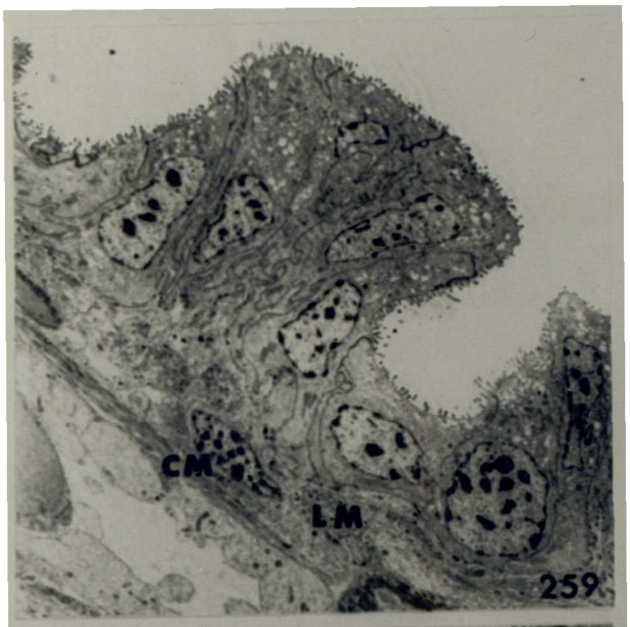
CM
LM
259

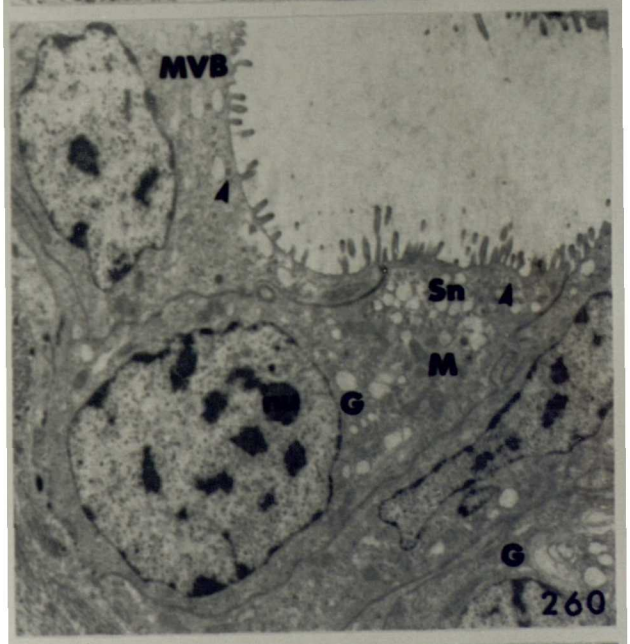
MVB
Sn
M
G
G
260

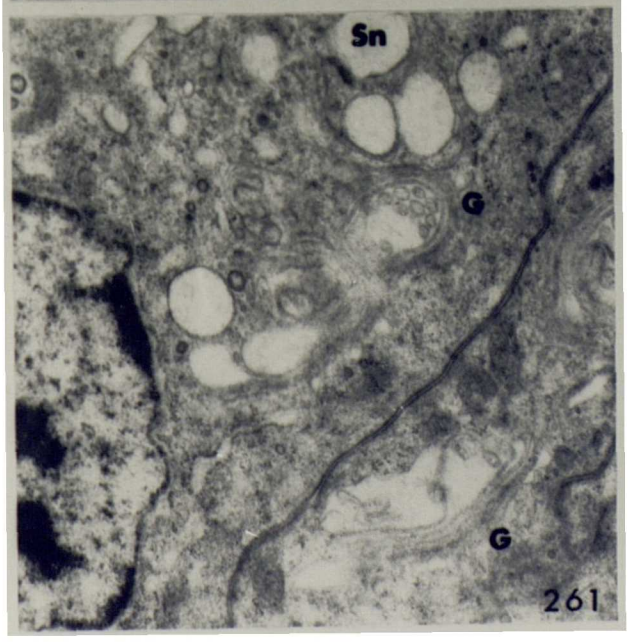
Sn
G
G
261

D.reticulatum, oviduct.

Fig. 262 Base of sub-epithelial oviducal gland cell (x2.5K).

Fig. 263 Oviducal gland cells (x1.5K).

Fig. 264 Gland cells opening into the lumen of the oviduct (x1.6K). The clear space is shrinkage artifact.

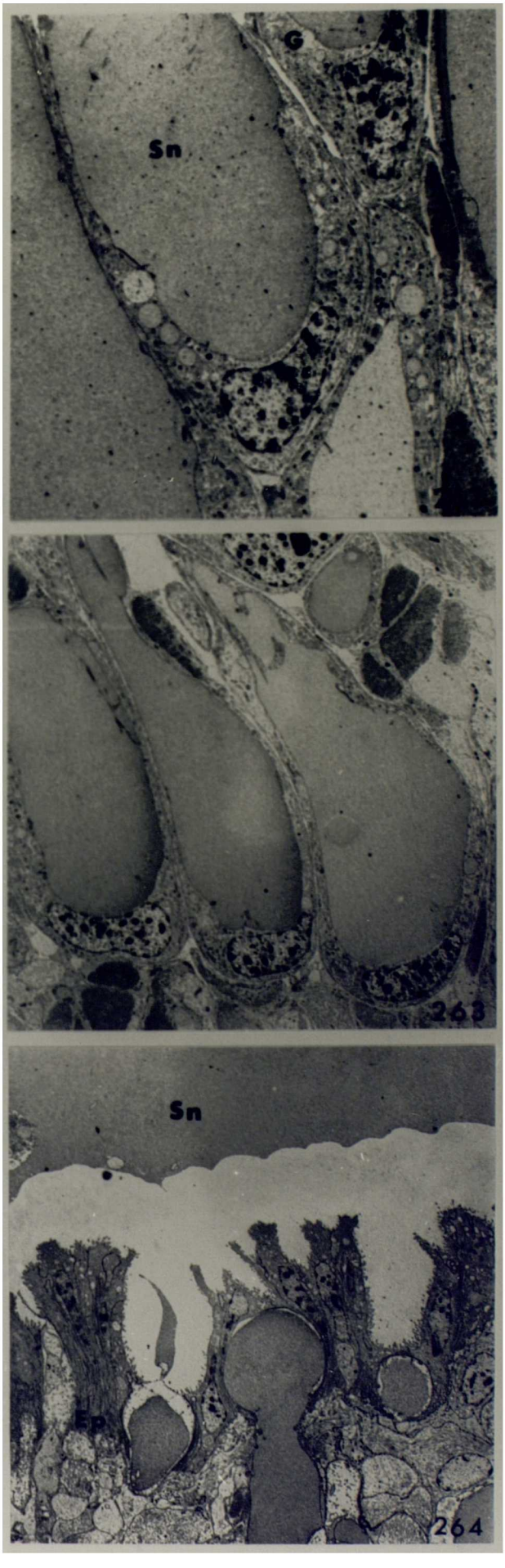
G
Sn
263
Sn
EP
264

D.reticulatum, oviduct.

Fig. 265 Arrangement of the nerve and muscle in the connective tissue surrounding the oviduct (x2.4K).

Fig. 266 Arrangement of the nerve and muscle in the connective tissue near the epithelium (x6.4K). The arrow indicates the position of a possible neuromuscular junction.

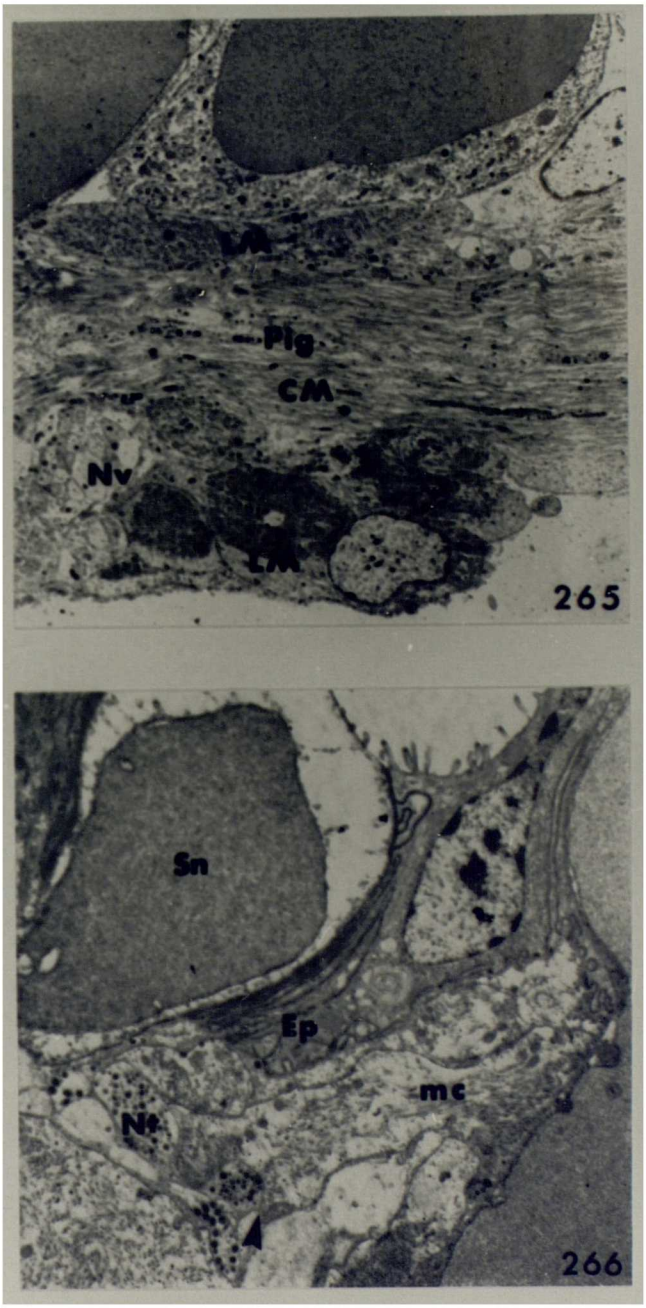
LM
Plg
CM
Nv
LM
265
Sn
Ep
mc
Nf
266

D.reticulatum, proximal region of the bursa copulatrix.

Fig. 267 Transverse section (x125).

Fig. 268 General view of the epithelium (x1.5K).

Fig. 269 Detail of the Golgi region in a typical epithelial cell (x37.5K).

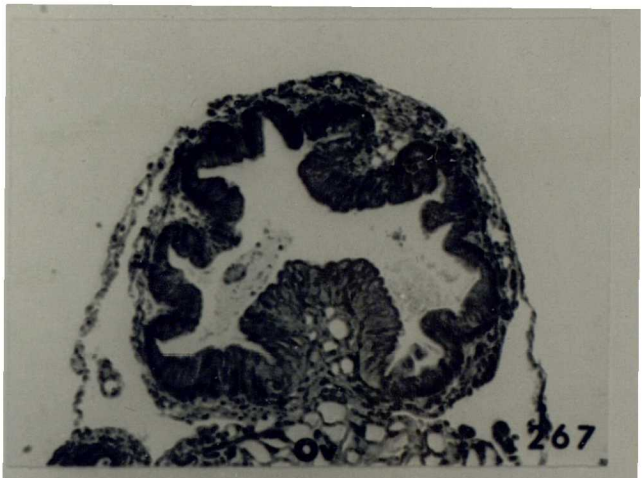
267

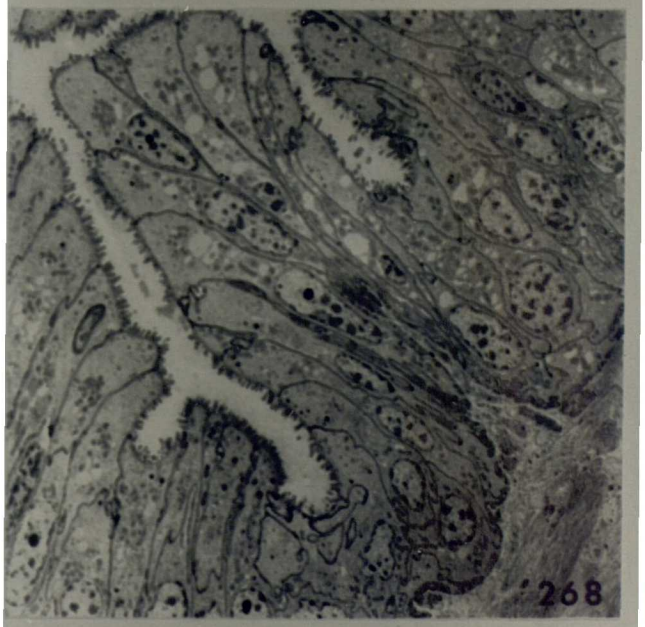
268

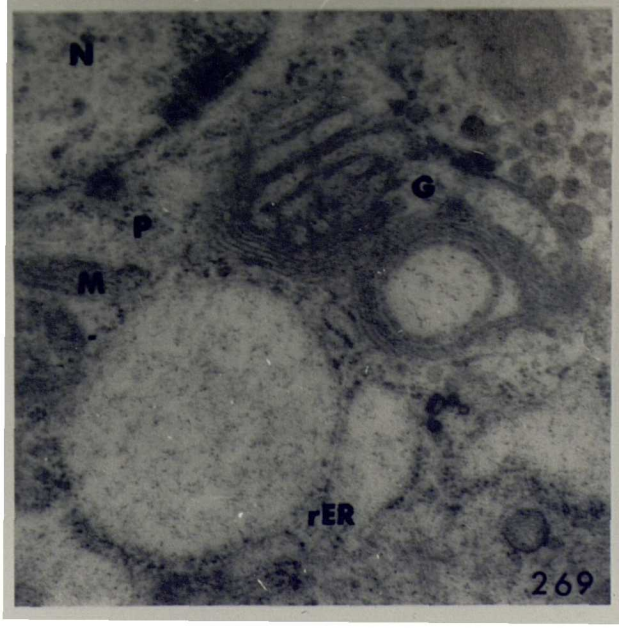
N
G
P
M
rER
269

D.reticulatum, mid-region of the bursa copulatrix.

Fig. 270 Detail of a cell apex swollen with accumulated secretion (x9K).

Fig. 271 Complex configuration of apical microvilli (x13.5K).

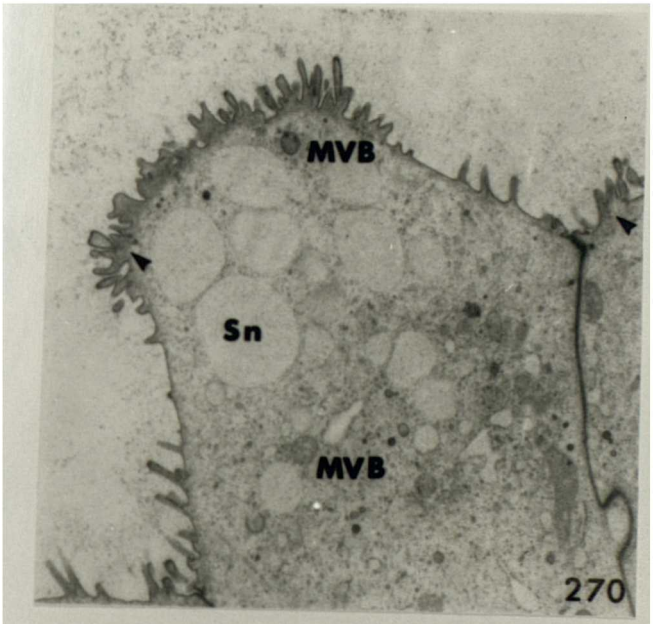
MVB
Sn
MVB
270

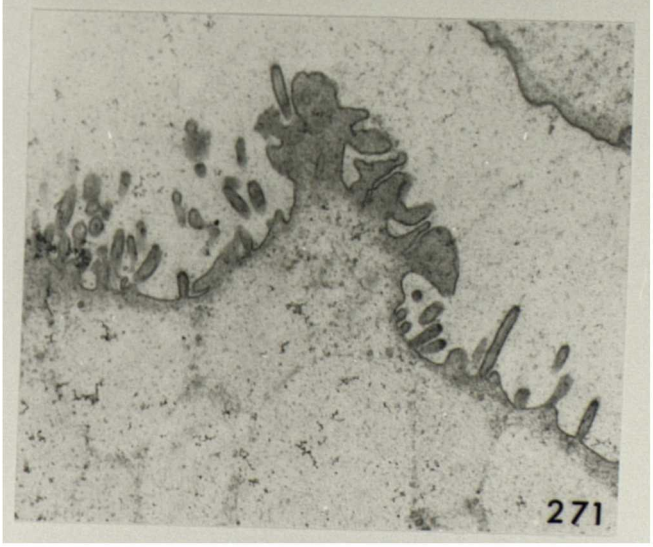
271

D.reticulatum, bursa copulatrix.

Fig. 272 Unciliated epithelium lining the mid-region of the bursa copulatrix (x160).

Fig. 273 Ciliated epithelium lining the distal region of the bursa copulatrix (x400).

Fig. 274 Transition from unciliated to ciliated epithelial cells (x2.2K).

Fig. 275 Arrangement of the muscle, nerve and pore cells in the connective tissue sheath (x 1.8K).

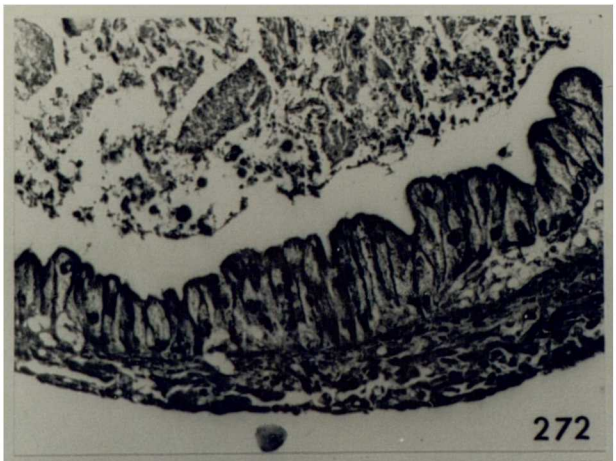

272

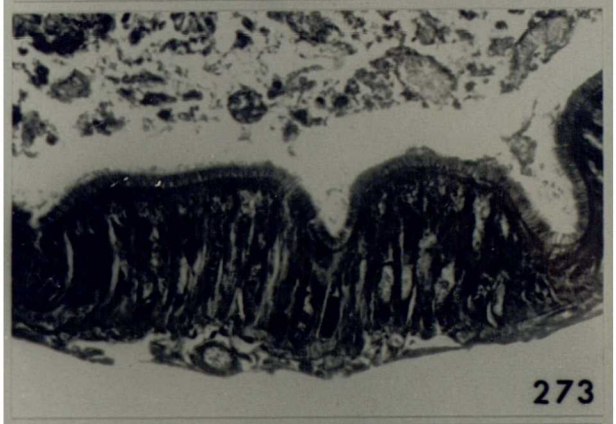

273

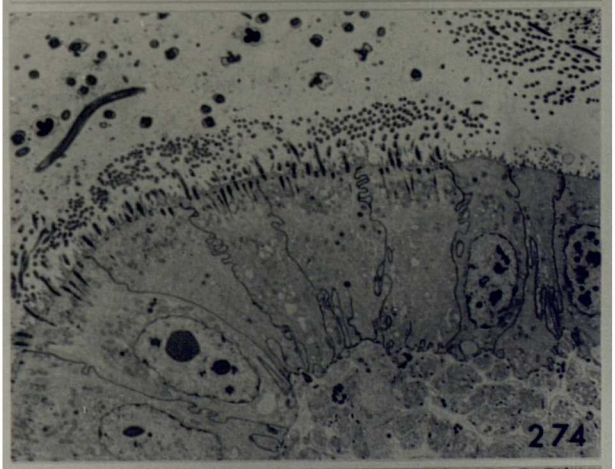

274

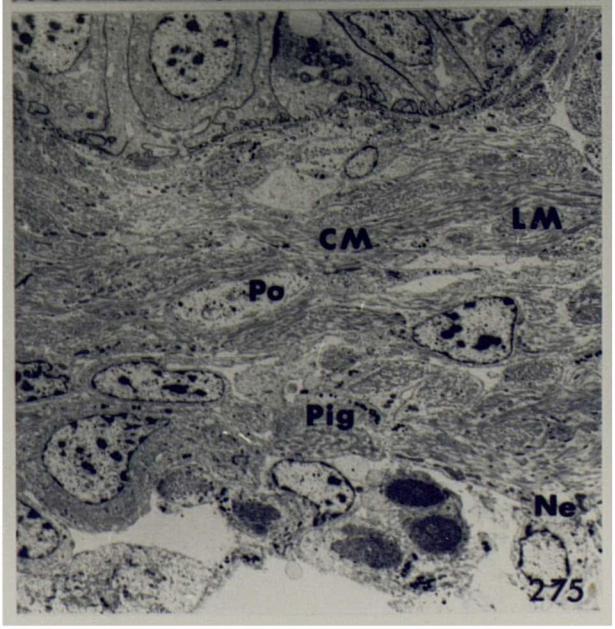

275

A. hortensis, lower atrium.

Fig. 276 Immature secretory cells (x 9K). Arrows indicate the rod or plate-like secretion granules.

Fig. 277 Detail of the smooth, tubular ER in the cytoplasm of a mature secretory cell (x 37.5K).

Fig. 278 Cytoplasmic detail of a mature secretory cell (x 22.5K). Arrow indicates a developing secretion granule.

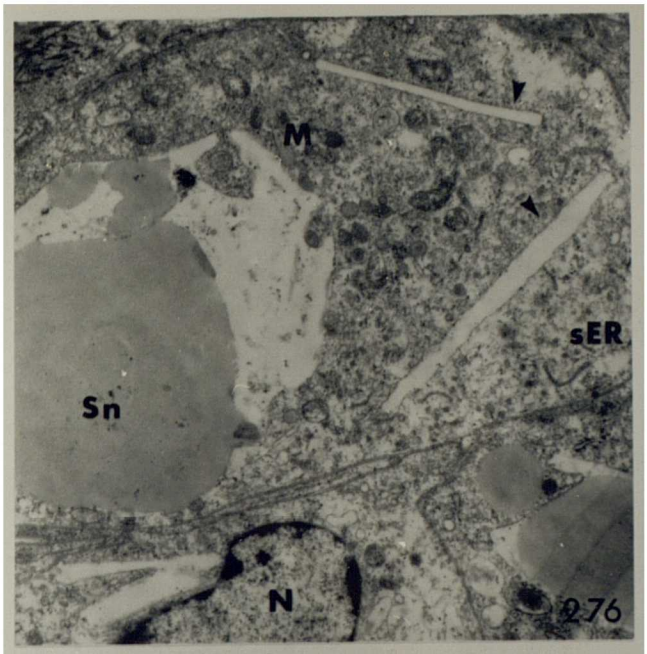
M
sER
Sn
N
276

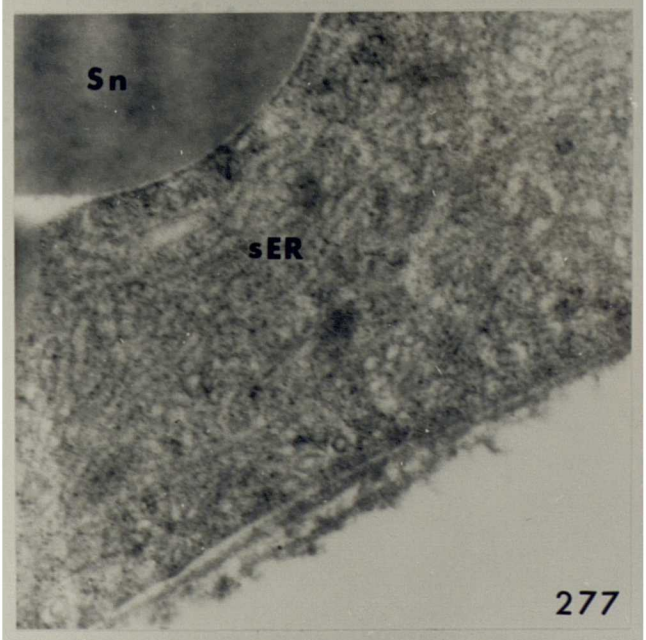
Sn
sER
277

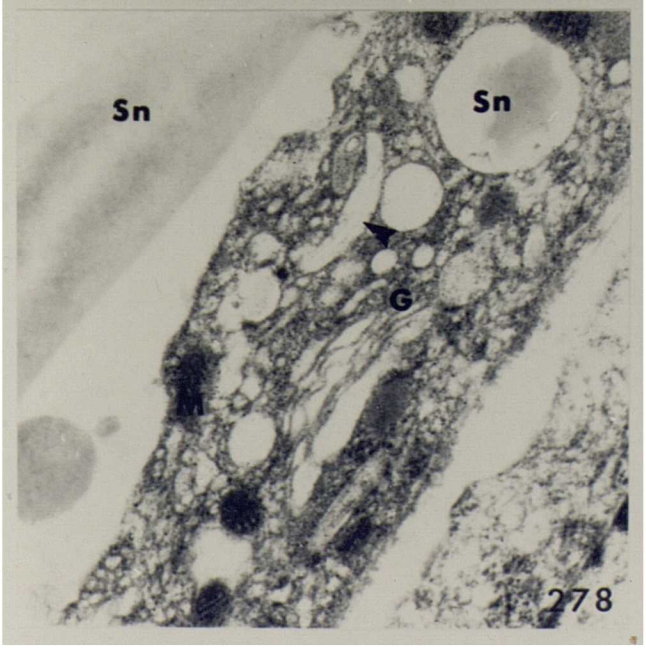
Sn
Sn
G
278

A. hortensis, lower atrium.

Fig. 279 Accumulation of secretion in the centre of the gland cell (x 6K).

Fig. 280 L.S. through the lower atrium (x 160).

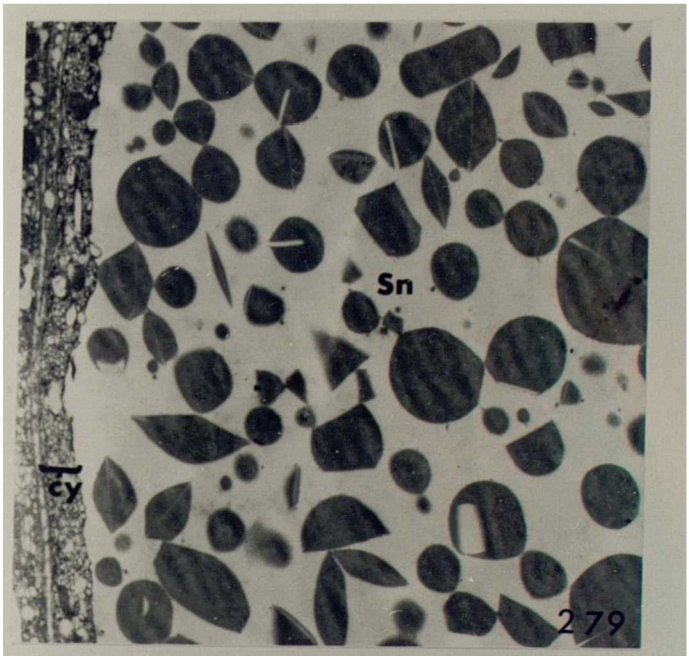

279

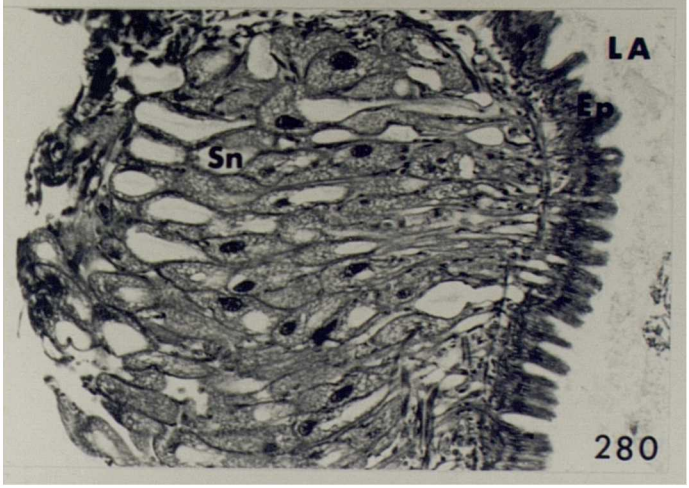

280

A.hortensis, vas deferens.

Fig. 281 Epithelial cells (x 6K). C-stage.

Fig. 282 Detail of a Golgi body and forming secretion granules (X 37.5K). E-stage. Arrows indicate electron-opaque vesicles.

Fig. 283 Epithelial cells (x3.75K). E-stage

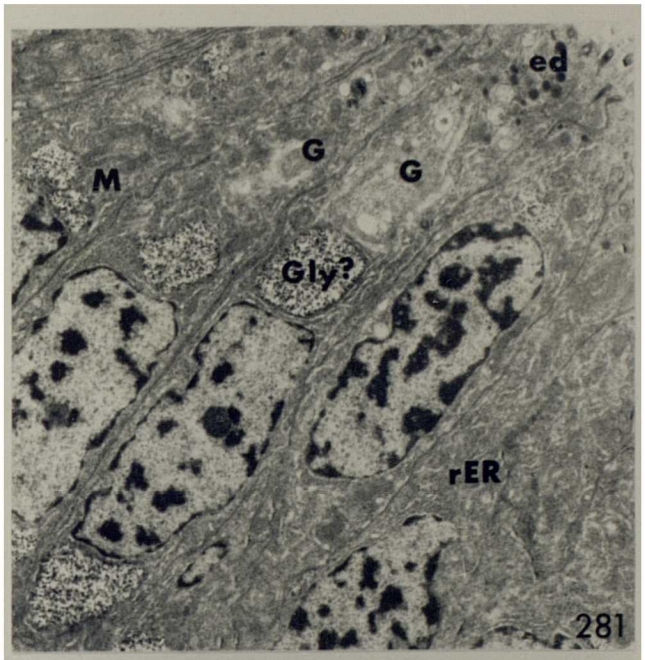
ed
G
G
M
Gly?
rER
281

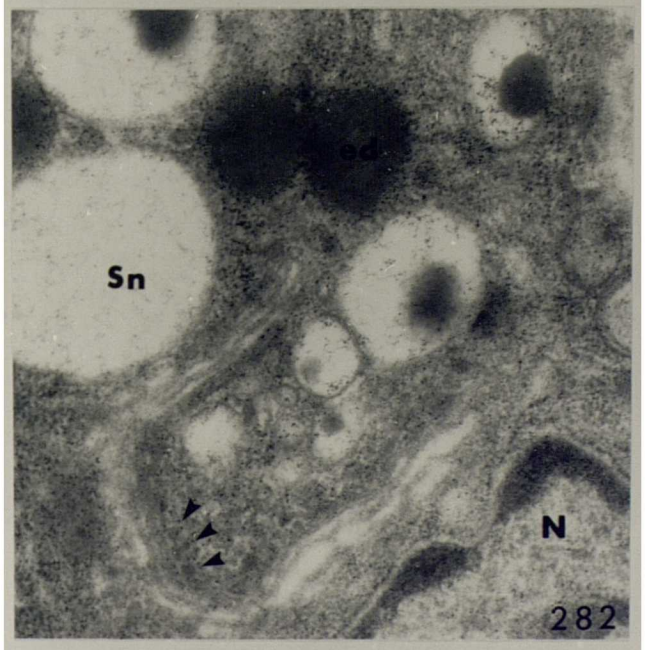
ed
Sn
N
282

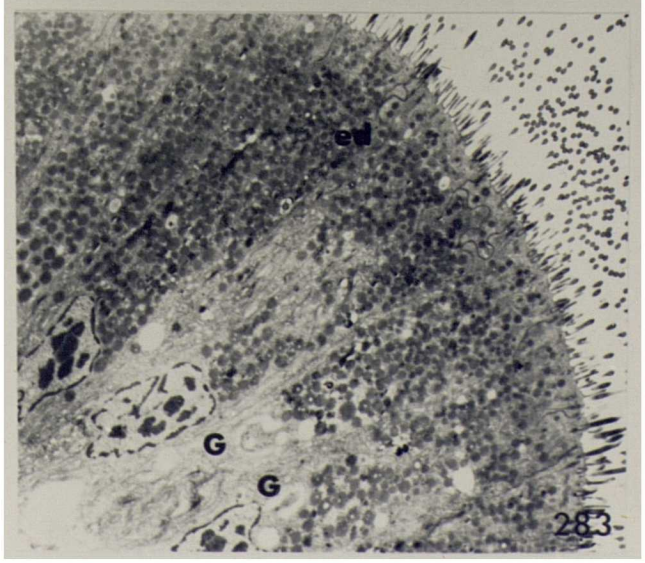
ed
G
G
283

A.hortensis, vas deferens.

Fig. 284 Arrangement of the muscle, nerve and pore cells in the connective tissue sheath (x1.5K). ? indicates unidentified cells with large inclusions.

Fig. 285 Spirochaetes in the connective tissue (arrowed) (x 22.5K).

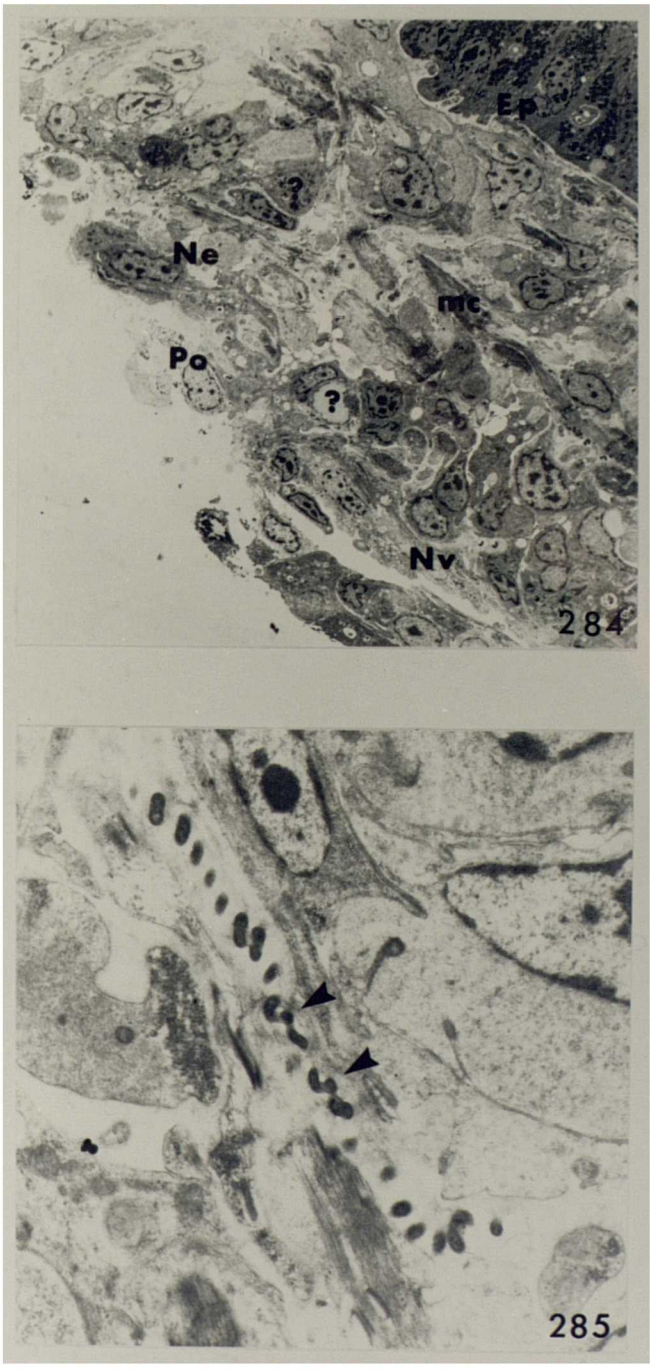
Ep
Ne
mc
Po
?
Nv
284
285

A.hortensis, epiphallus.

Fig. 286 Papillae lining the epiphallus, S.E.M. (x1.3K).

Fig. 287 L.S. through the epiphallus (x250).

Fig. 288 General view of epithelium with underlying calcium cells (x2.25K).

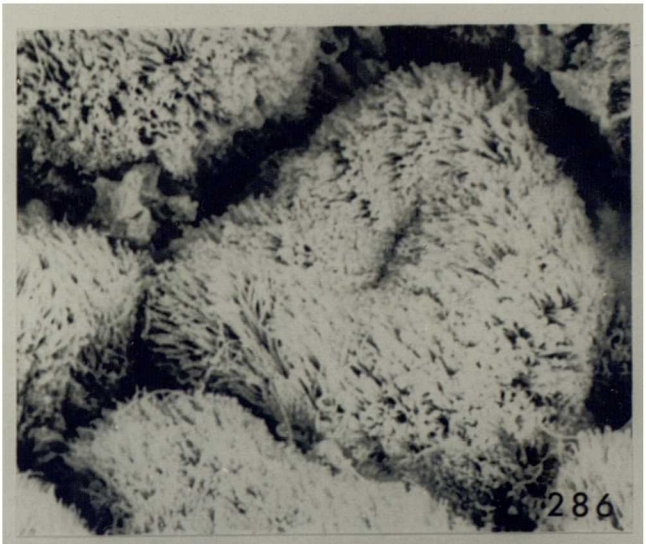

286

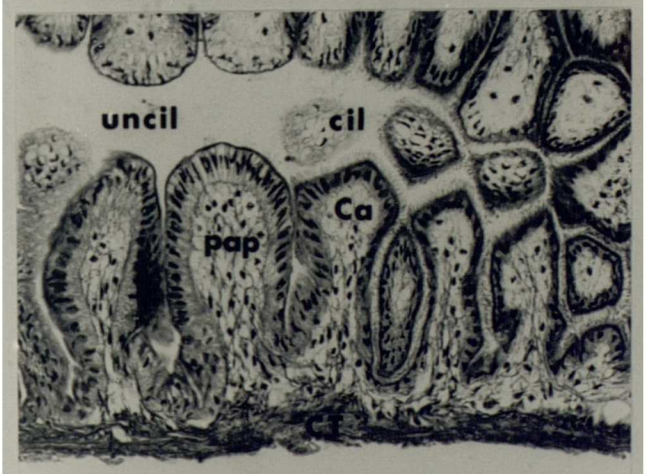

287

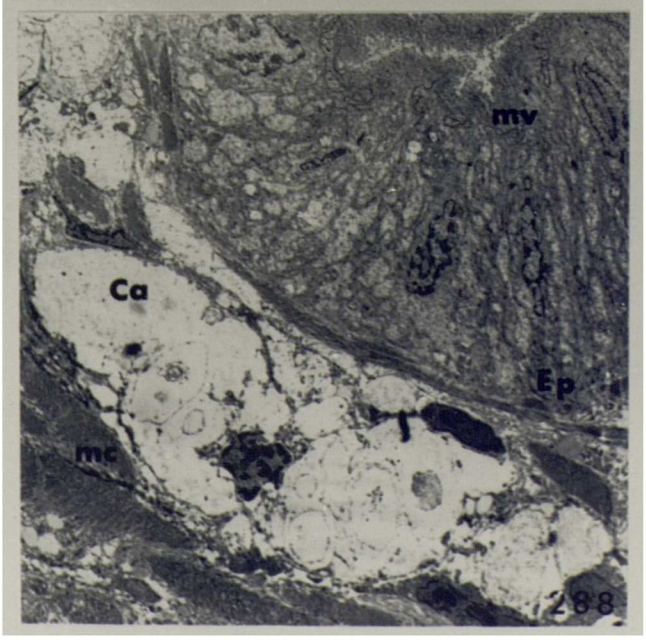

288

A.hortensis, epiphallus

Fig. 289 Epithelial cells (x6K). Arrow indicates hemidesmosome on basal membrane.

Fig. 290 Arrangement of muscle, granular cell and calcium cells in the connective tissue sheath (x2.25K).

Fig. 291 Detail of calcium concretions within the calcium cell (x15K).

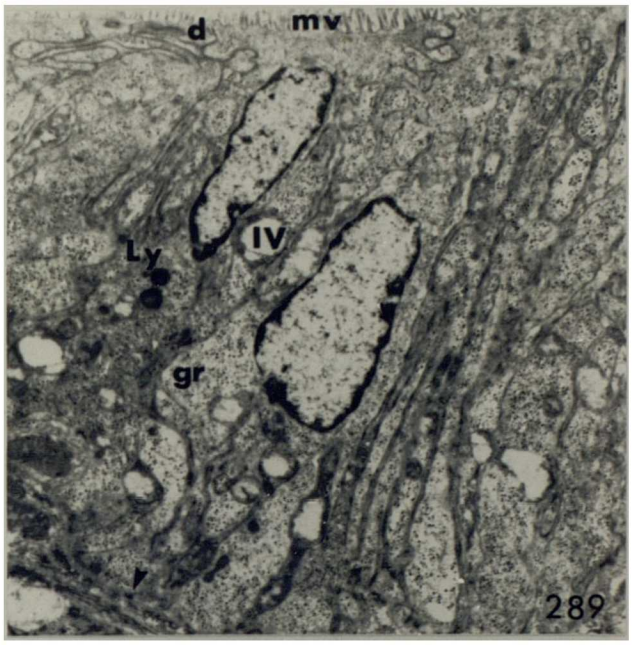
d
mv
Ly
lV
gr
289

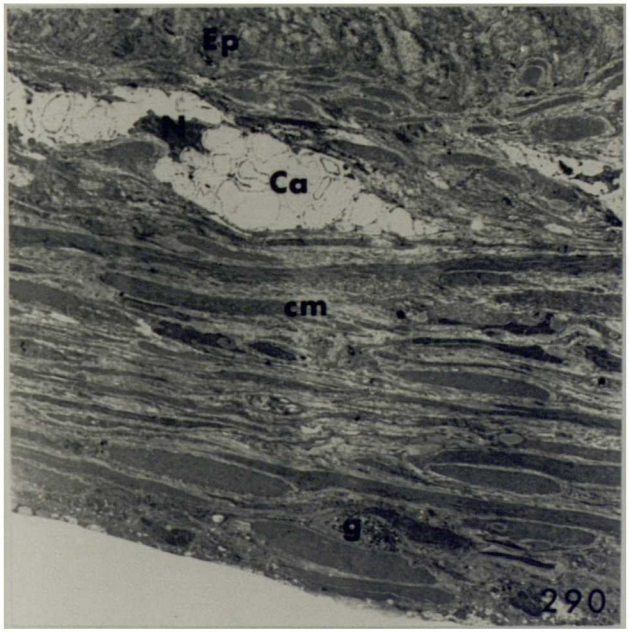
Ep
Ca
cm
g
290

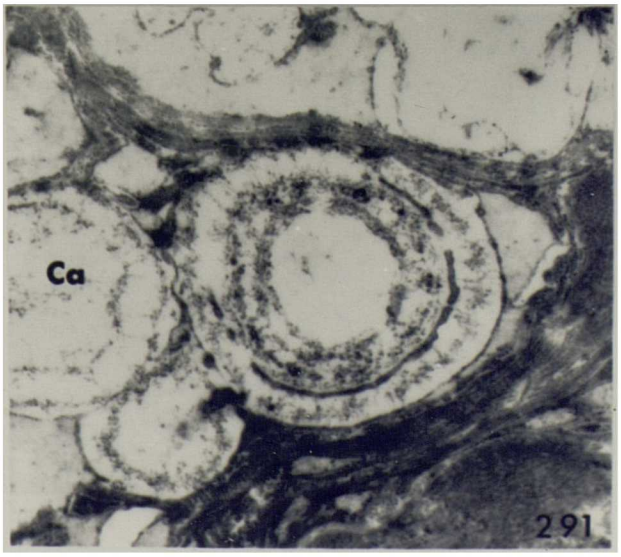
Ca
291

A.hortensis, thick oviduct.

Fig. 292 General view of epithelium (x2.25K).

Fig. 293 Detail of a Golgi body and forming secretory vesicles (x37.5K).

Fig. 294 Detail of cell apices (x22.5K). Arrow indicates the position of a desmosome.

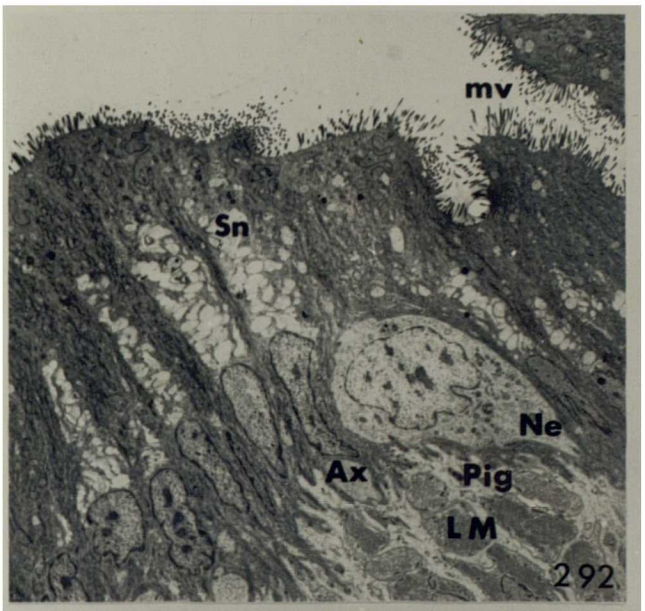
mv
Sn
Ne
Ax
Pig
LM
292

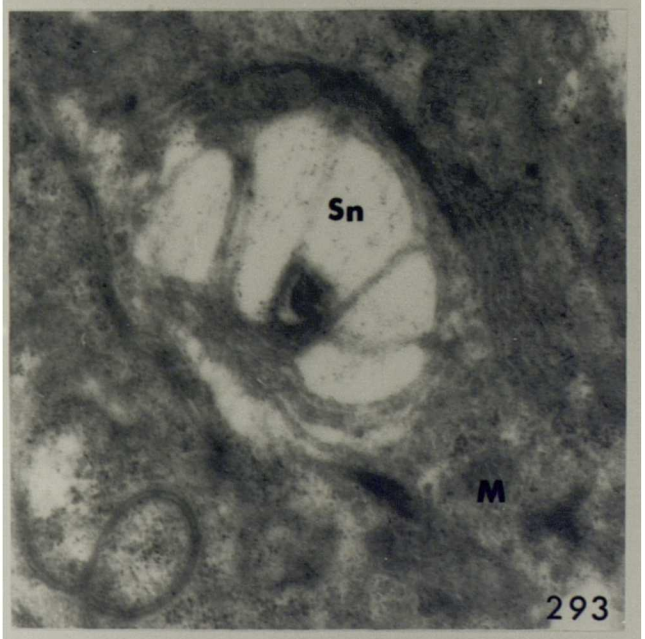
Sn
M
293

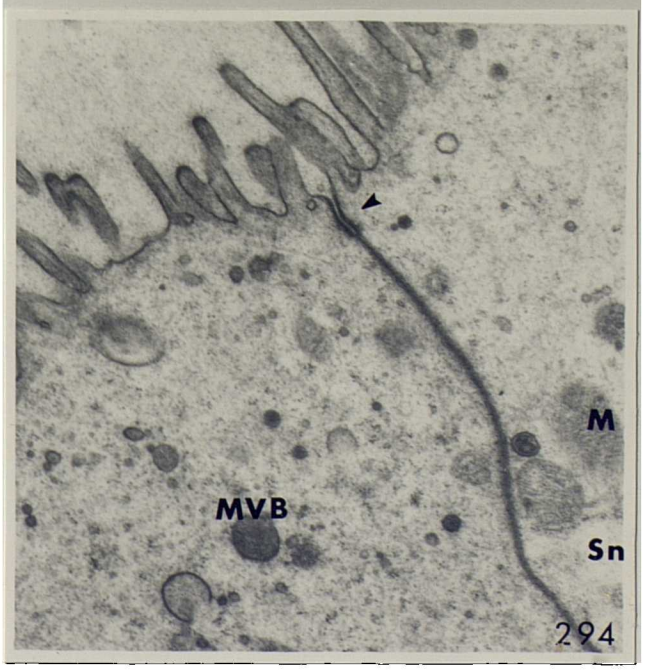
M
MVB
Sn
294

A.hortensis, thick oviduct.

Fig. 295 Detail of cell bases showing the relationship with the underlying nerve plexus (x15K). Arrows indicate hemidesmosomes in apposition to the thick basement membrane.

Fig. 296 T.S. through the thick oviduct (x164).

Fig. 297 Arrangement of the muscle and nerve cells in the inner region of the connective tissue sheath (x3.36K).

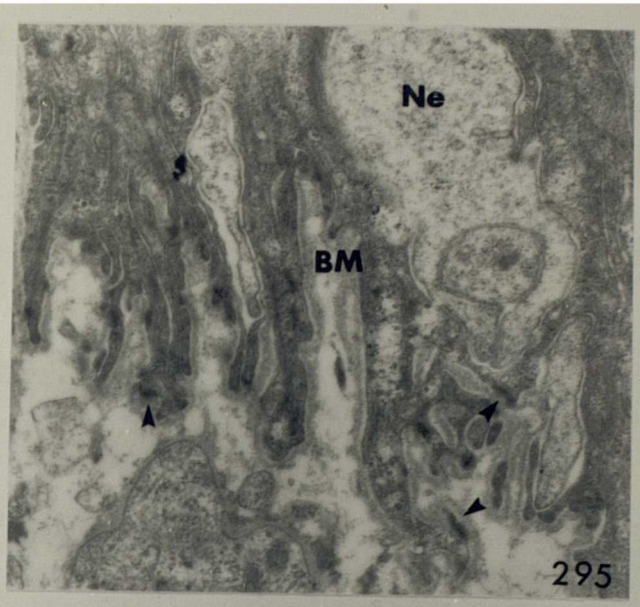
Ne
BM
295

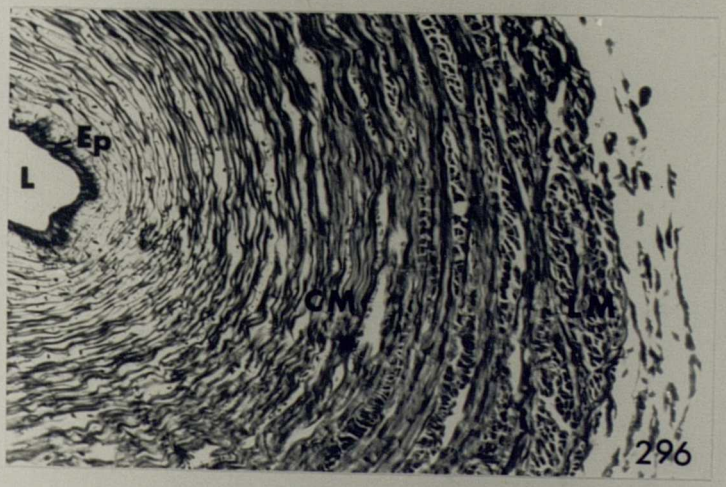
Ep
L
CM
LM
296

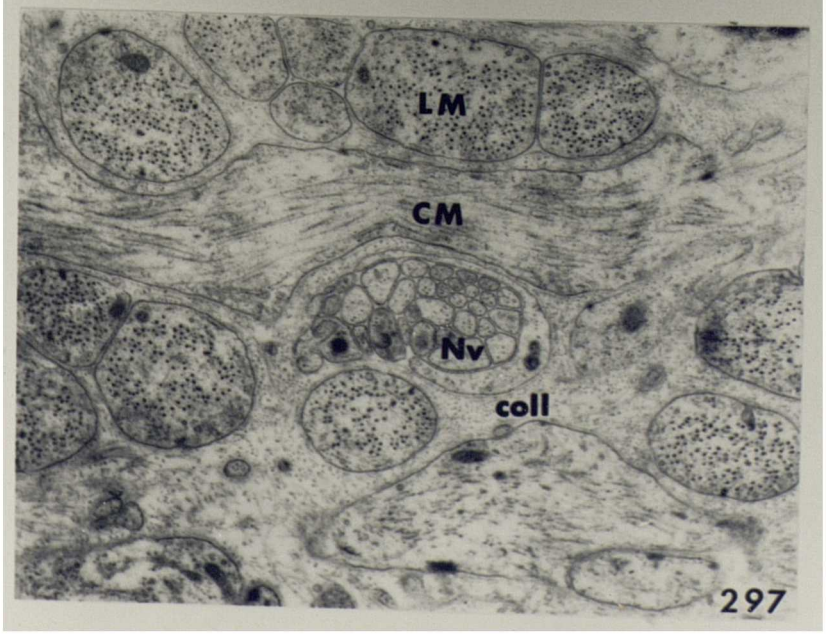
LM
CM
Nv
coll
297

A.hortensis, thick oviduct.

Fig. 298 Arrangement of the muscle and nerve cells in the central region of the connective tissue sheath (x4.32K).

Fig. 299 Detail of the muscle/nerve relationship (x9K). Arrow indicates possible neuromuscular junction.

Fig. 300 Arrangement of the nerve and muscle cells at the periphery of the connective tissue sheath (x5.16K).

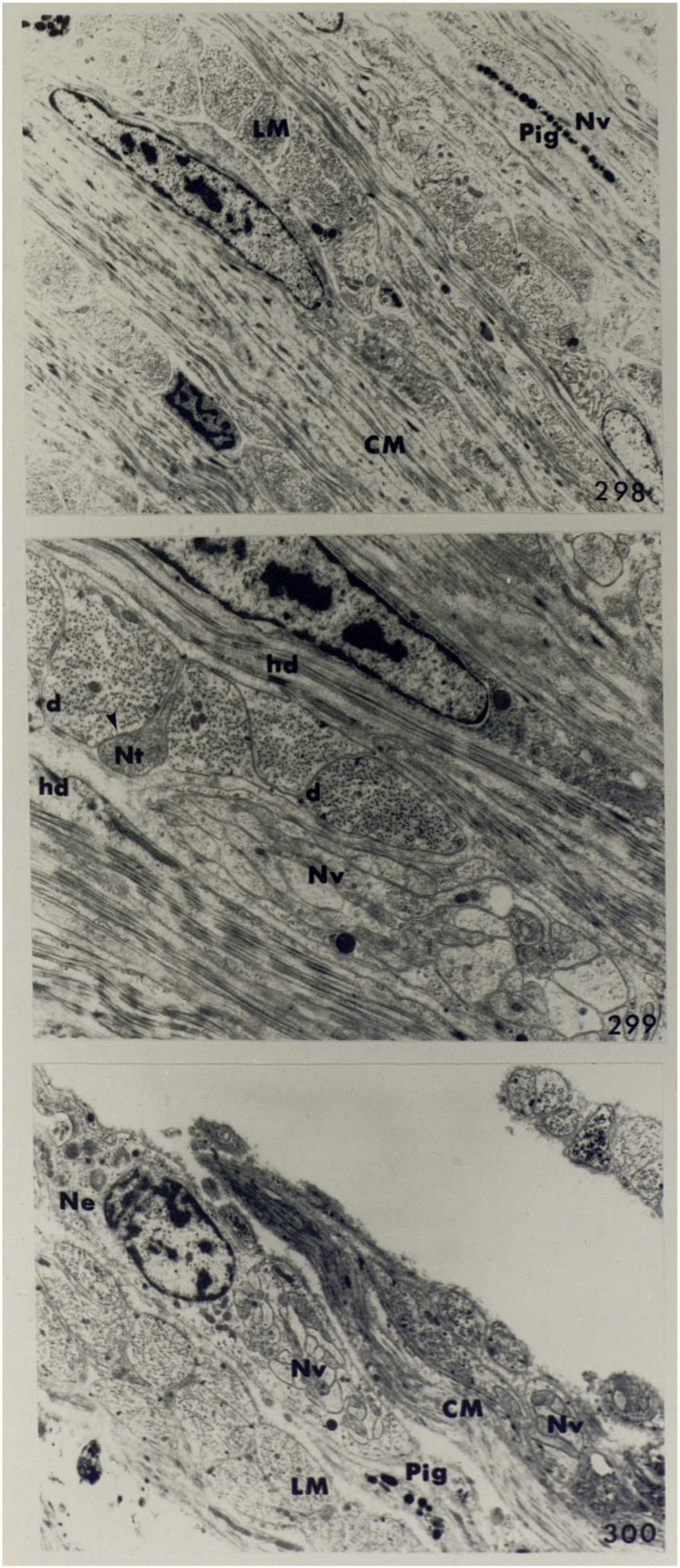
LM
Pig
Nv
CM
298
hd
d
Nt
hd
d
Nv
299
Ne
Nv
CM
Nv
LM
Pig
300

A.hortensis, thin oviduct.

Fig. 301 General view of epithelium (x3.75K). Small arrows indicate granular accumulations in the cytoplasm, large arrows indicate lipid-like droplets.

Fig. 302 Detail of Golgi apparatus (x37.5K).

Fig. 303 Arrangement of muscle and nerve cells in the connective tissue sheath (x2.25K).

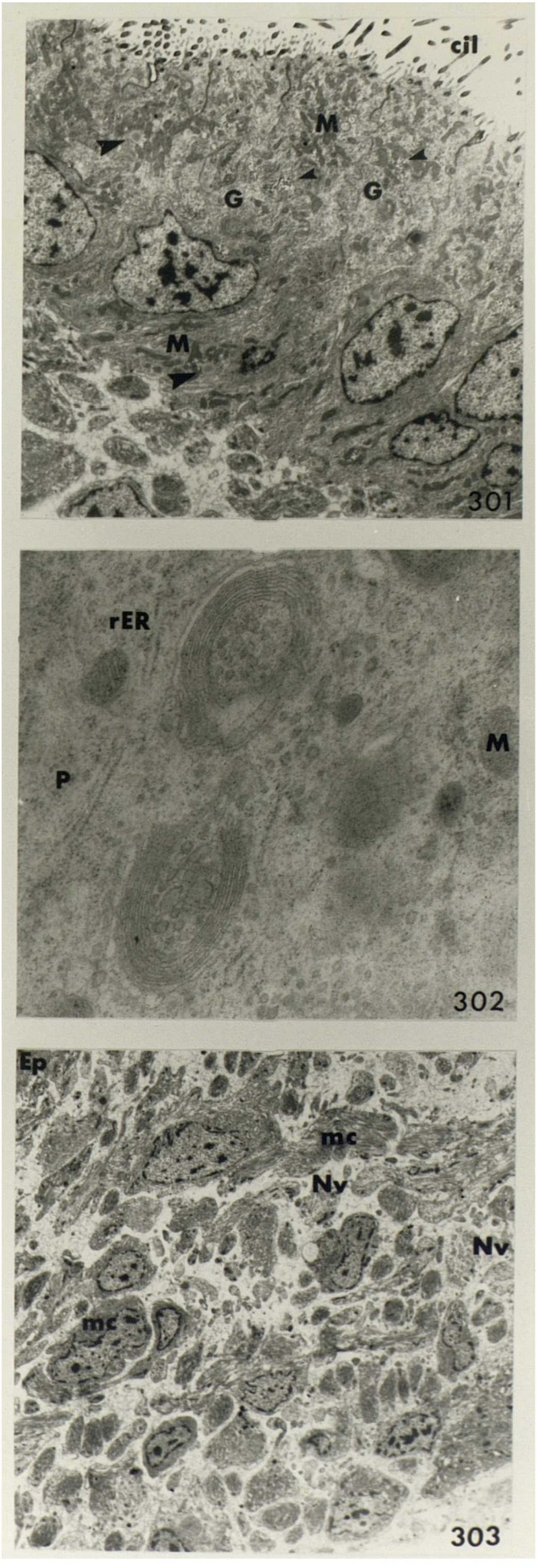
cil
M
G
G
M
301
rER
M
P
302
Ep
mc
Ny
Nv
mc
303

Fig. 304 Tracing of a thin layer chromatogram of lipid extracts from the lower atria of A.hortensis.

A. aqueous extract

B. first ether extract

C. second ether extract

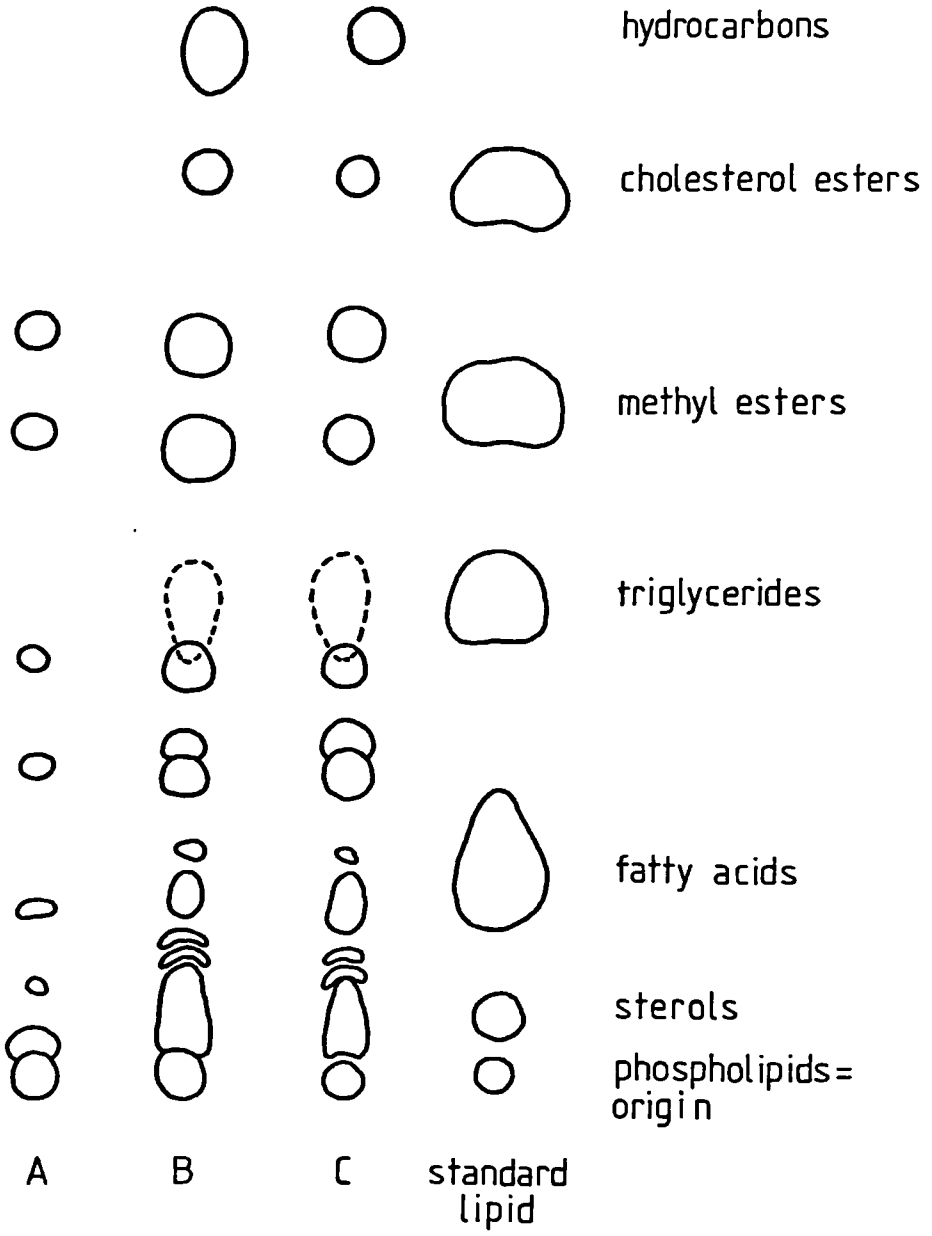
hydrocarbons
cholesterol esters
methyl esters
triglycerides
fatty acids
sterols
phospholipids=
origin
A
B
C
standard
lipid

Fig. 304

Fig. 305 Diagram showing the variety of form of the anterior genital ducts in representative Stylommatophora.

a. Generalized plan

b. Helix aspersa

c. Pellicula depressa

d. Testacella haliotidea

e. A.hortensis

f. Milax budapestensis

g. Limax maximus

h. D. reticulatum

i. Lehmannia marginata

j. Philomycus carolinianus

Key: a, atrium; b, bursa copulatrix; c, caecum; CD, common duct; div, diverticulum; ds, dart sac; e, epiphallus; f, flagellum; lg, lobed gland; mg, mucous gland; o, oviduct; p, penis; pm, penial mass; ta, trifid appendage; vd, vas deferens.

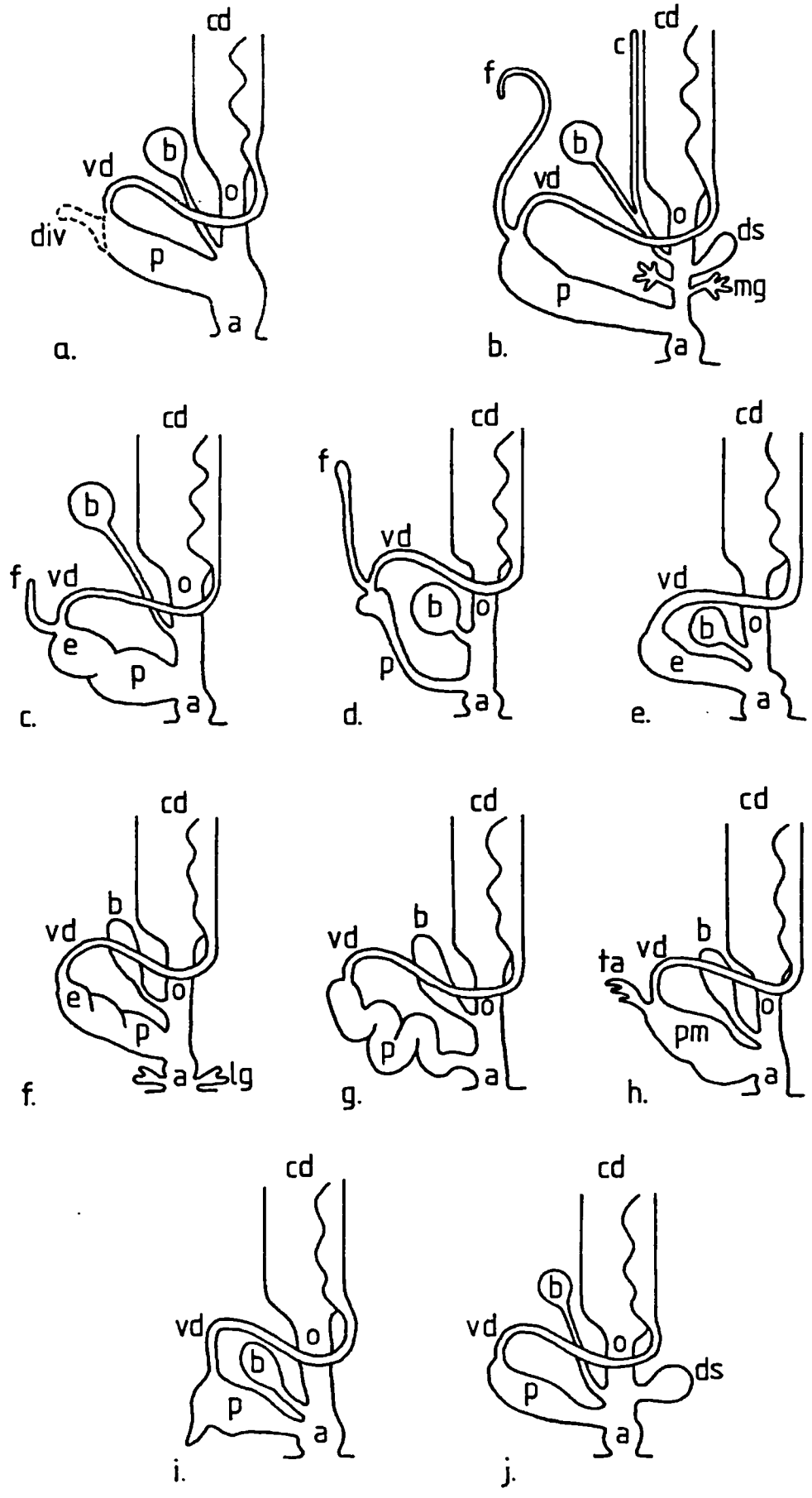
cd
vd
b
o
div
p
a
a.
cd
c
f
b
vd
o
ds
mg
p
a
b.
cd
b
f
vd
o
e
p
a
c.
cd
f
vd
b
o
p
a
d.
cd
vd
b
o
e
a
e.
cd
b
vd
e
o
p
a
lg
f.
cd
vd
b
o
p
a
g.
cd
b
vd
ta
o
pm
a
h.
cd
vd
b
o
p
a
i.
cd
b
vd
o
p
ds
a
j.

Fig. 305

Fig. 306 Variation in the origin of the bursa copulatrix at morphogenesis in representative *Stylommatophora*.

a. Helix pomatia

b. A. hortensis

c. D. reticulatum, Limax maximus

d. Arion ater

Key: cd, common duct; ga, genital atrium;
♀, female duct; ♂, male duct.
Bursa copulatrix, stippled.

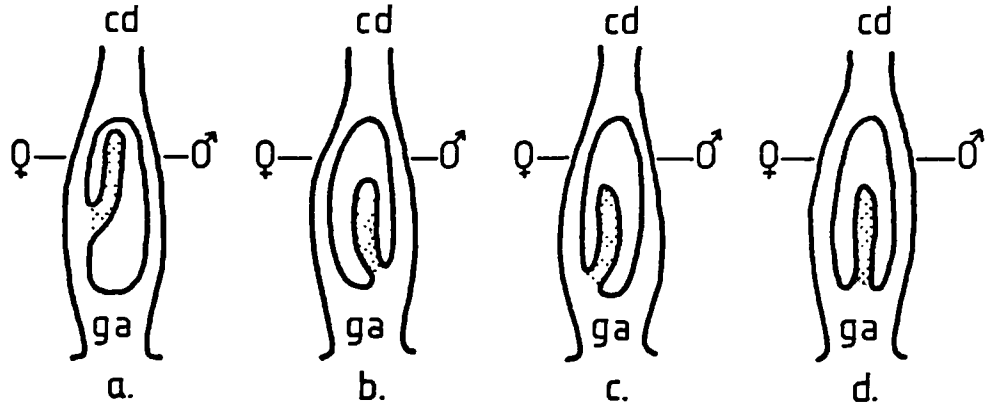

Fig. 306

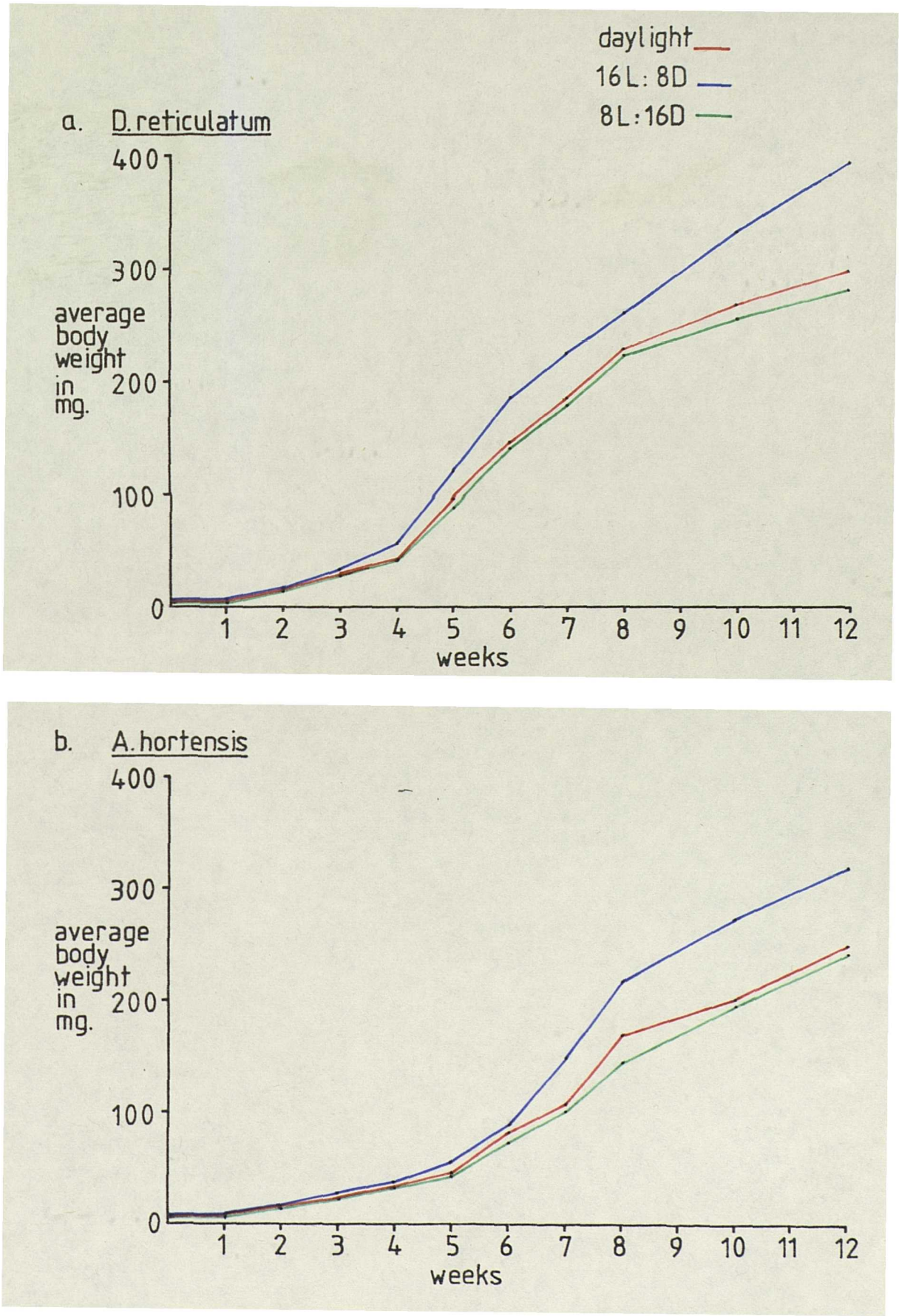

Fig. 307 The effect of photoperiod on growth

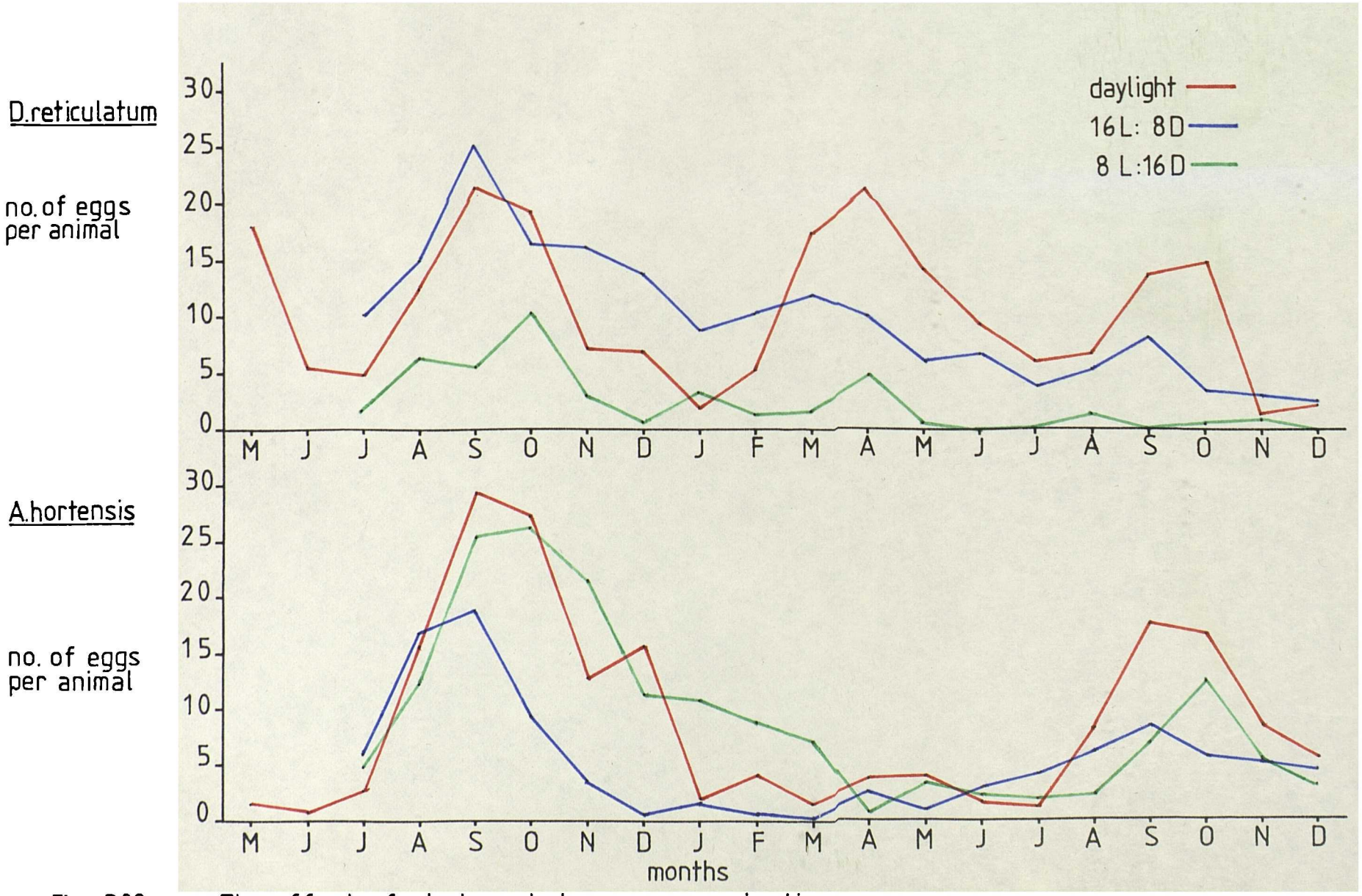

Fig. 308 The effect of photoperiod on egg production

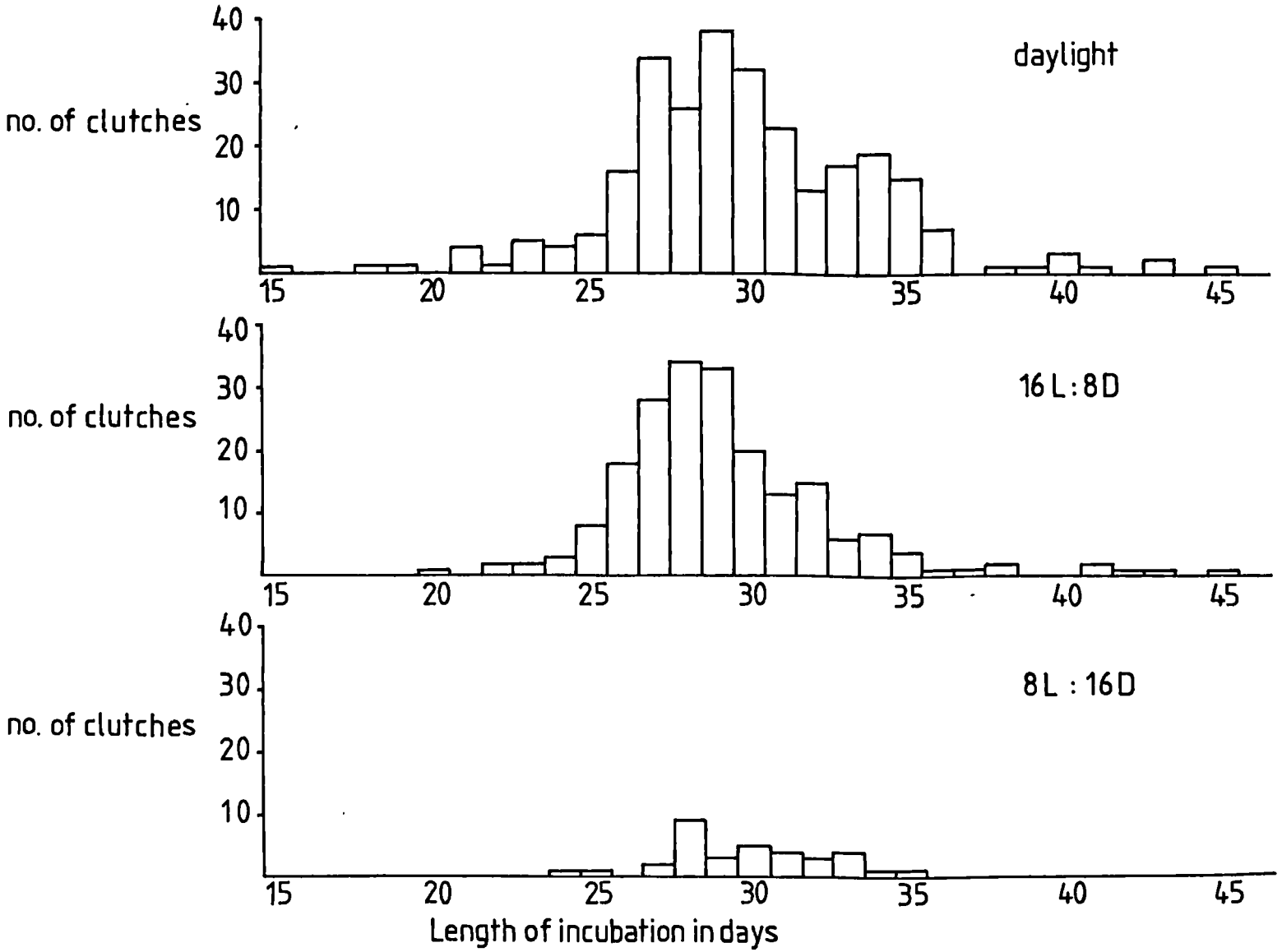

Fig. 309 a The effect of photoperiod on the length of incubation in D.reticulatum

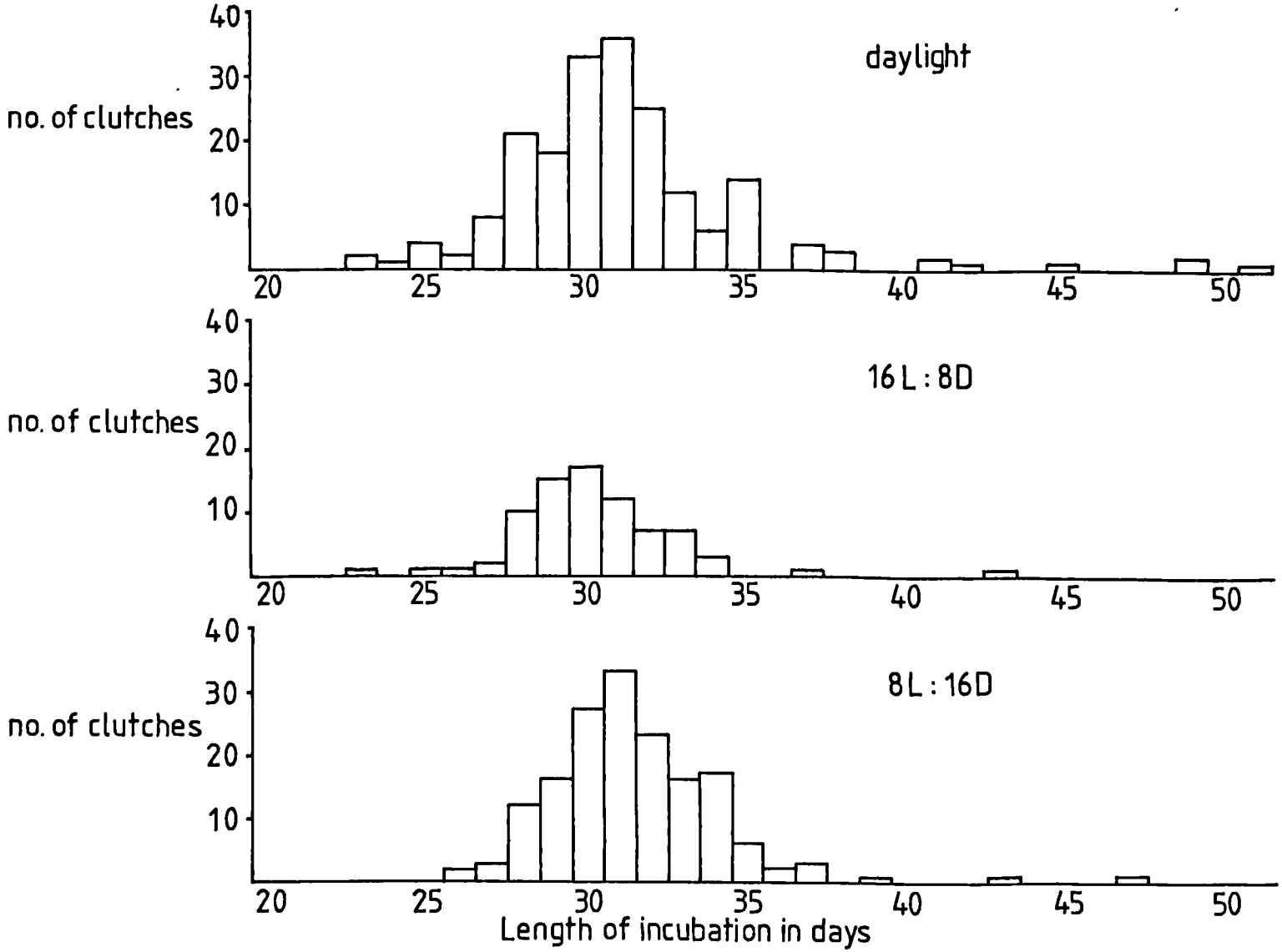

Fig. 309b The effect of photoperiod on the length of incubation in A.hortensis

Fig. 310 Abnormal development of A. hortensis , changes in pigmentation

a. animal taken from the field.

b. animal after six months in captivity.

c. second generation animal.


a
b
c
310

Abnormal development of A. hortensis.

Fig. 311 Gonad at 26 weeks (x160).

Fig. 312 Carrefour at 26 weeks (x160).

Fig. 313 Anterior genital ducts at 26 weeks (x160).


b
a
311
al
ah
dl
312
♀
b
♂
313

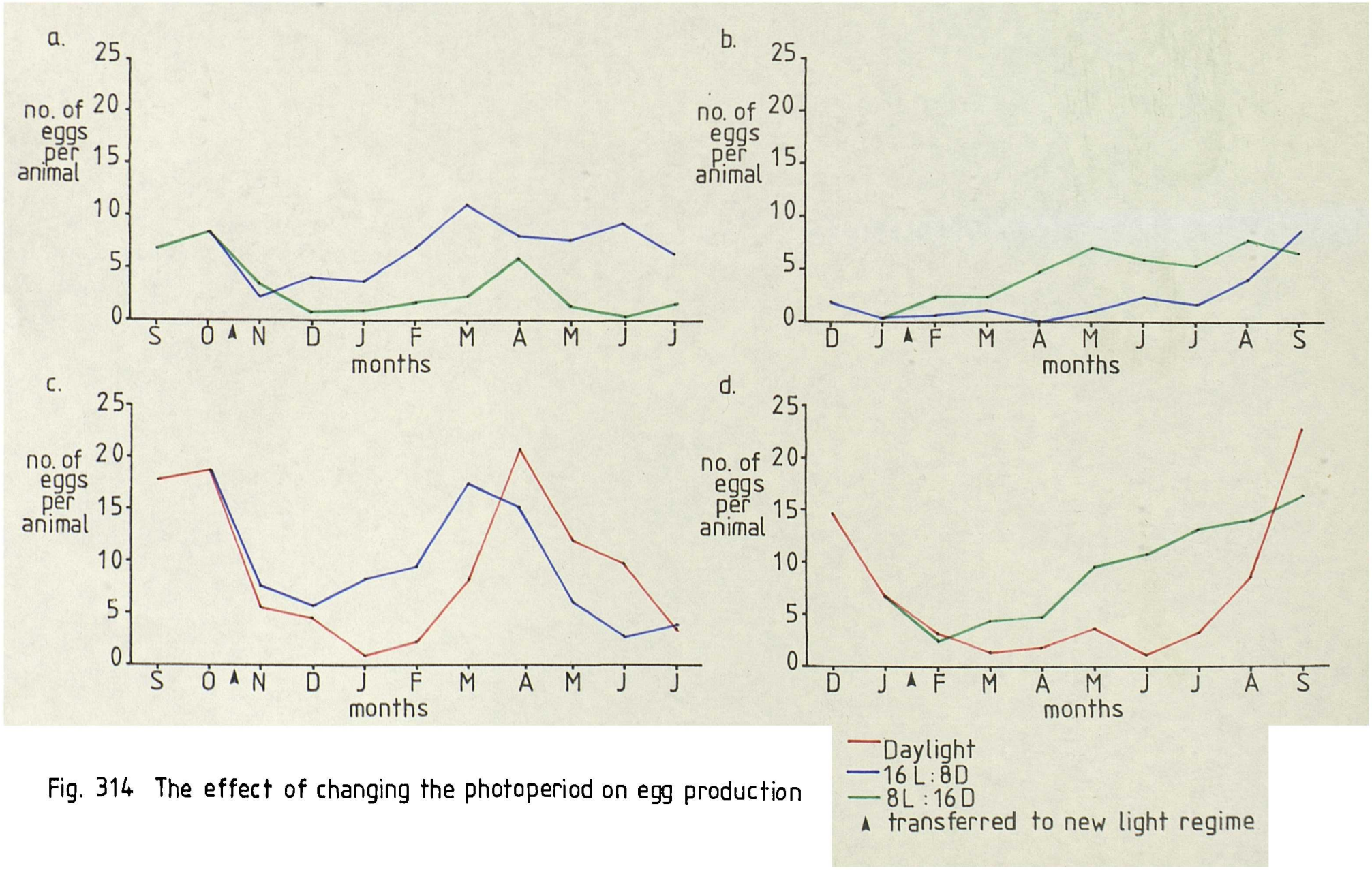

Fig. 314 The effect of changing the photoperiod on egg production

Fig. 315 Courtship behaviour of D. reticulatum .

a. Position assumed during the early stages of courtship.

b. Circling away from one another.

c. Position assumed during the later stages of courtship.

Broken arrows indicate the direction of movement.

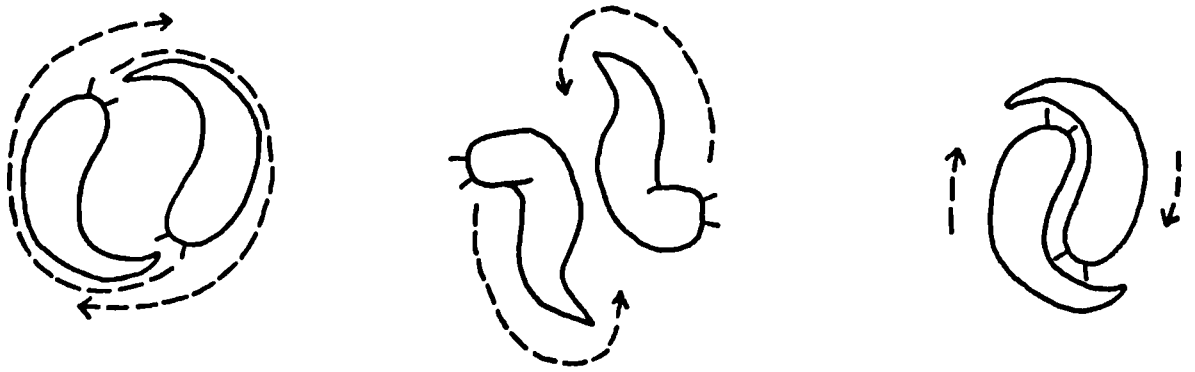

a. b. c.

Fig. 315

Fig. 316 D. reticulatum, courtship and copulation under laboratory conditions.

a. caressing with the tips of their sarcobella.

b. pair moving closer together.

c. sarcobella erected.

d. penial sacs partially everted.

e. penial sacs completely everted. The blue colouration is due to the blood pigment, haemocyanin.

f. exchange of sperm packages.

g. exchange of sperm packages. Arrows indicate the fully-everted trifid appendages.

h. exchange of sperm packages.

Fig. 316

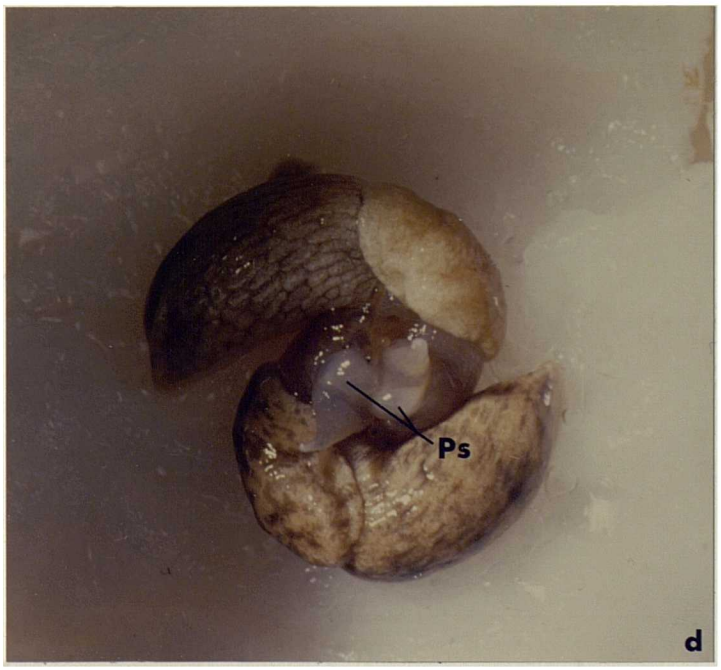

Fig. 316 cont.

Fig. 316 cont.

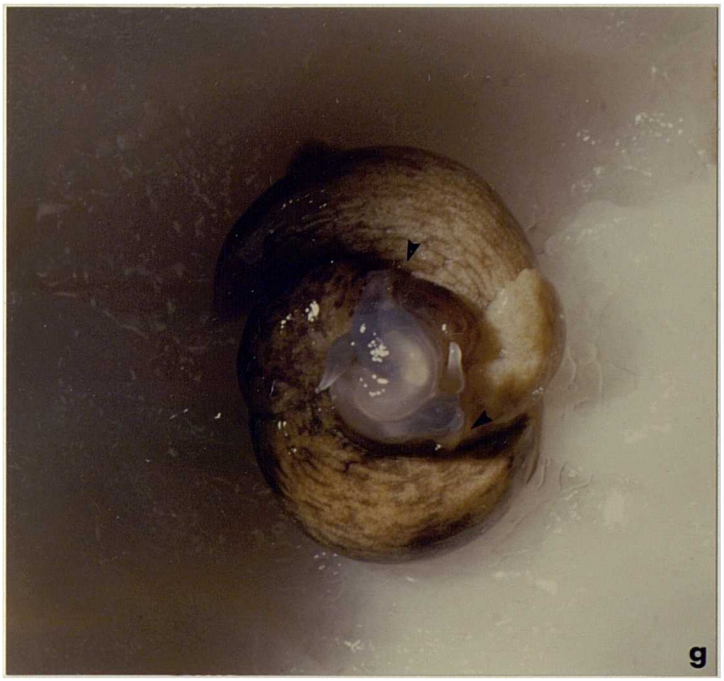

Fig. 316 cont.

Fig. 317 D. reticulatum, courtship and copulation in the field.

a-b pair circling slowly while caressing with the tips of their sarcobella.

c. bases of the sarcobella apposed.

d. caressing with the sarcobella.

e. pair moving closer together.

f. genital openings apposed, sarcobella erected.

g. partial eversion of penial sacs, sarcobella displaced.

h. complete eversion of penial sacs. Arrows indicate the fully-everted trifid appendages.

i. exchange of sperm packages (arrowed).

Fig. 317

Fig. 317 (cont.)

Fig. 317 (cont.)

Fig. 317 (cont.)

Fig. 317 (cont.)

D, reticulatum, 10 minutes after protrusion of sarcobellum.

Fig. 318 Sperm in the anterior, slender region of the hermaphrodite duct and entering the pouched diverticulum of the carrefour (x240).

Fig. 319 Sperm filling the base of the carrefour (x240).

Fig. 320 Sperm entering the male groove of the common duct (x125).

Fig. 321 Increased activity of the sub-epithelial mucocytes associated with the carrefour diverticula (x240).

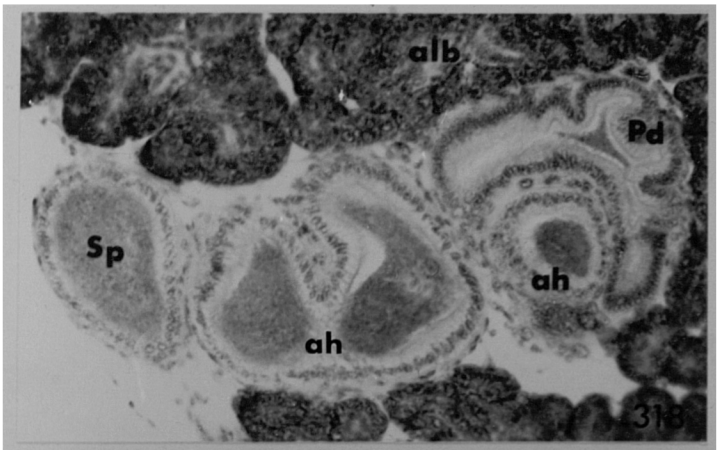
alb
Pd
Sp
ah
ah
318

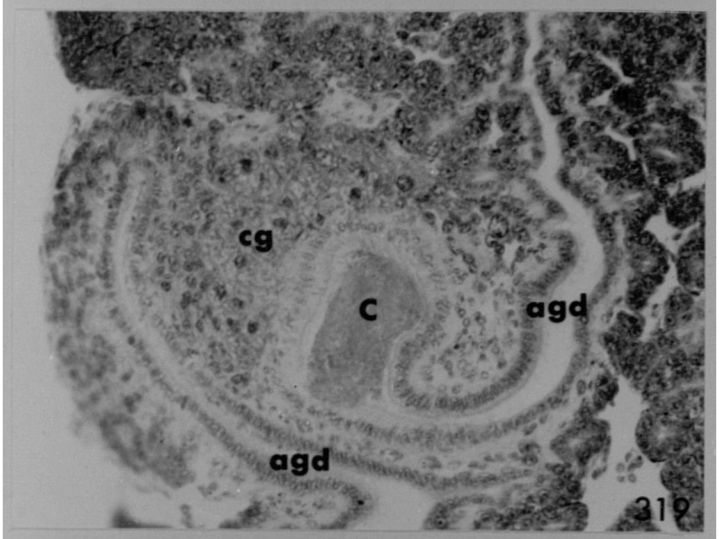
cg
C
agd
agd
319

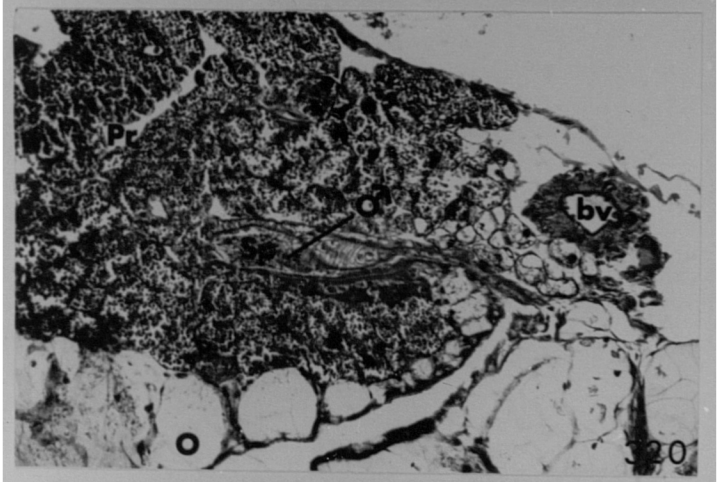
Pr
bv
O
320

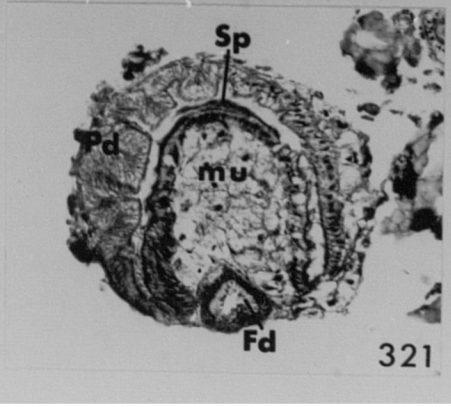
Sp
Pd
mu
Fd
321

D. reticulatum, 15 minutes after protrusion of the sarcobellum.

Fig. 322 T.S. through distal half of hermaphrodite duct (x160).

Fig. 323 T.S. through carrefour, pouched diverticulum swollen with sperm (x160).

Fig. 324 T.S. through carrefour, albumen gland ducts filled with albumen, male groove filled with secretion from the carrefour gland (x125).

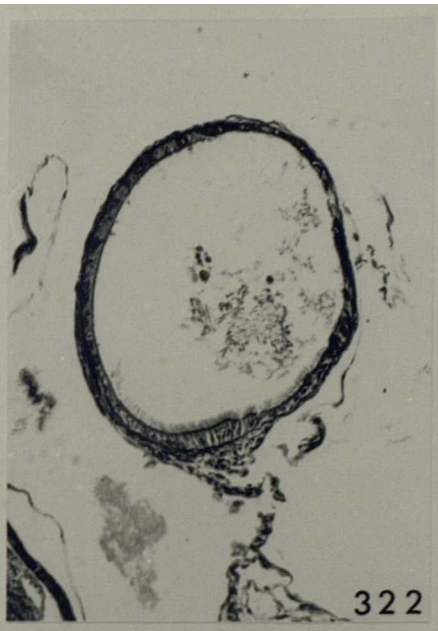
322

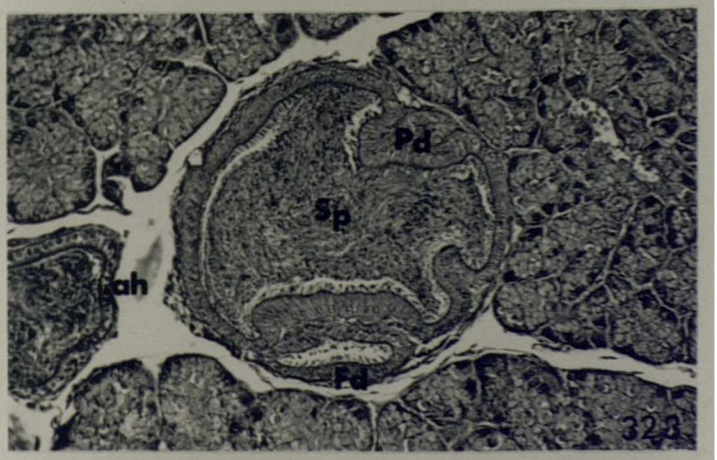
Pd
Sp
ah
Pd
323

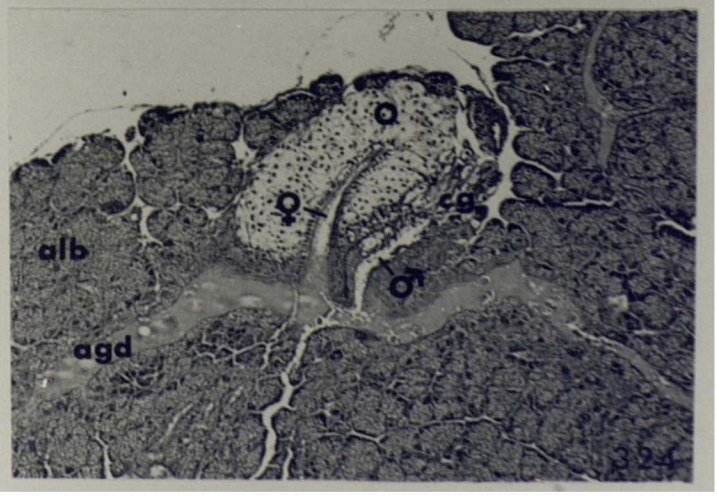
♀
♀
♂
alb
agd
324

D. reticulatum, 15 minutes after protrusion of the sarcobellum.

Fig. 325 Prostate gland, tubules containing prostate secretion (x160).

Fig. 326 Prostate secretion filling the male groove of the common duct (x155).

Fig. 327 Prostate secretion containing a small volume of sperm filling the penial sac (x25).

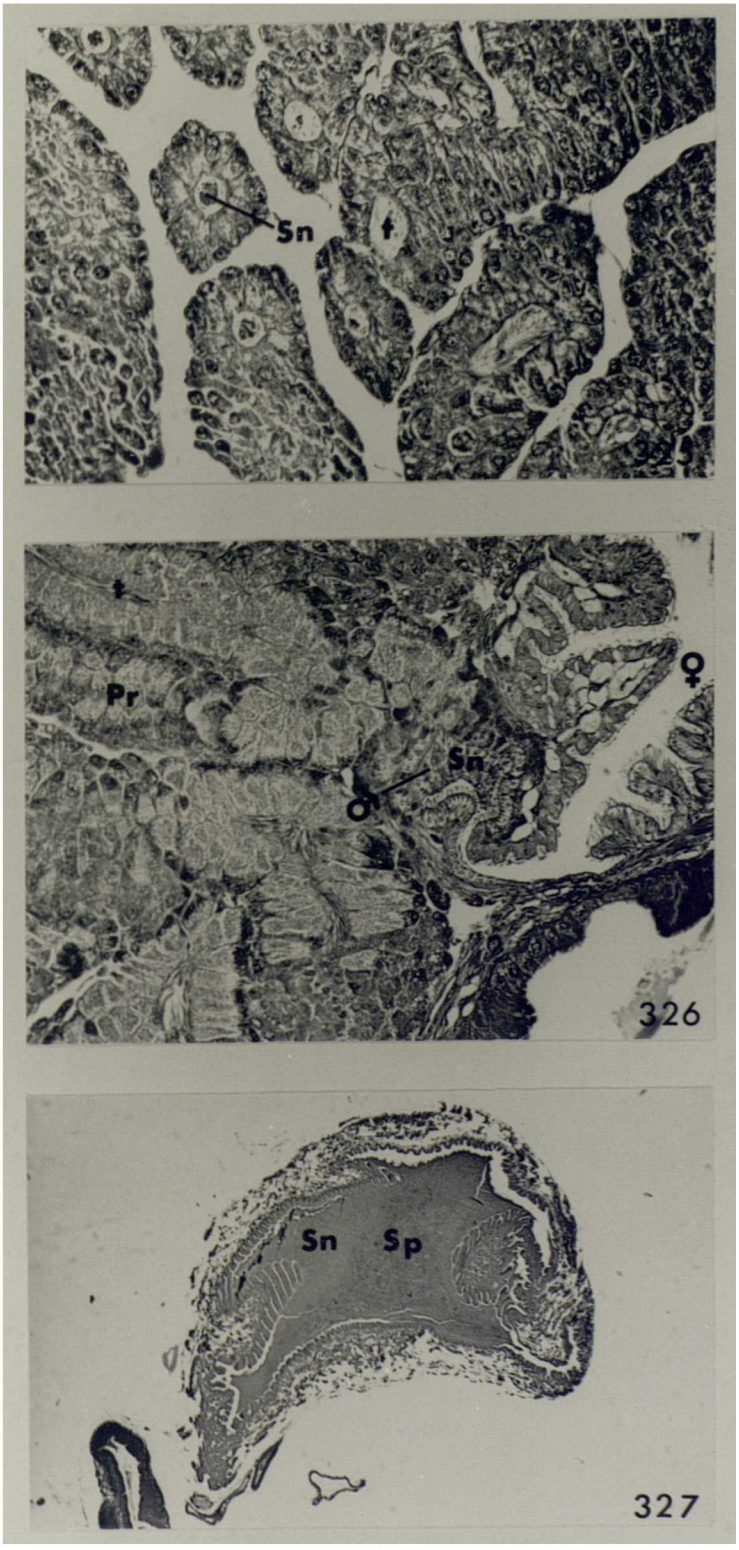
Sn
t
t
Pr
♀
Sn
♂
326
Sn
Sp
327

D. reticulatum, 20 minutes after protrusion of the sarcobellum.

Fig. 328 T.S. through carrefour diverticula (x205).

Fig. 329 Sperm filling the male groove of the common duct (x100).

Fig. 330 T.S. through the vas deferens. Sperm arranged into discrete bundles and surrounded by prostate secretion (x160).

Fig. 331 Sperm and secretion filling penial sac and vas deferens (x40).

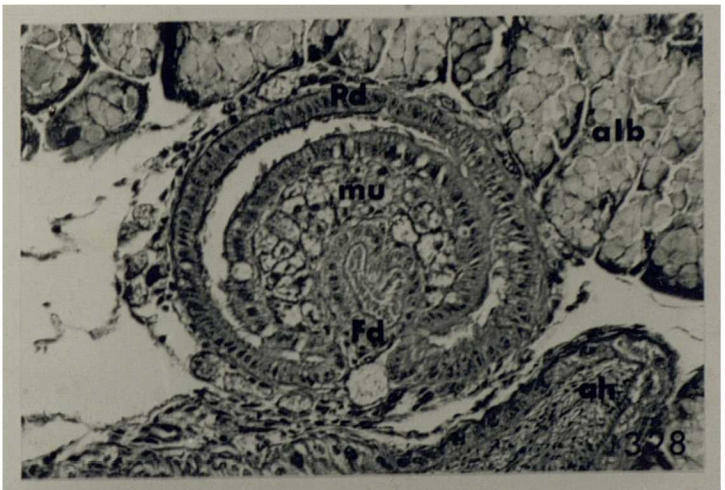
Rd
alb
mu
Fd
328

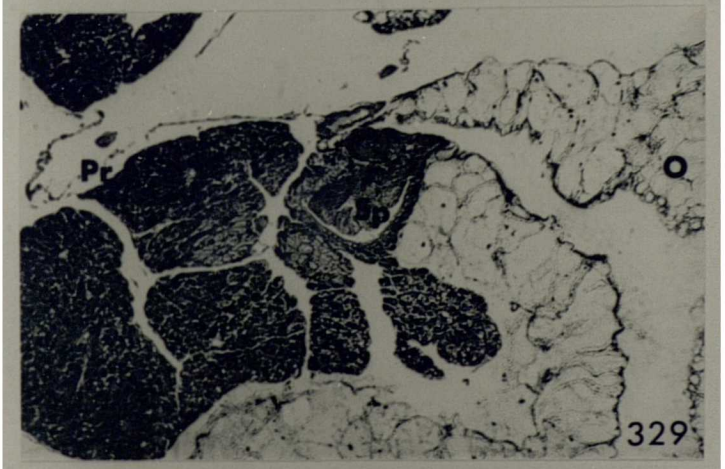
Pr
Sp
O
329

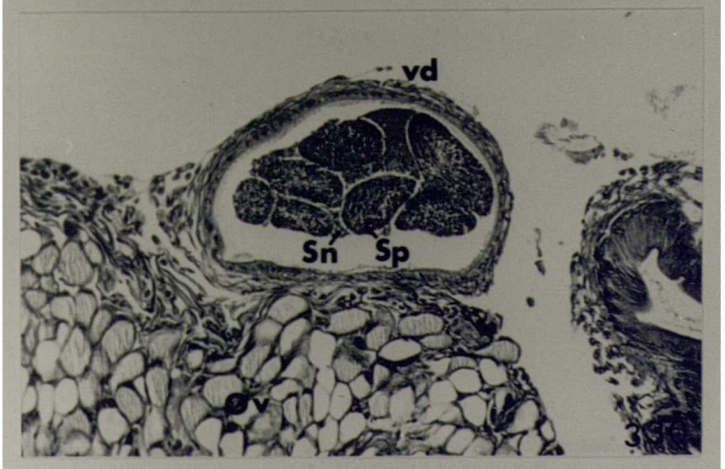
vd
Sn
Sp
Ov

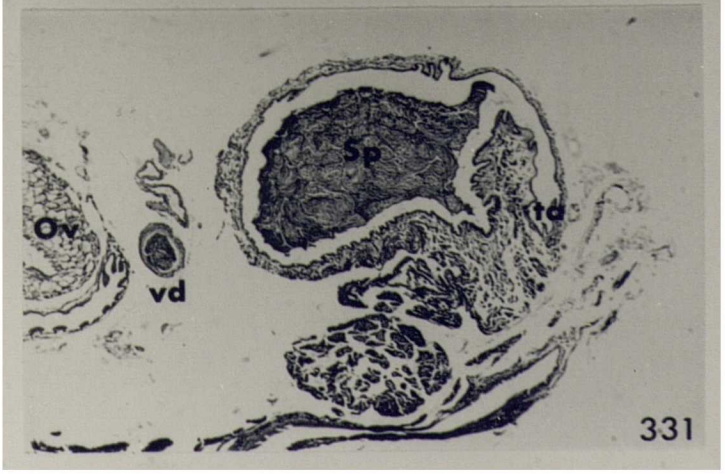
Sp
Ov
vd
331

D. reticulatum, 20 minutes after protrusion of the sarcobellum.

Fig. 332 T.S. and L.S. through the diverticula of the trifid appendage (x125). Prostate secretion fills the side branches (arrowed).

Fig. 333 T.S. through a side branch of one of the trifid diverticula (x160).

Fig. 334 Detail of the epithelium lining the trifid appendage (x400). Arrow indicates the transition from cuboidal to squamous epithelium.

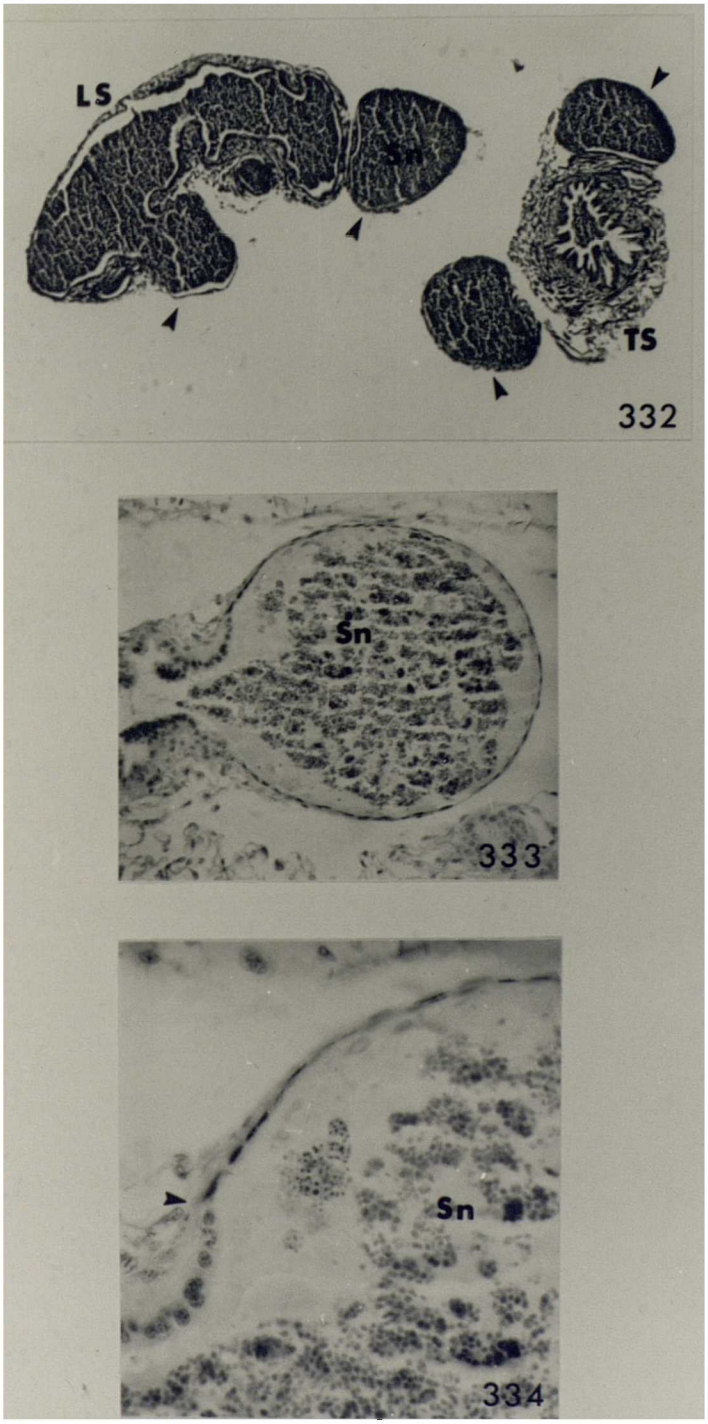
LS
Sn
TS
332
Sn
333
Sn
334

D. reticulatum, 30 minutes after protrusion of the sarcobellum.

Fig. 335 T.S. through the anterior region of the common duct (x125). Prostrate secretion fills the main groove.

D. reticulatum, 40 minutes after protrusion of the sarcobellum.

Fig. 336 Sperm entering the efferent ductules of the gonad (x160).

335

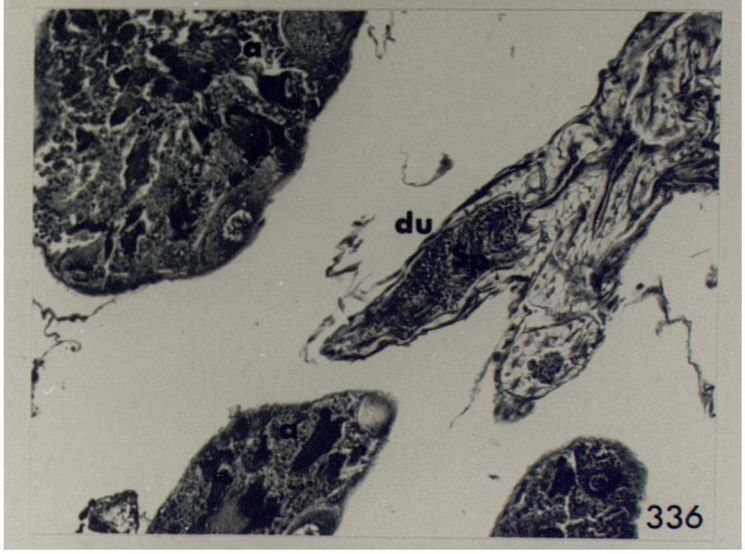

336

D. reticulatum, 40 minutes after protrusion of the sarcobellum.

Fig. 337 Sperm package filling the penial sac (x25).

Fig. 338 Detail of sperm package (x160).

Fig. 339 T.S. through one of the trifid diverticula (x250). Side branch filled with prostate secretion (arrowed).

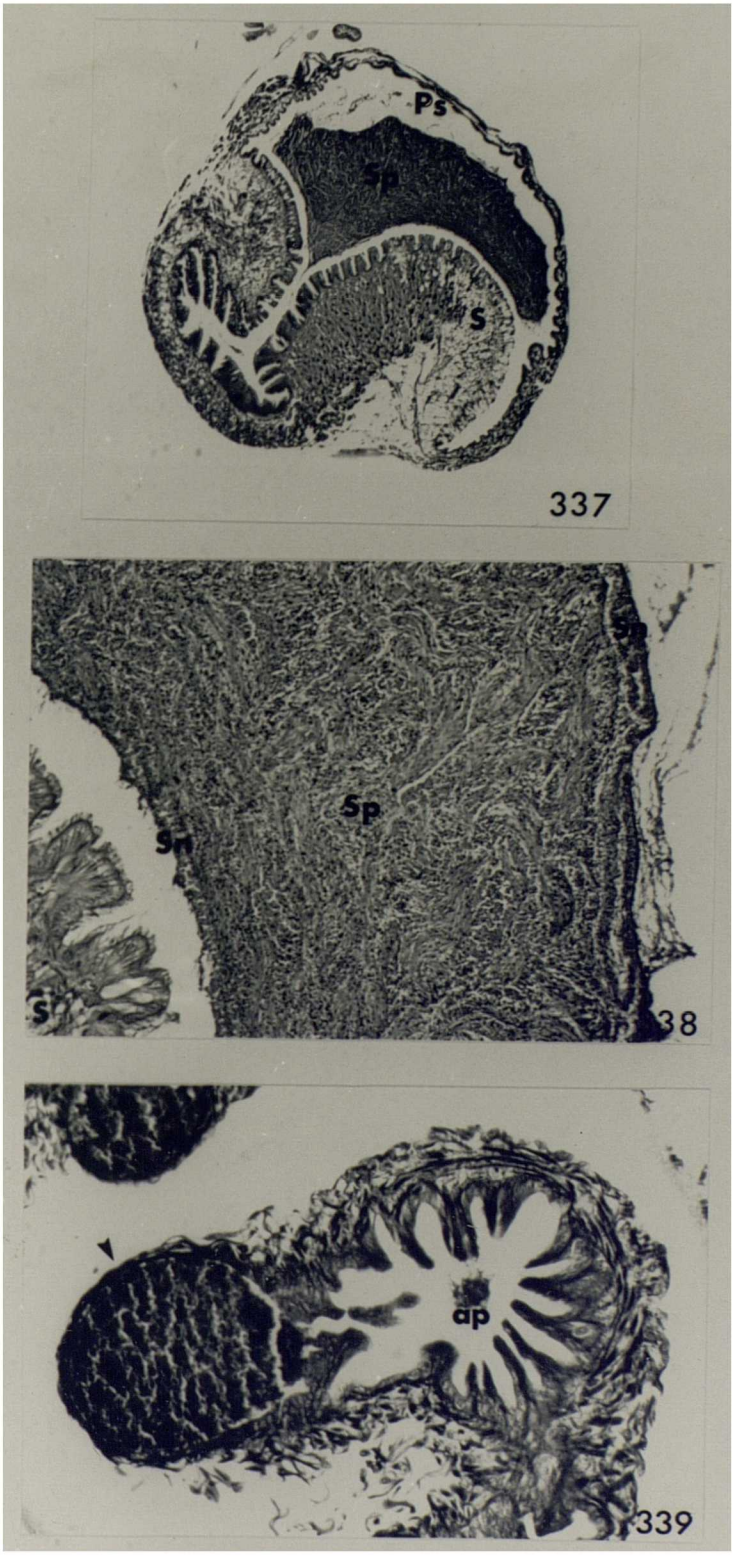
Ps
Sp
S
337
Sp
Sm
S
38
ap
339

D. reticulatum, prostate gland secretion.

The granule types are arrowed.

Fig. 340 Type A (x250)

Fig. 341 Type B (x250)

Fig. 342 Type C (x250)

Fig. 343 Type D (x300)

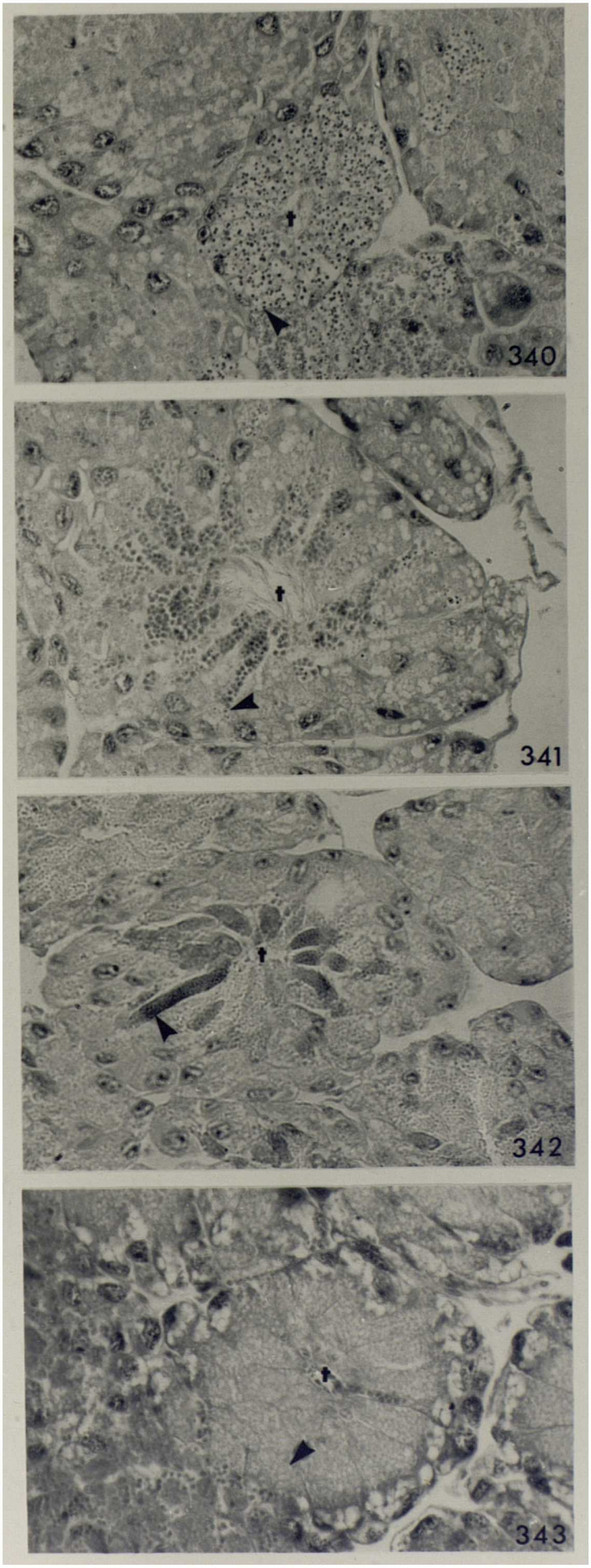
340
341
342
343

D. reticulatum, prostate gland secretion. Granule types A, B, C and D.

Fig. 344 Sperm package on the surface of the everted penial sac (x30).

Fig. 345 Sperm package on the surface of the everted penial sac (x40). Arrows indicate the position of Figs. 346 and 347.

Fig. 346, Fig. 347 Detail of the prostate secretion surrounding the sperm package (x310).

Fig. 348 Detail of the prostate secretion within the trifid appendage (x310). Arrows indicate clusters of type A granules.

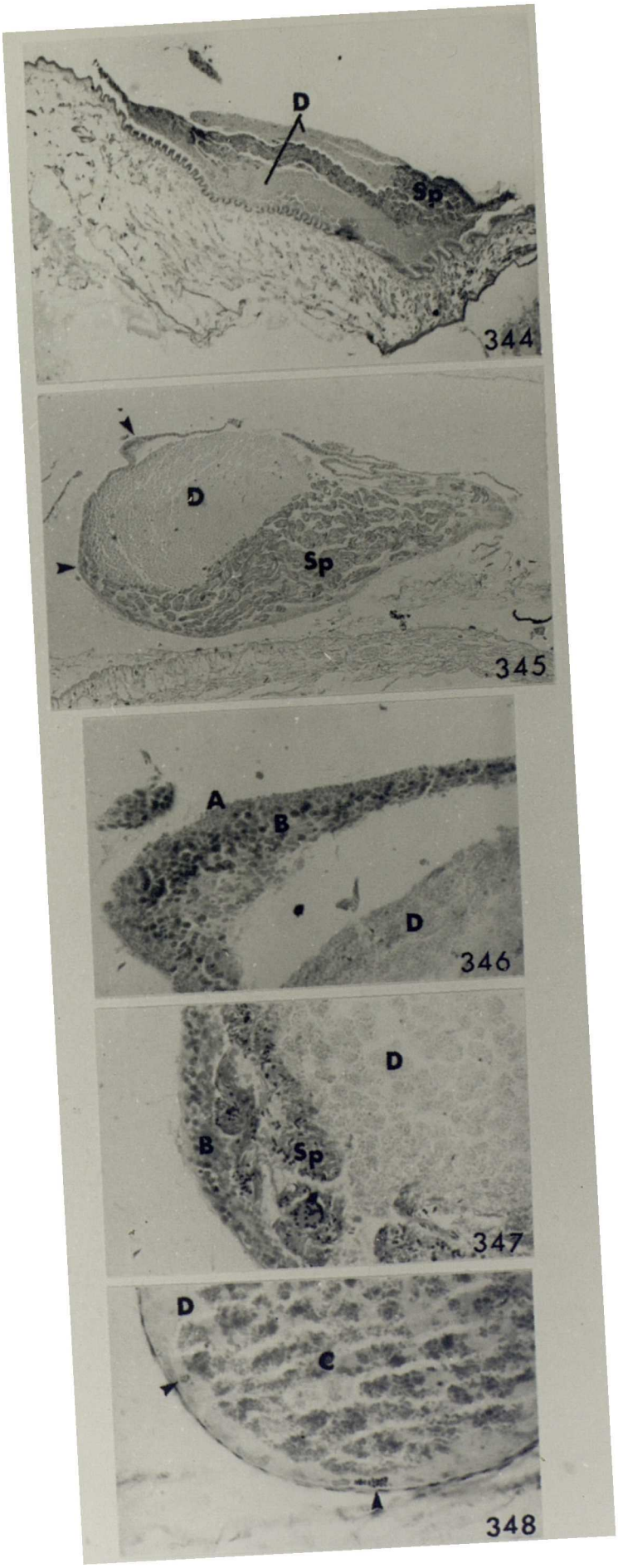
D
Sp
344
D
Sp
345
A
B
D
346
D
B
Sp
347
D
C
348

D. reticulatum, sperm package.

Fig. 349 Two sperm packages removed during copulation (x20).

Fig. 350 Surface detail of the sperm package, S.E.M. (x100).

Fig. 351 Surface detail of the sperm package, S.E.M. (x1.7K).

349

350

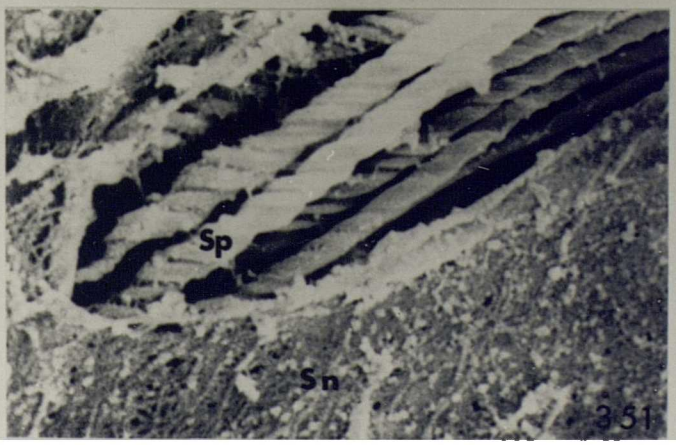

351

D. reticulatum, at copulation.

Fig. 352 Penial mass everted at copulation (x18). Arrows a and b indicate the positions of Figs. 353a and 353b respectively.

Fig. 353 Detail of the epithelium of the everted penial sac at positions a (x160) and b (x400) in Fig. 352.

Fig. 354 Groove formed between the everted penial sac and body wall, leading into the bursa copulatrix (x40). Arrow indicates the direction of movement of the sperm package.

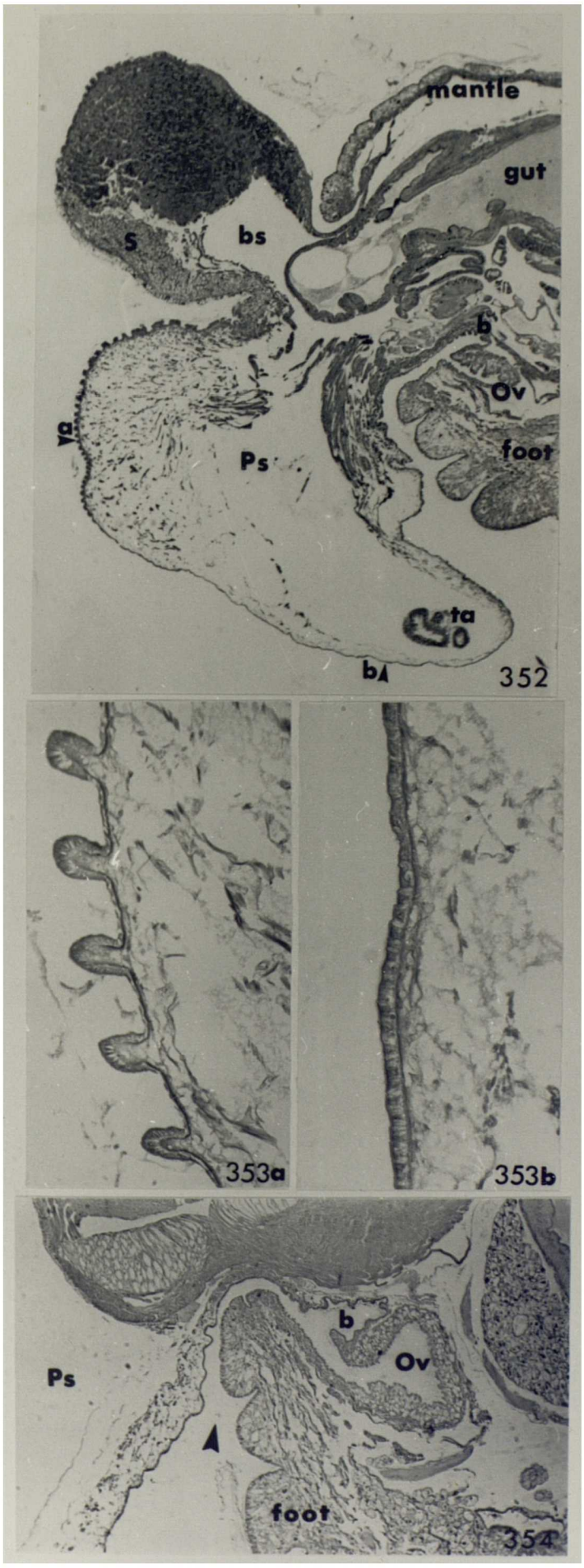
mantle
gut
S
bs
b
Ov
va
Ps
foot
ta
ba
352
353a
353b
b
Ov
Ps
foot
354

D. reticulatum, at copulation.

Fig. 355 Penial mass everted at copulation (x18).

Fig. 356 Sperm package in the groove which develops between the everted penial sac and the body wall (x25). Arrow indicates the direction of movement.

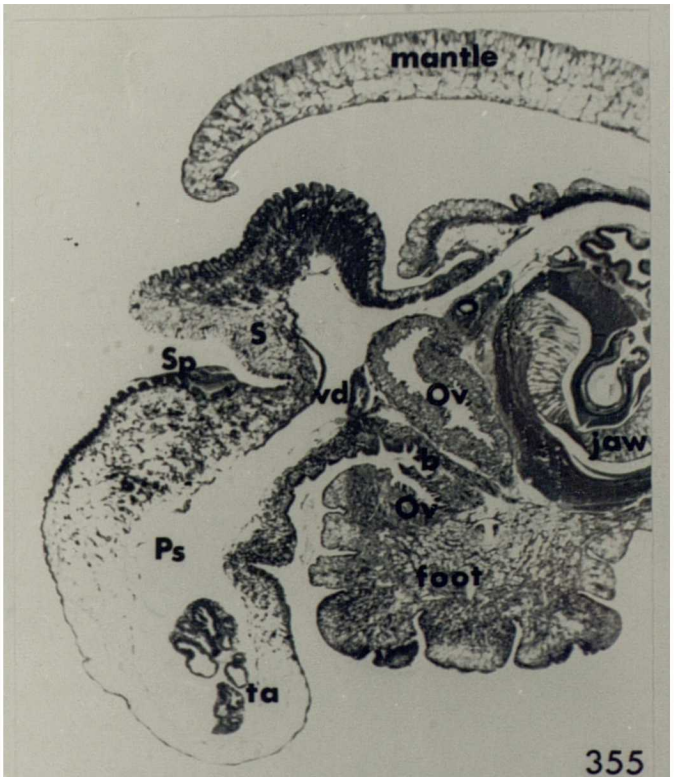

355

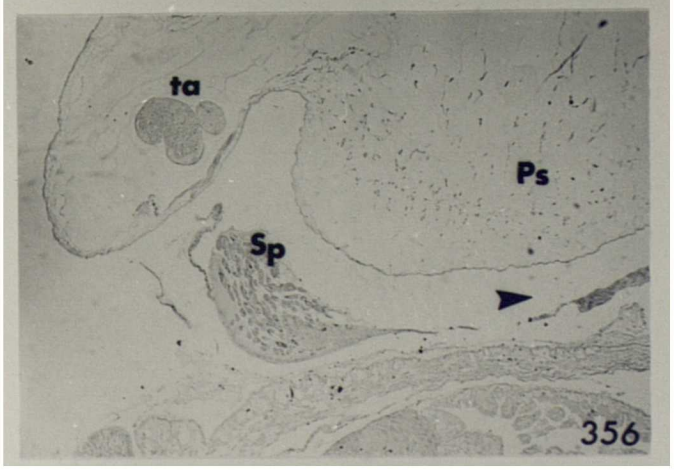

356

D. reticulatum, at copulation.

Fig. 357 L.S. through partially everted trifid appendage (x50).

Fig. 358 T.S. through partially everted trifid appendage (x100).

Fig. 359 L.S. through fully everted trifid appendage (x25).

Fig. 360 T.S. through sarcobellum (x33).

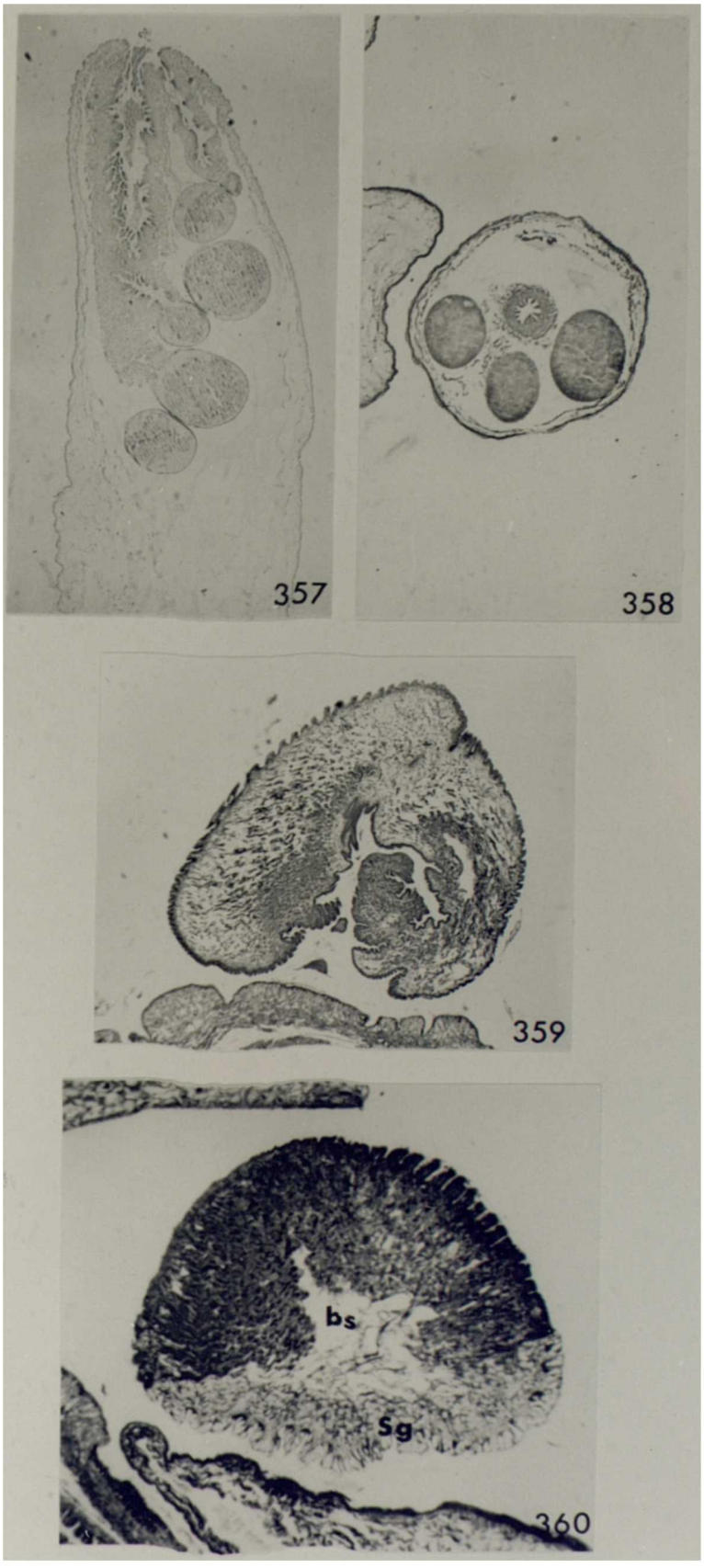
357
358
359
bs
Sg
360

D. reticulatum, 10 minutes after copulation.

Fig. 361 Foreign sperm package in the penial sac (x25).

Fig. 362 Foreign sperm package entering the bursa copulatrix (x25).

Fig. 363 L.S. through the partially everted trifid appendage (x60).


b
Sp
Ps
S
361
Ov
Ps
b
Sp
362
363

D. reticulatum, 30 minutes after copulation.

Fig. 364 Foreign sperm package entering the bursa copulatrix (x25).

D. reticulatum, 60 minutes after copulation.

Fig. 365 T.S. through bursa copulatrix (x25).

Fig. 366 L.S. through bursa copulatrix (x25).


b
Sp
Ov
Ps
S
364
Ov
b
Ps
vd
sp
S
365
Sp
b
Ps
vd
sp
366

D.reticulatum, 75 minutes after copulation.

Fig. 367 T.S. through the bursa copulatrix (x30).

D.reticulatum, 90 minutes after copulation.

Fig. 368 Foreign sperm in the penial sac (x25).

Fig. 369 T.S. through the carrefour, sperm in finger-like diverticulum (arrowed) (x200).

367

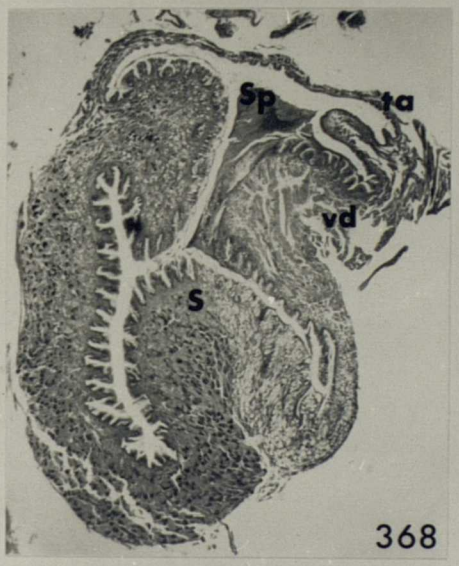

368

369

D.reticulatum, 6 hours after copulation.

Fig. 370 T.S. through the carrefour, sperm in pouched diverticulum (x120).

D.reticulatum, 8 hours after copulation.

Fig. 371 T.S. through the carrefour (x200).

Fig. 372 T.S. through the anterior, slender region of the hermaphrodite duct (x300).

D.reticulatum, 24 hours after copulation.

Fig. 373 T.S. through the bursa copulatrix (x25).

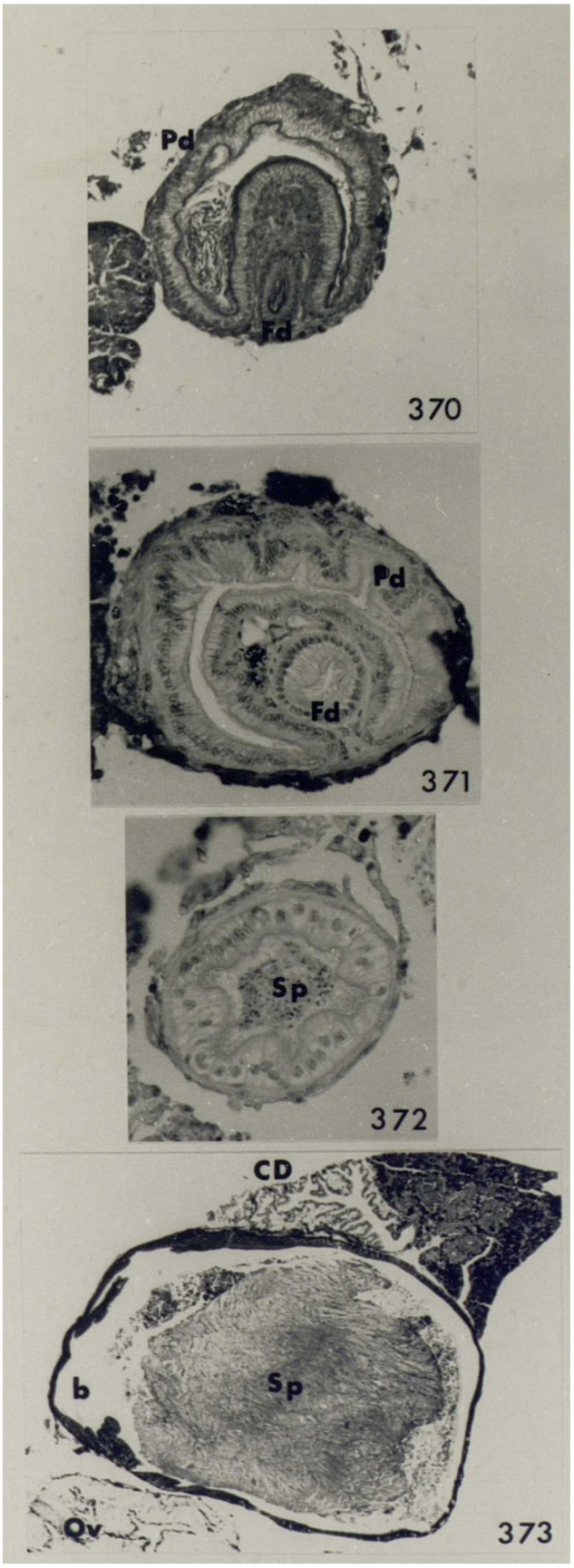
Pd
Fd
370
Pd
Fd
371
Sp
372
CD
b
Sp
Ov
373

Fig. 374 A.hortensis, courtship and copulation under laboratory conditions.

a. courtship position.
b. slight separation revealing the genital opening of one partner (arrowed).
c. upper atrium partially everted by one partner (A) exposing the core of the epiphallus and the entrance to the bursa copulatrix (arrowed).
d. eversion of the upper atria.
e. upper atria completely everted.
f. expansion of upper atria, the thick oviduct can be seen through the thin transparent wall.

Fig. 374

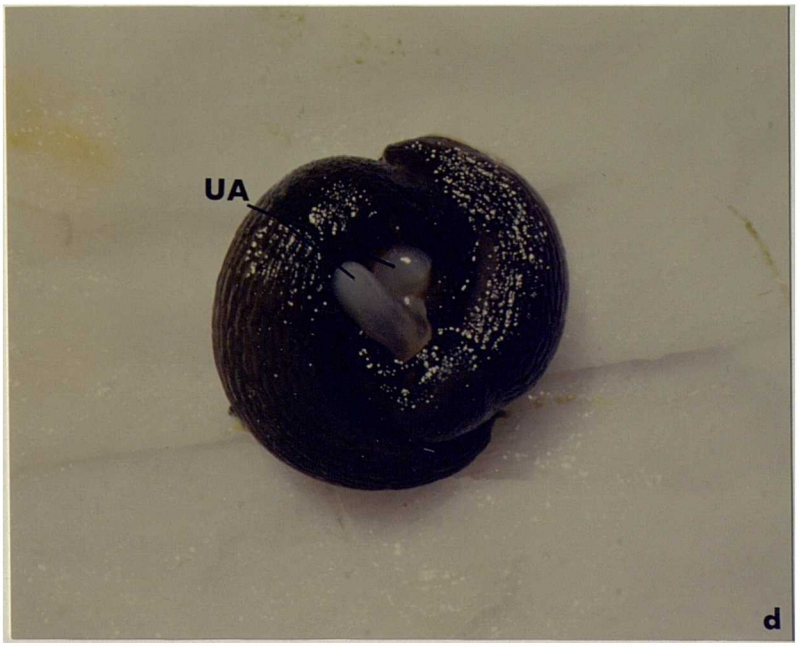

Fig. 374 (cont.)

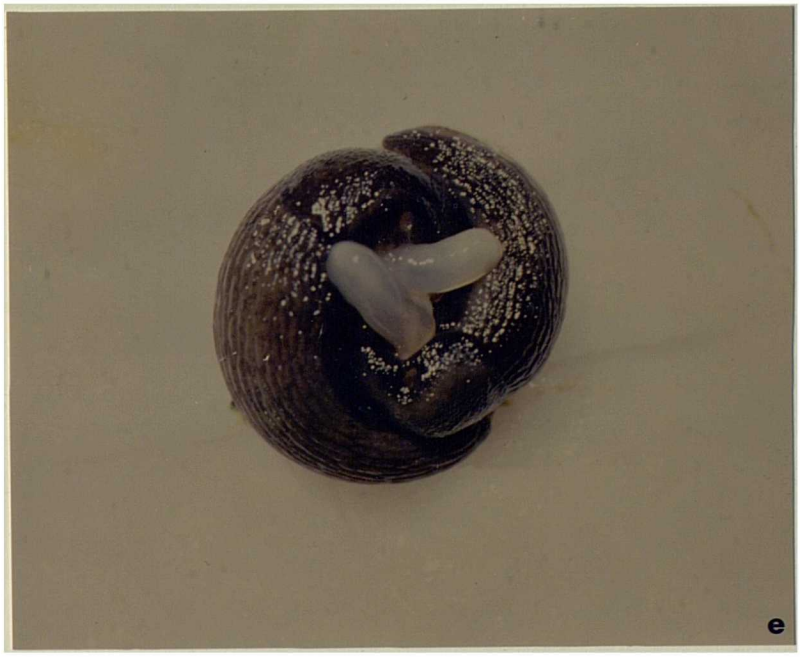

Fig. 374 (cont.)

Fig. 375 A.hortensis, upper atria everted. The epiphallic cone of animal A has entered the channel leading to the bursa copulatrix of animal B (arrowed). The cone of animal B is about to enter the entrance to the bursa of animal A.

Fig. 376 A.hortensis, 30 minutes after the start of courtship. Carrefour gland secretion filling the proximal region of the male groove of the common duct (x63).


'A'
'B'
ec
b
375

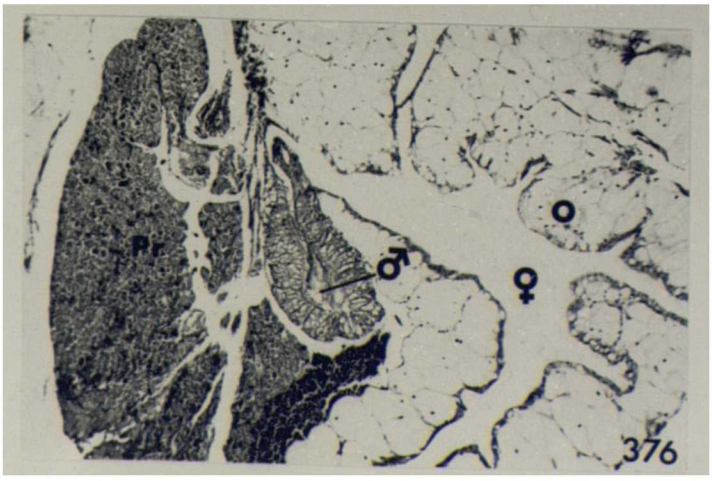
Pr
♂
♀
♀
376

A.hortensis, 90 minutes after the start of courtship.

Fig. 377 T.S. through the carrefour loop (x160). Small amount of sperm has entered the base of the ascending limb.

Fig. 378 T.S. through the carrefour loop (x160). Mid-region.

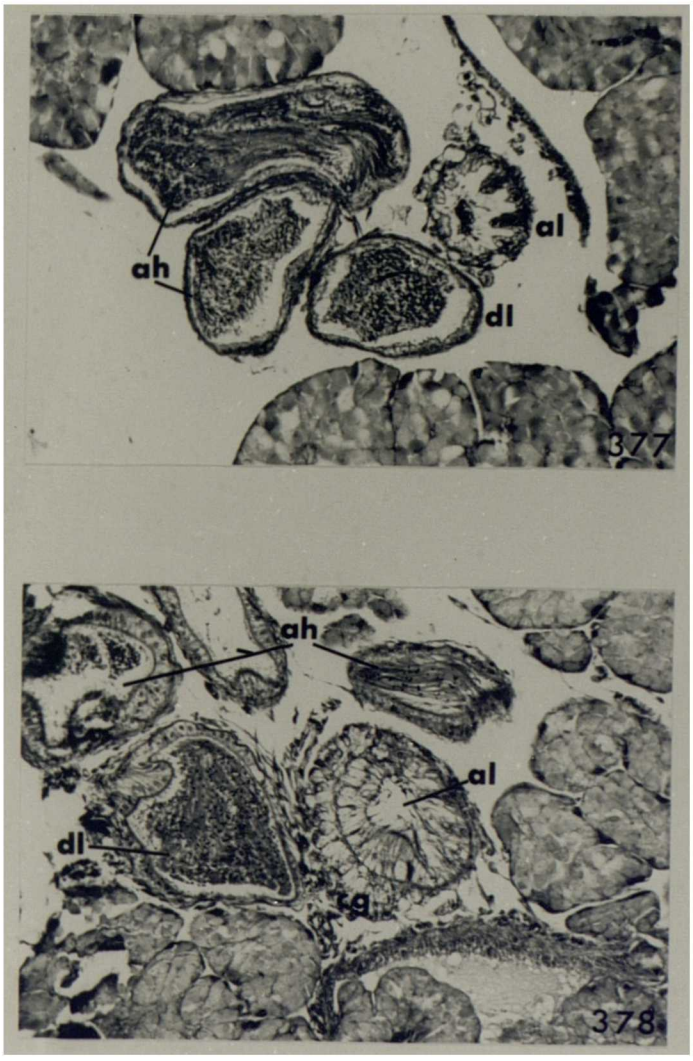
ah
al
dl
377
ah
al
dl
rg
378

A.hortensis, 120 minutes after the start of courtship.

Fig. 379 Sperm filling the male groove at the anterior end of the common duct and the vas deferens (x40).

Fig. 380 T.S. through the prostate gland (x63). Secretion entering the tabules.

Fig. 381 T.S. through the prostate gland (x250). Cells depleted of secretion.

Fig. 382 Sperm and prostate secretion filling the male groove of the common duct (x100).

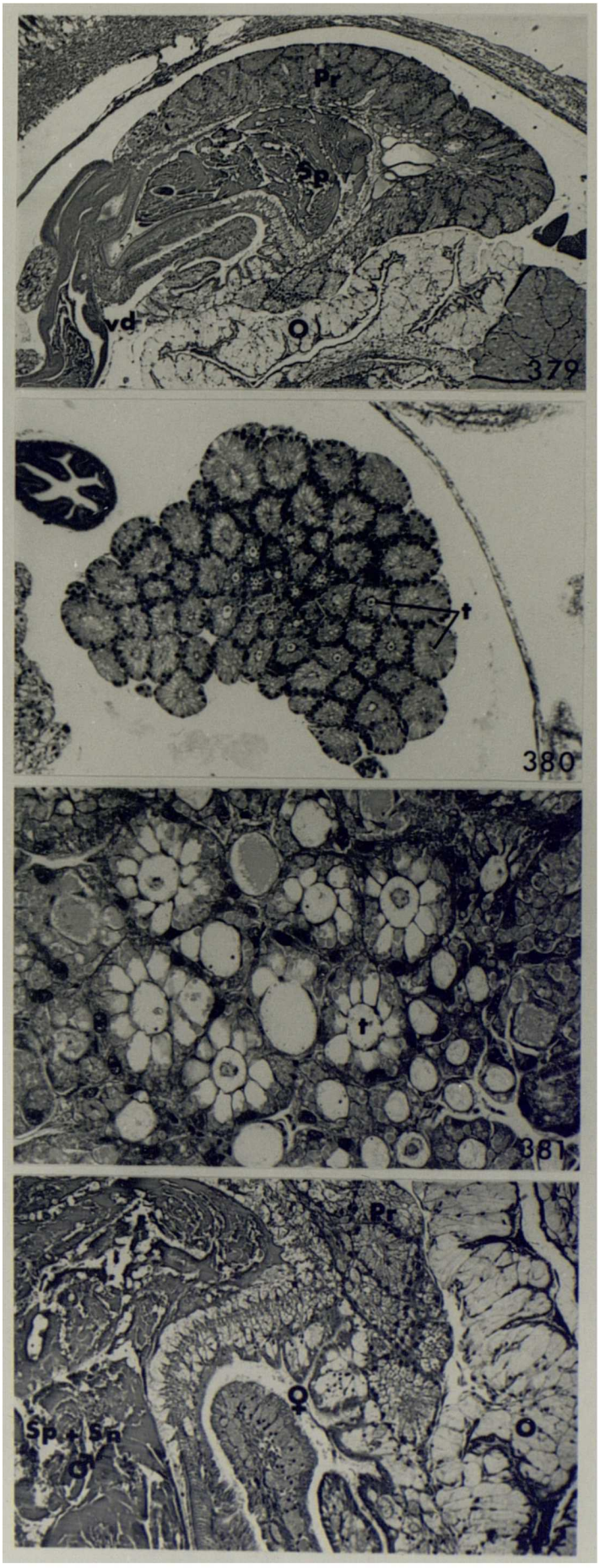
Pr
Sp
vd
O
379
t
380
t
381
Pr
♀
O
Sp + Sn
♂

A.hortensis, spermatophore.

Fig. 383 T.S. through mid-region of spermatophore (x400).

Fig. 384 T.S. through anterior region of spermatophore (x400). Prostate granule types labelled B and D.

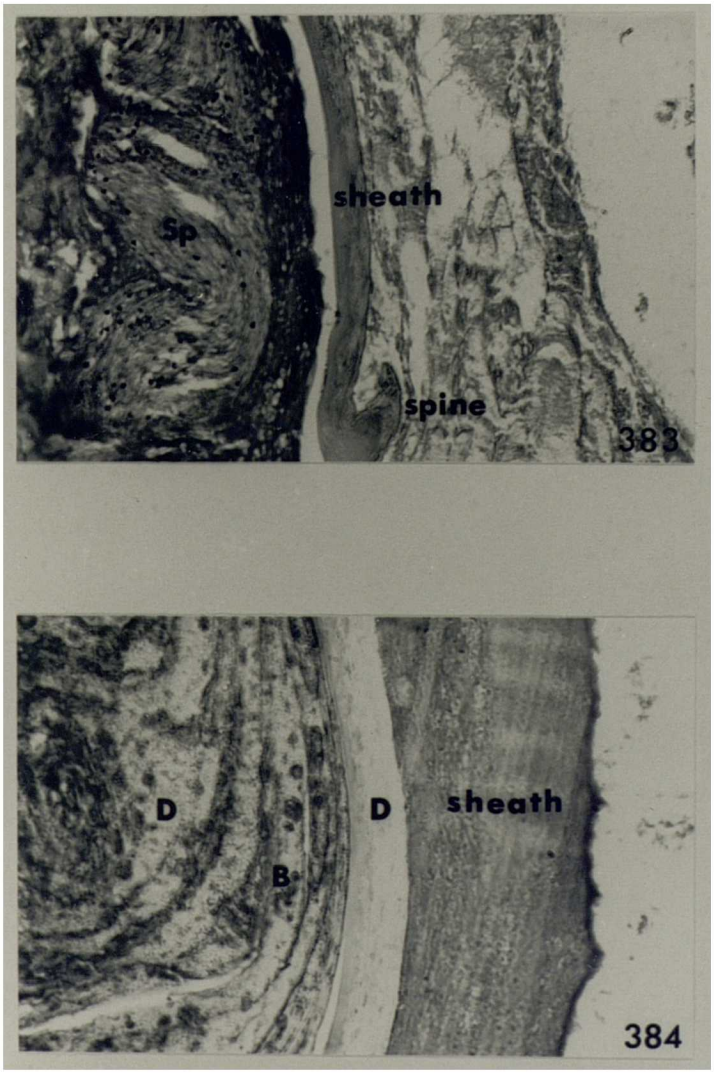
Sp
sheath
spine
383
D
B
D
sheath
384

A.hortensis, at copulation.

Fig. 385 Upper atrium everted exposing epiphallic cone (x18).

Fig. 386 Upper atrium completely everted (x25).

Fig. 387 Detail of the epithelium lining the everted upper atrium (x250).

Fig. 388 Detail of the epithelium lining the everted lower atrium (x125).

Fig. 389 Detail of the epithelium and muscle layers lining the everted upper atrium (x100).

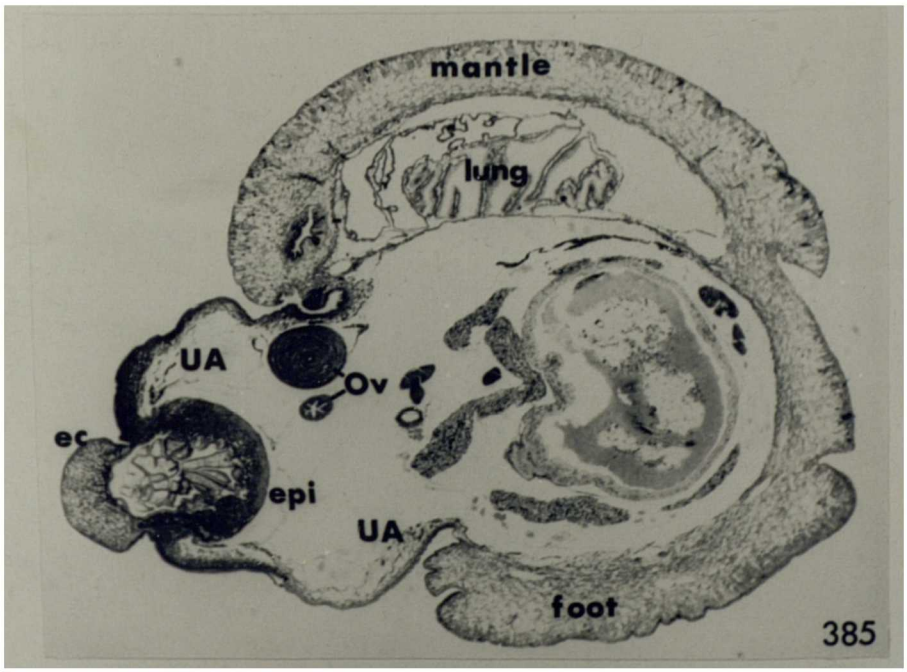
mantle
lung
UA
Ov
ec
epi
UA
foot
385

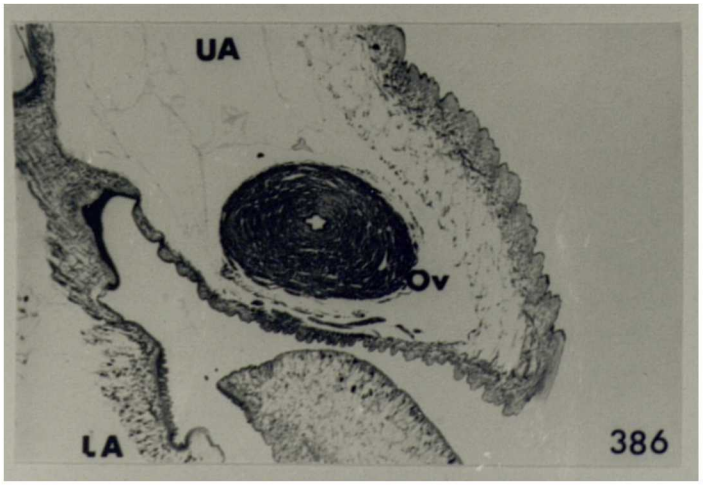
UA
Ov
LA
386

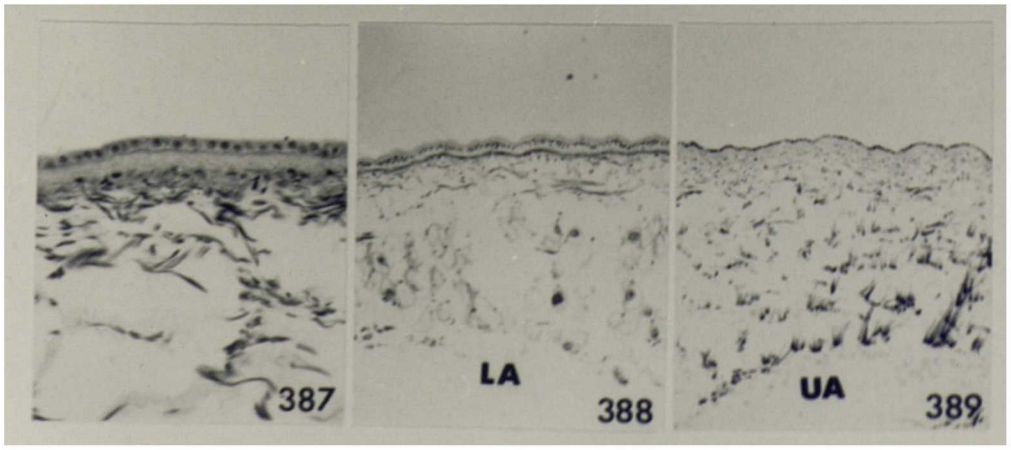
387
LA
388
UA
389

A.hortensis, at copulation.

Fig. 390 Upper atria everted (x18).

Fig. 391 Epiphallic cone engaged in the channel leading to the partner's bursa copulatrix (x18).

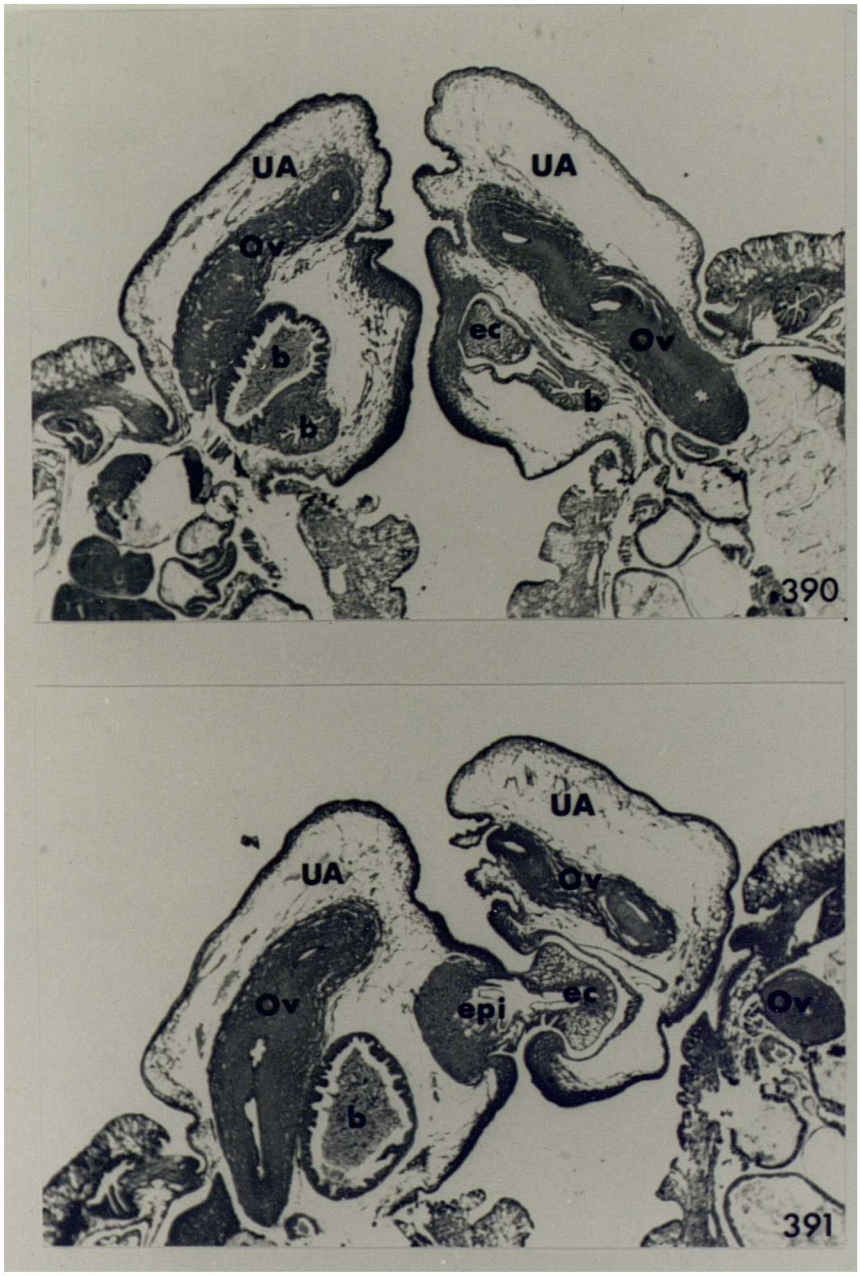
UA
Ov
b
b
UA
ec
Ov
b
390
UA
UA
Ov
Ov
epi
ec
Ov
b
391

A.hortensis, at copulation.

Fig. 392 Epiphallic cone engaged in the channel leading to the partner's bursa copulatrix (x50). Detail of Fig. 391.

Fig. 393 Spermatophore material filling the posterior region of the epiphallus (x100).

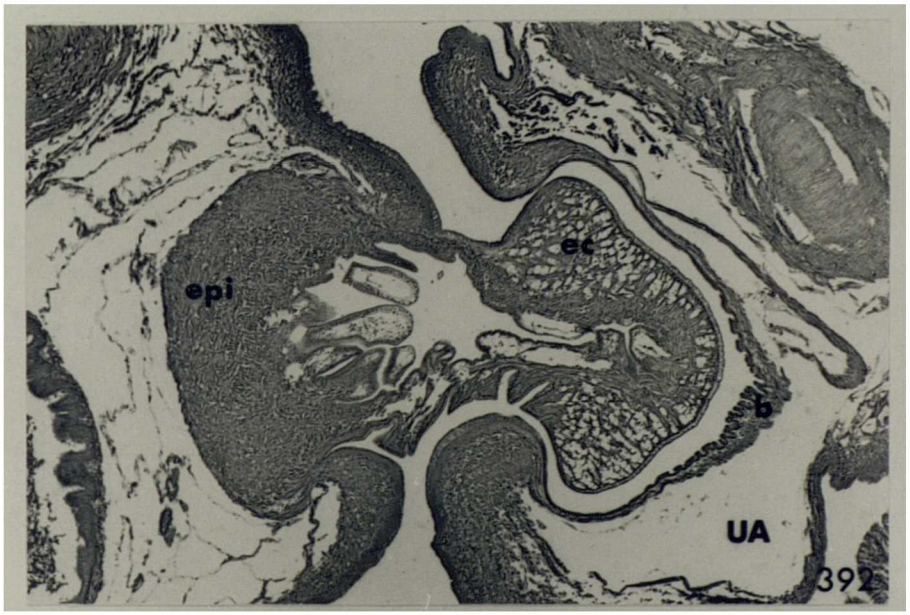
epi
ec
b
UA
392

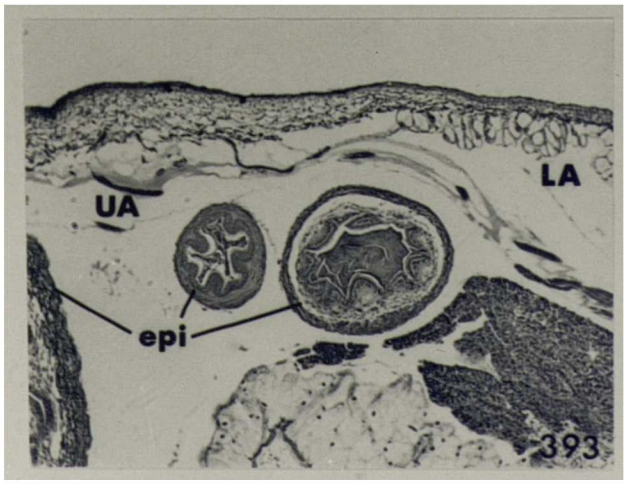
UA
LA
epi
393

A.hortensis, immediately after copulation.

Fig. 394 Anterior region of the foreign spermatophore filling the entrance to the bursa copulatrix (x25).

Fig. 395 Posterior region of the foreign spermatophore in the upper atrium (x25).

Fig. 396 L.S. through the lower atrium (x100).

Fig. 397 T.S. through the oviduct (x63).

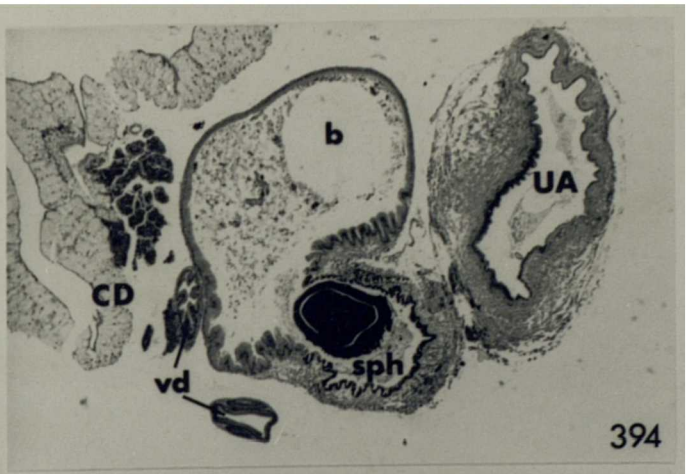

394

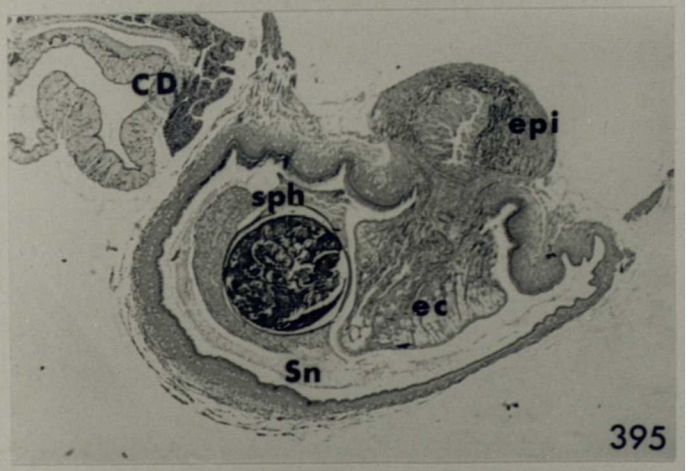

395

396

397

A.hortensis, 2 hours after copulation.

Fig. 398 Foreign sperm remaining in the upper atrium (x25).

A. hortensis, 4 hours after copulation.

Fig. 399 Foreign sperm in the oviducal side of the common duct near its junction with the carrefour (x63).

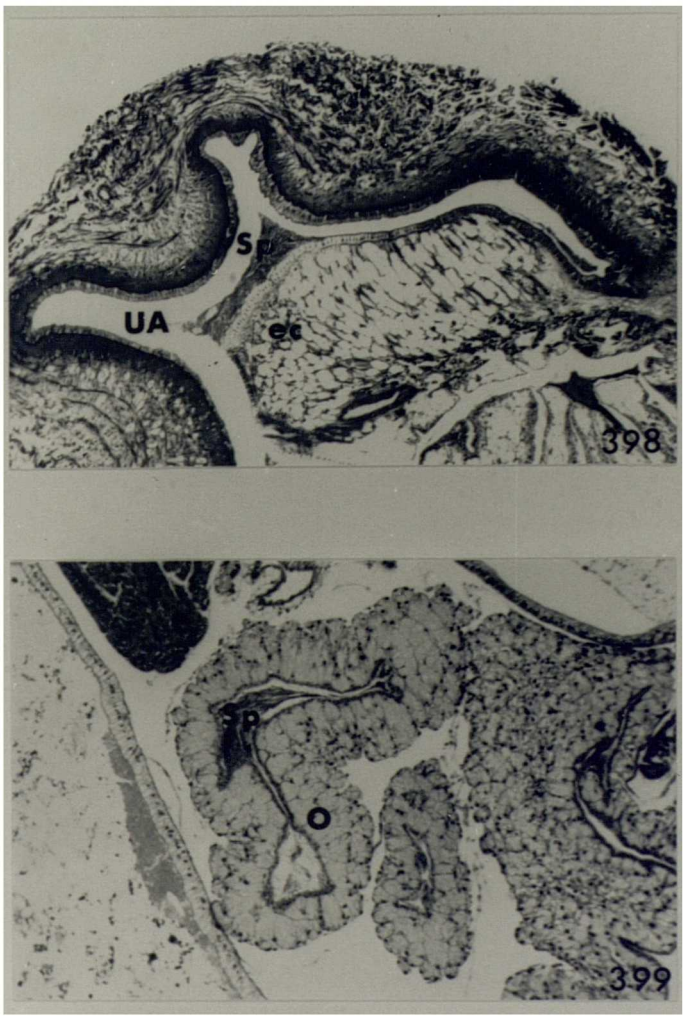
UA
398
399

D.reticulatum, changes in the reproductive tract prior to egg-laying.

Fig. 400 Oocyte passing through the seminal vesicle (x250).

Fig. 401 Oocytes filling the pouched diverticulum of the carrefour (x125).

Fig. 402 Detail of oocytes in the pouched diverticulum (x250). Arrow indicates the transition from columnar to squamous epithelial cells (x250).

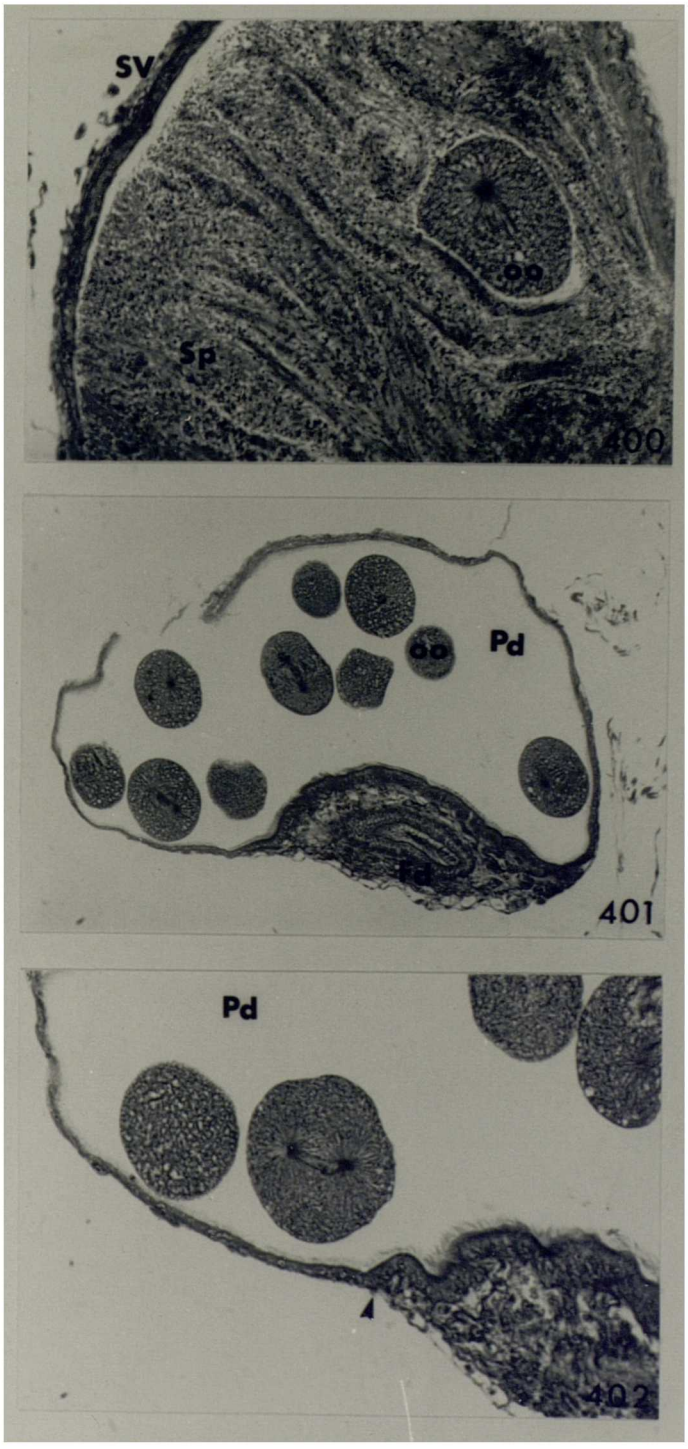
SV
oo
Sp
400
Pd
oo
401
Pd
402

D.reticulatum, changes in the reproductive tract prior to egg-laying.

Fig. 403 Detail of oocyte containing spindle (x400).

Fig. 404 Sperm in the pouched diverticulum of the carrefour (x250).

Fig. 405 Albumen gland duct filled with secretion (x100).

Fig. 406 Egg receiving shell layers during its passage through the oviducal groove of the common duct (x30).

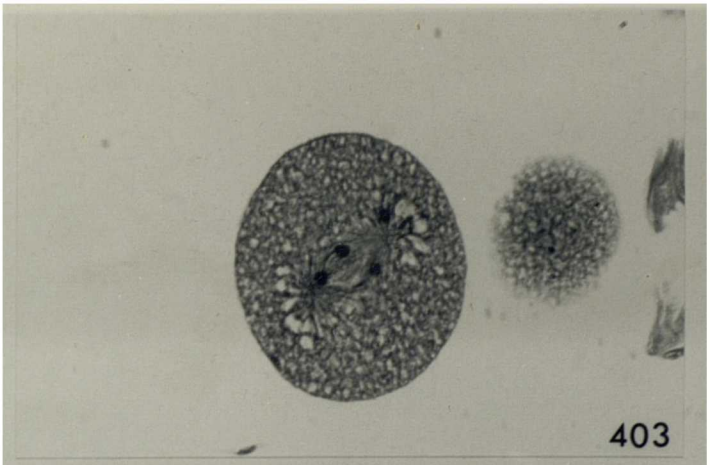

403

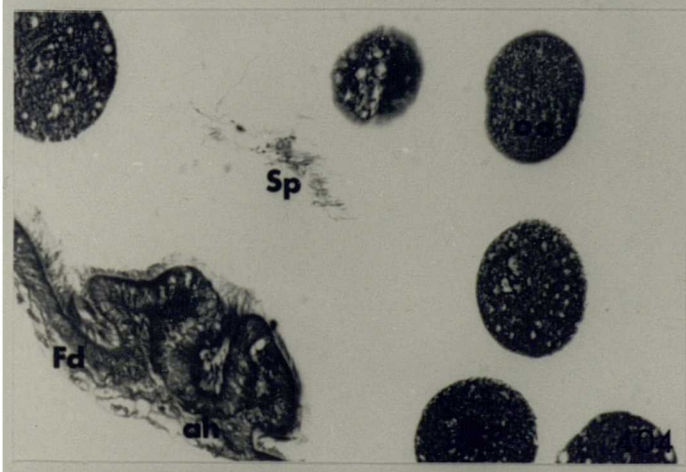

405

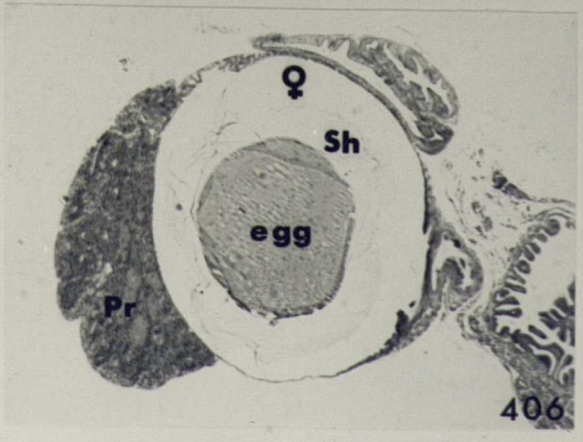

406

D.reticulatum, egg formation.

Fig 407 Eggs at different levels along the common duct showing the addition of successive jelly and shell layers (x250).

a. formation of perivitelline membrane.
b. addition of innermost, dense jelly layer.
c-e. addition of jelly layer.
f-g. addition of shell layer.
h. fully-formed egg.

Fig. 408 Oocyte, with spindle, surrounded by perivitelline fluid (x400).

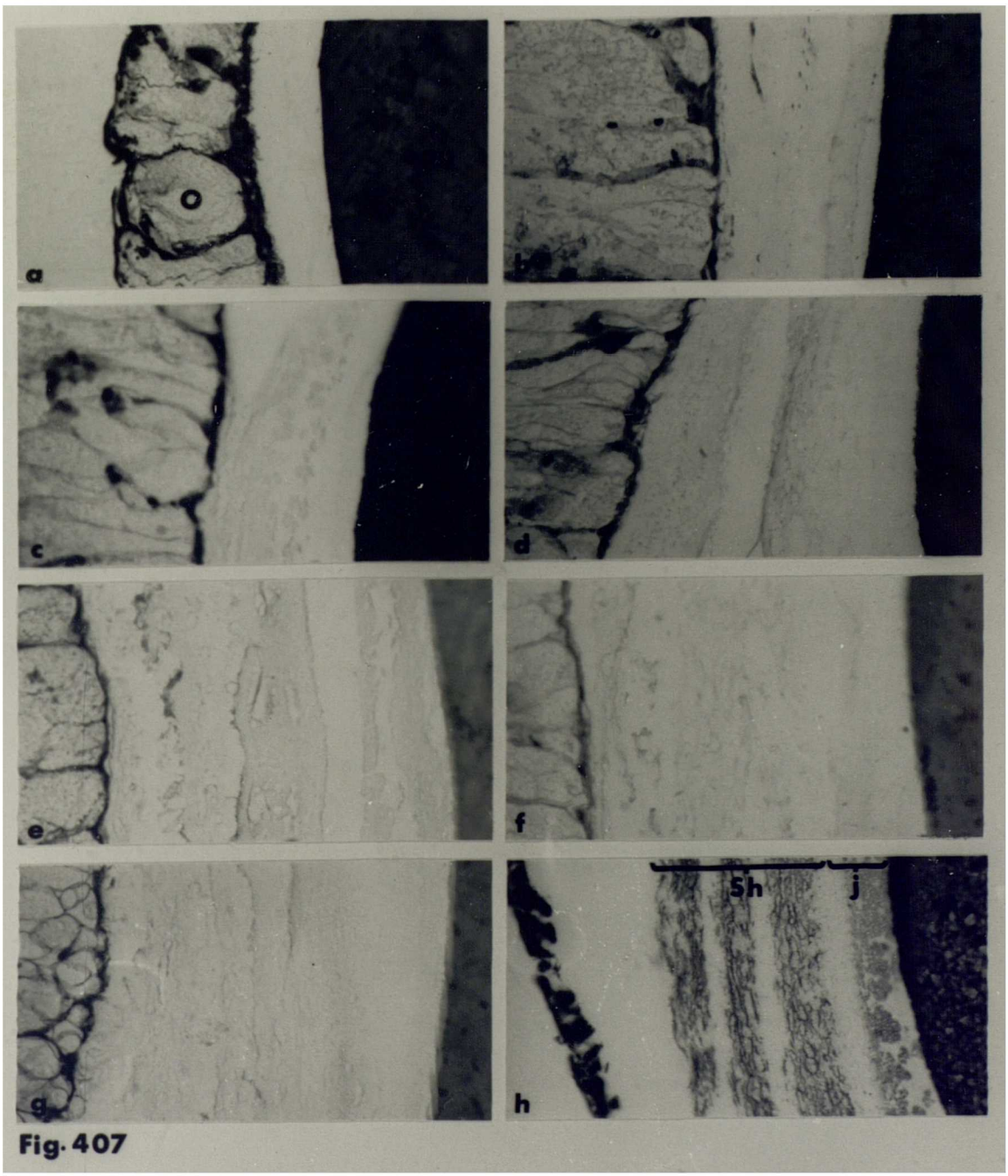

Fig. 407

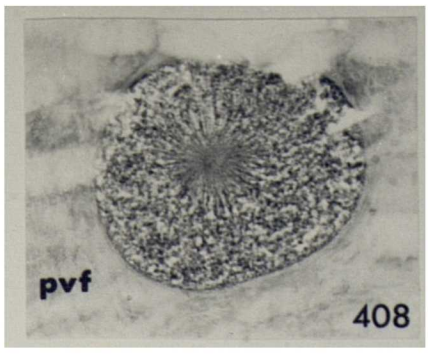

408

A.hortensis, changes in the reproductive tract prior to egg-laying.

Fig. 409 Oocytes with spindles in the gonad (x250).

Fig. 410 Oocyte with spindle in the gonad (x160).

Fig. 411 Oocyte leaving the follicle at ovulation (x250).

Fig. 412 Oocyte passing along an efferent ductule from an acinus into the posterior, slender region of the hermaphrodite duct (x160).

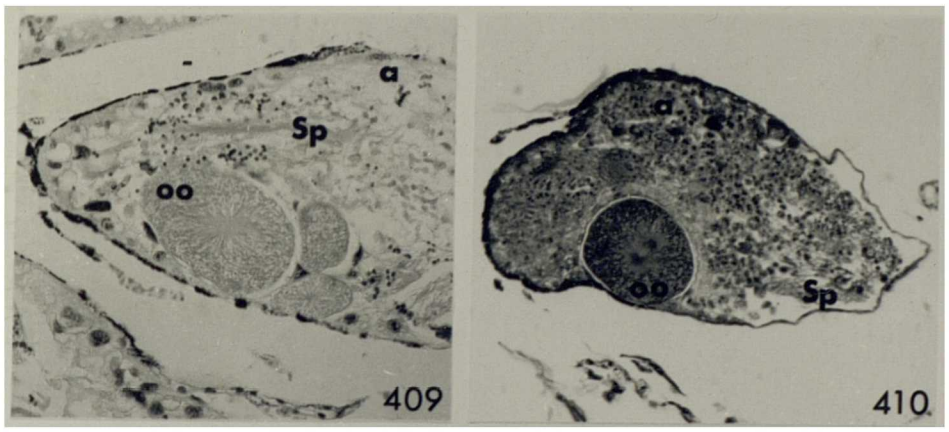
a
Sp
oo
409
a
oo
Sp
410

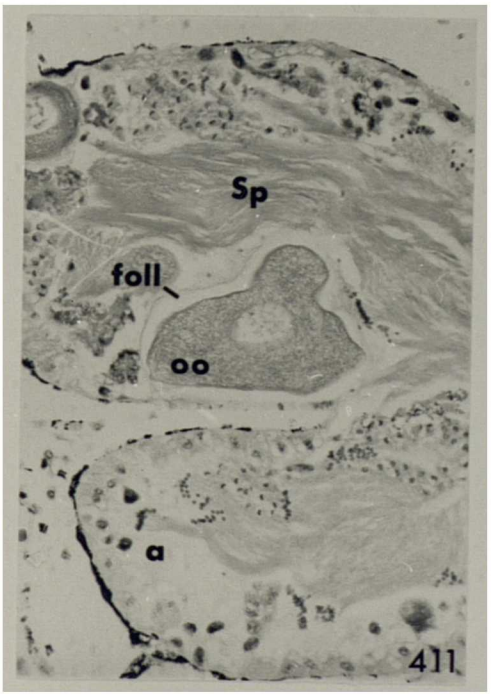
Sp
foll
oo
a
411

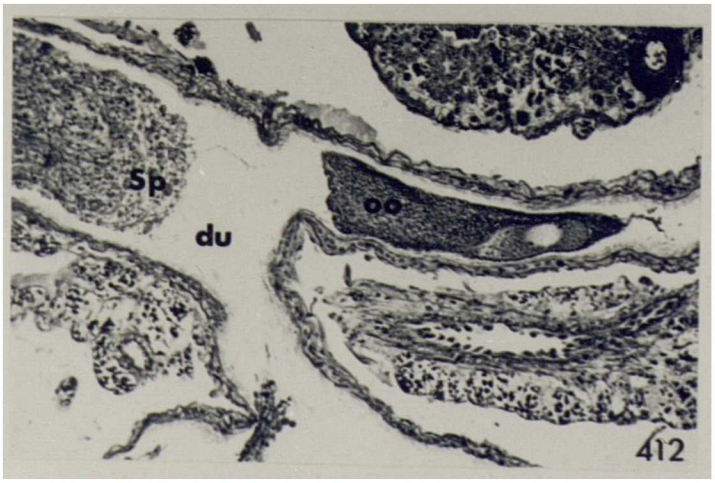
Sp
du
oo
412

A.hortensis, changes in the reproductive tract prior to egg-laying.

Fig. 413 Oocyte passing through the seminal vesicle (x160).

Fig. 414 Perivitelline oocyte cluster (arrowed) entering the hermaphrodite duct (x160).

Fig. 415 Oocytes (arrowed) filling the ascending limb of the carrefour loop (x300).

413

414

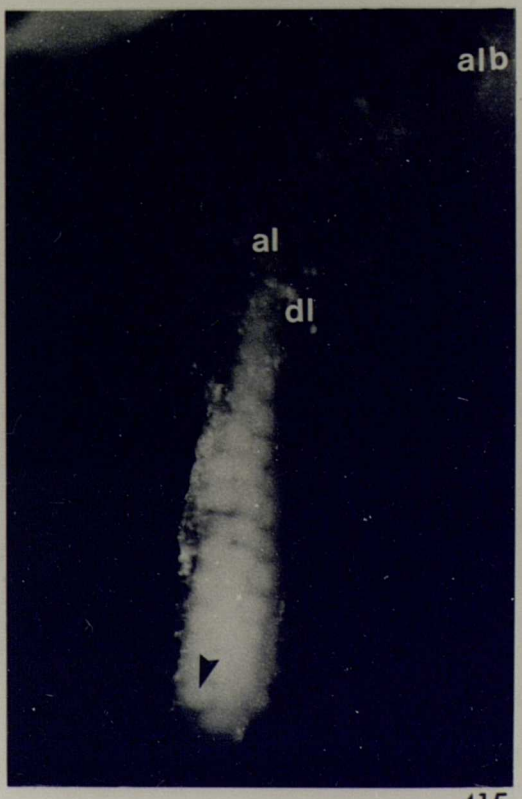

415

A.hortensis, changes in the reproductive tract prior to egg-laying.

Figs. 416-418 Oocytes filling the ascending limb of the carrefour loop (x160).

Fig. 416 T.S. through the mid-region of the carrefour loop.

Fig. 417 T.S. near the base of the carrefour loop.

Fig. 418 T.S. through the base of the carrefour loop.

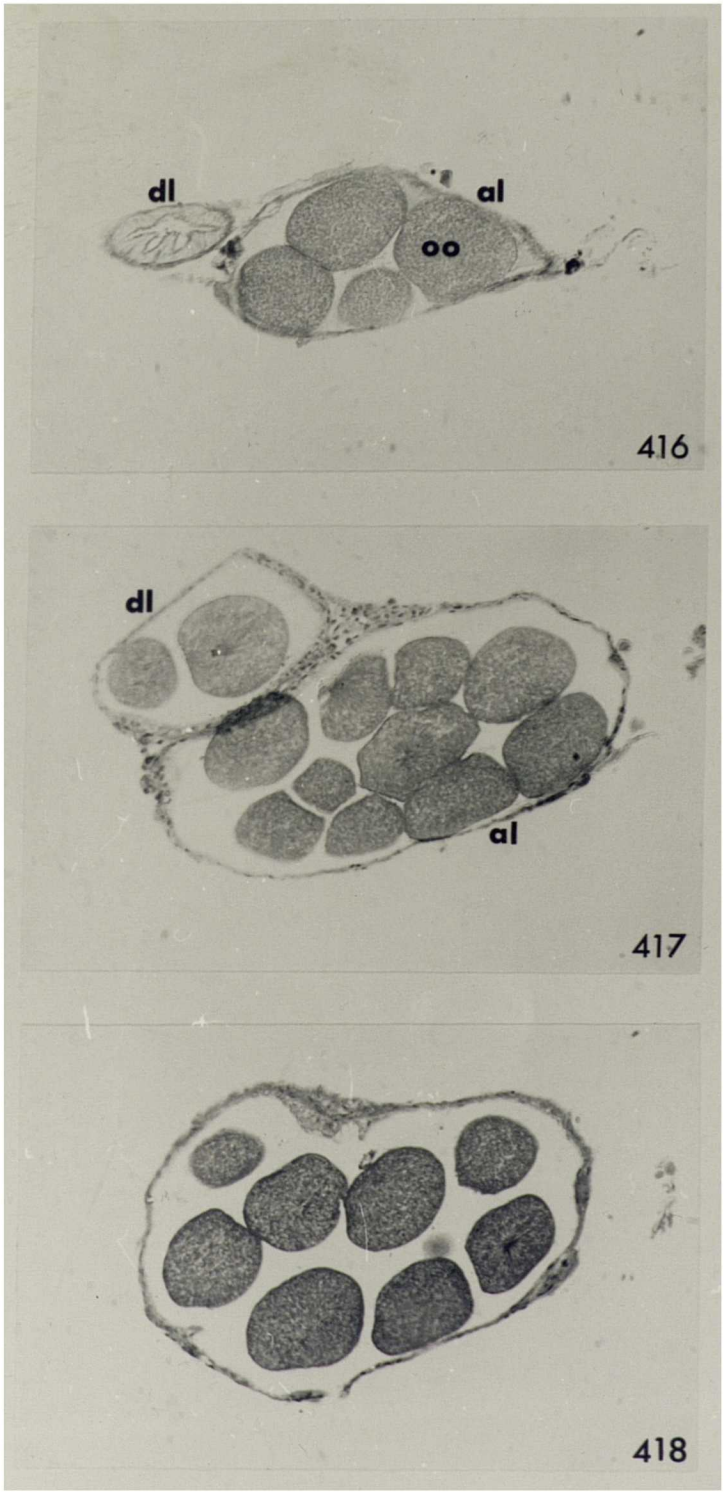
dl
al
oo
416
dl
al
417
418

A.hortensis, changes in the reproductive tract prior to egg-laying.

Fig. 419 Oocyte and sperm in the base of the carrefour loop (x160).

Fig. 420 Detail of oocyte with spindle in the ascending limb of the carrefour loop (x400).

Fig. 421 Detail of oocyte with polar body in the ascending limb of the carrefour loop (x400).

Fig. 422 L.S. through the ascending limb of the carrefour loop (x200).

Fig. 423 Oocytes containing the sperm and egg nuclei (x500). Detail of Fig. 422.

419

420

421

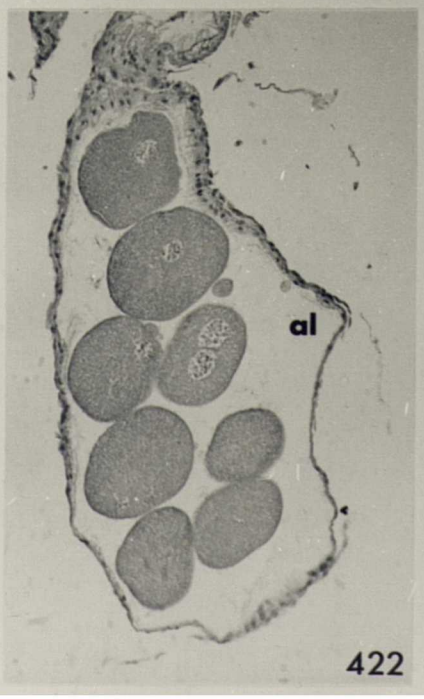

422

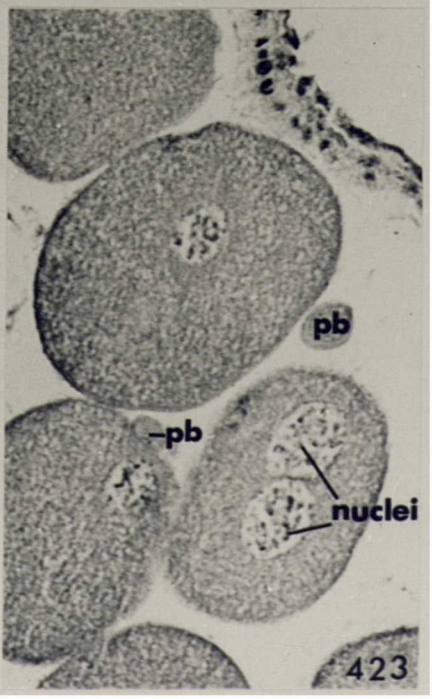

423

A.hortensis, egg-formation.

Fig. 424 Eggs removed at different levels along the common duct showing the addition of successive jelly and shell layers (x400).

a. formation of perivitelline membrane.

b. addition of innermost jelly layer.

c-f. addition of jelly layer.

f(i) is a detail of the whole egg seen in f(ii) (x25).

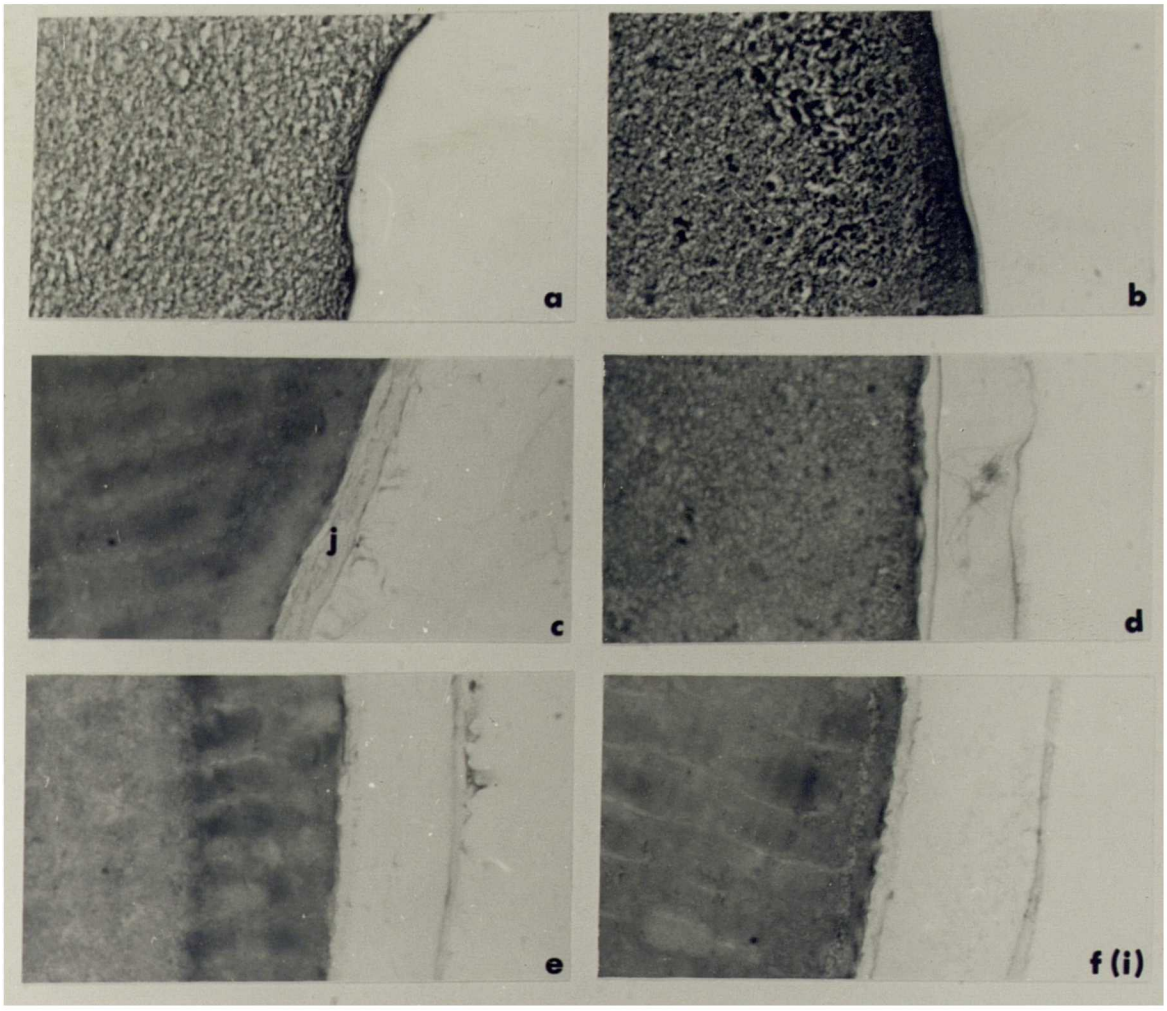

Fig. 424

A.hortensis, egg formation.

Fig. 424 (cont.) Eggs removed at different levels along the common duct showing the addition of successive jelly and shell layers (x400).

g-k. addition of outer shell layers.
l. fully-formed egg in upper atrium.

Fig. 425 Oocyte, with polar body, surrounded by perivitelline fluid.

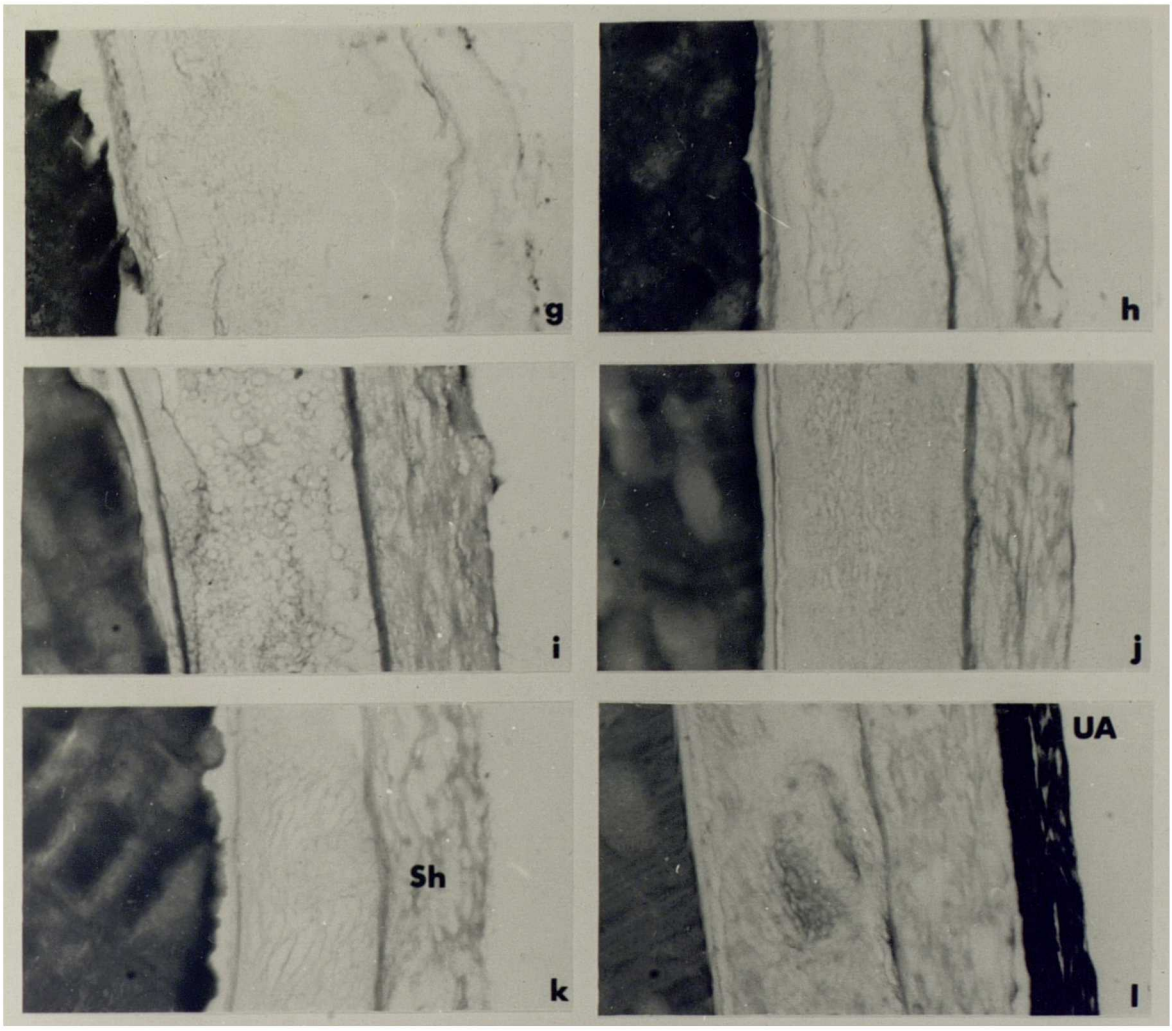

Fig. 424 (cont.)

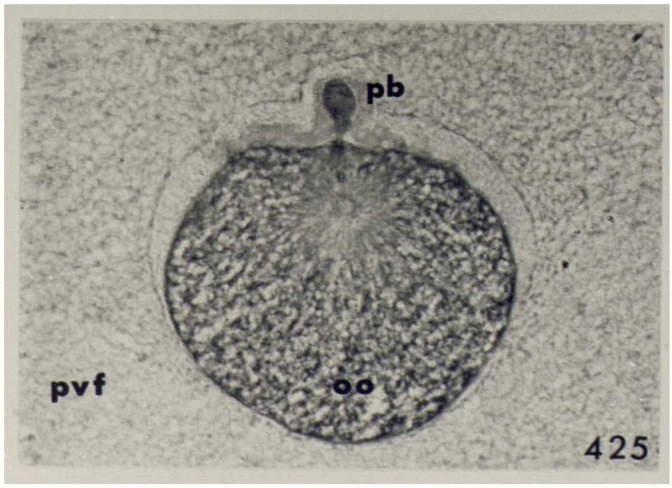

A.hortensis, egg-laying.

Fig. 426 T.S. of egg in the thin oviduct (x40).

Fig. 427 T.S. of egg in the thick oviduct (x25).

Fig. 428 Egg filling the upper atrium (x25).

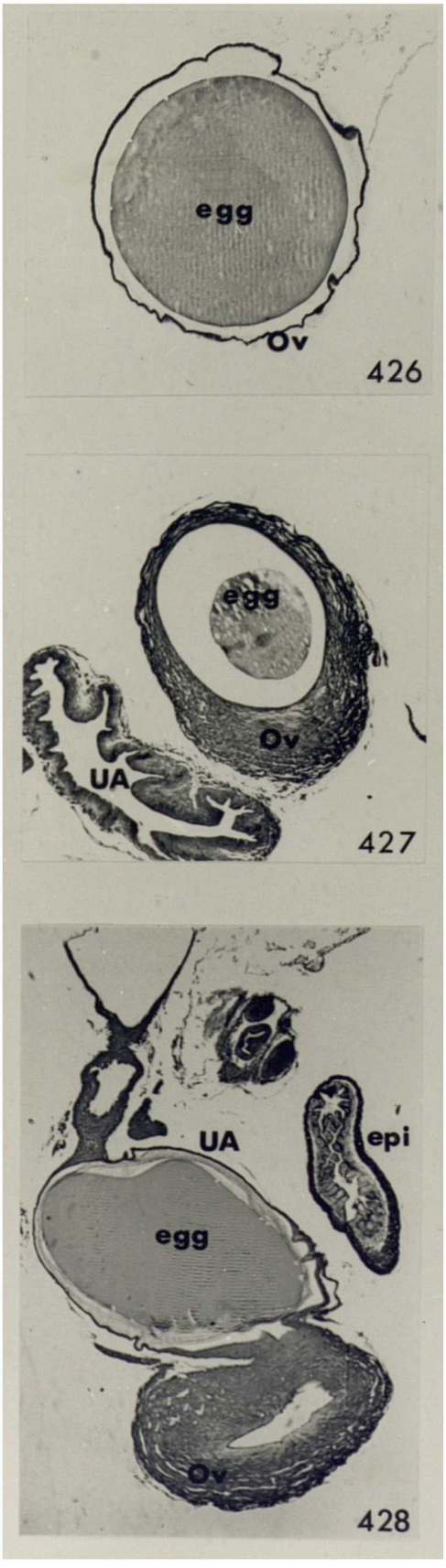
egg
Ov
426
egg
Ov
UA
427
UA
epi
egg
Ov
428

Fig. 429 Diagrams showing the position of the sperm package at intervals during courtship and copulation in D.reticulatum.

a. at rest.
b. during courtship, sarcobellum (striped) protruding through the genital opening. Sperm package (stippled) in penial sac.
c. sperm package lying on the surface of everted penial sac.
d. direction of movement of the sperm packages.
e. immediately after copulation.
f. 40 minutes after copulation.
g. 75 minutes after copulation.

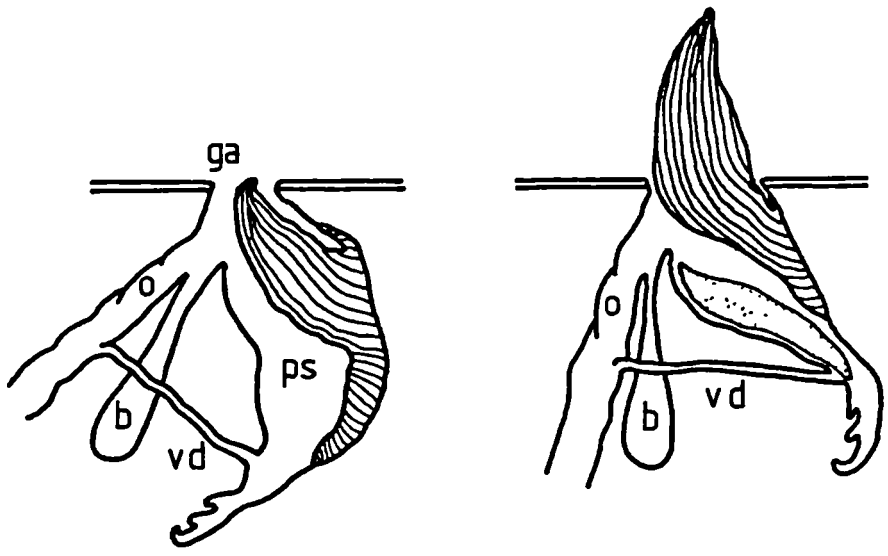

a. b.

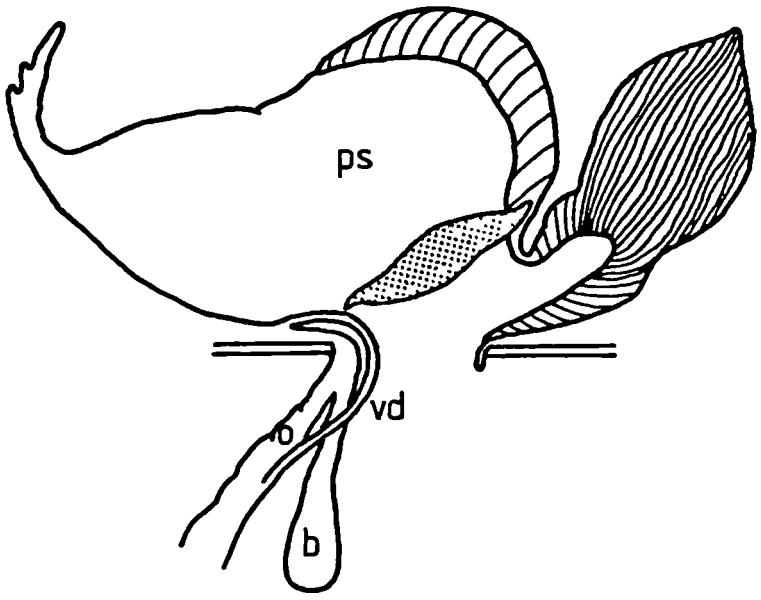

c.

Fig. 429

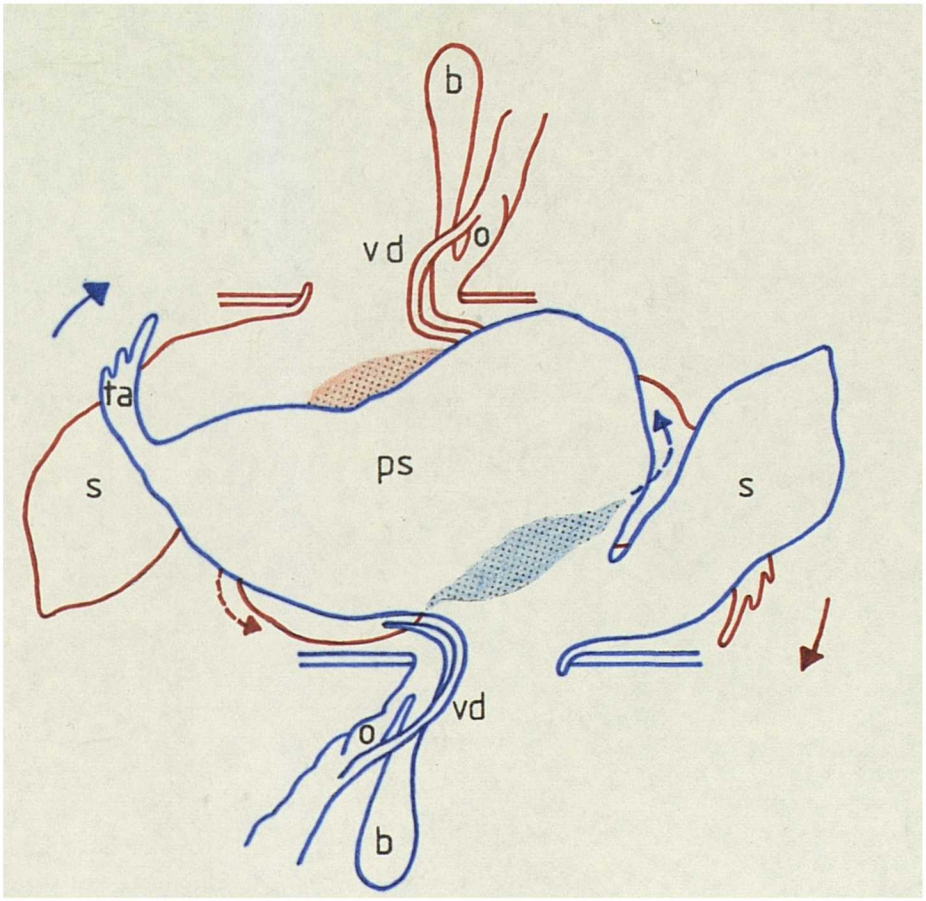

d.

circling movement of animals

movement of sperm package

Fig. 429 (cont.)

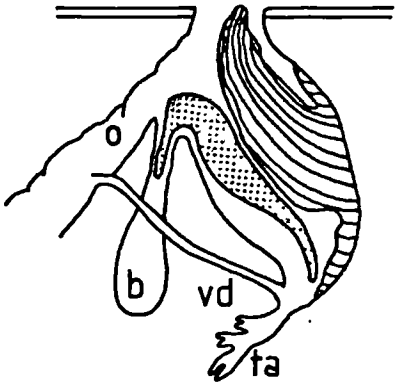

e.

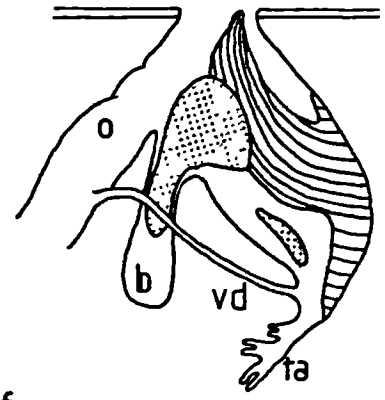

f.

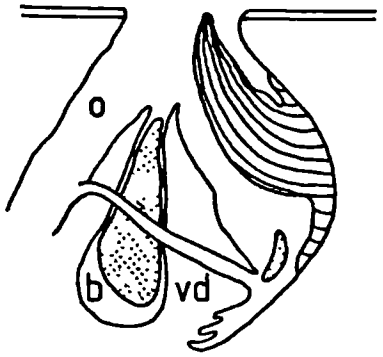

g.

Fig. 429 (cont.)

Fig. 430 Diagram to show the variety of form of spermatophores produced by A.hortensis.

a. elaborate, spined spermatophore.
b. simple, smooth spermatophore
(after Quick, 1960).

Fig. 431 Diagrams showing the position of the spermatophore at intervals during courtship and copulation in A.hortensis.

a. 2 hours after the start of courtship.
b. partial eversion of upper atrium.
c. complete eversion of upper atrium.
d. epiphallic cones engaged. Spermatophore transferred directly into the bursa copulatrix. (arrows show direction of movement).
e. immediately after copulation.

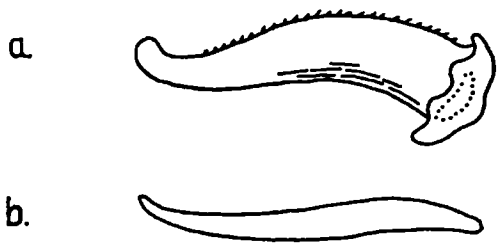

Fig. 430

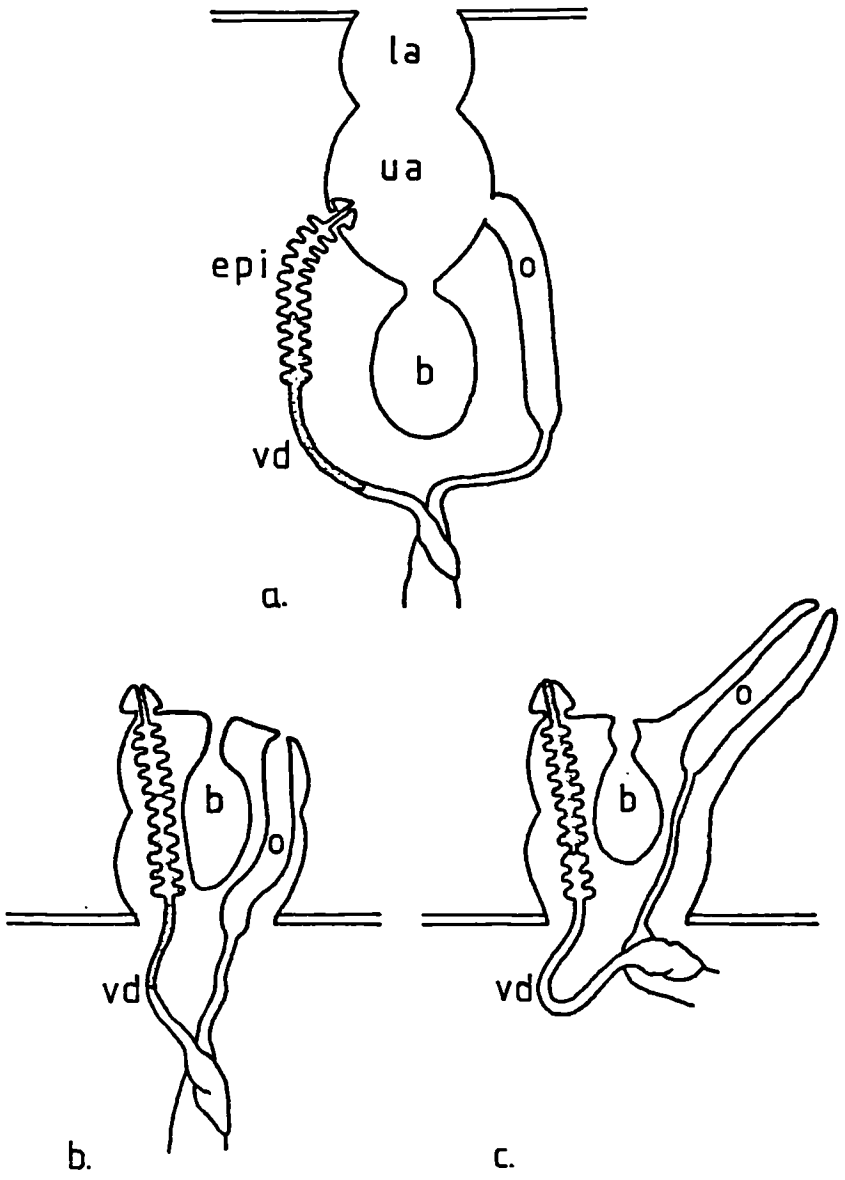

Fig. 431

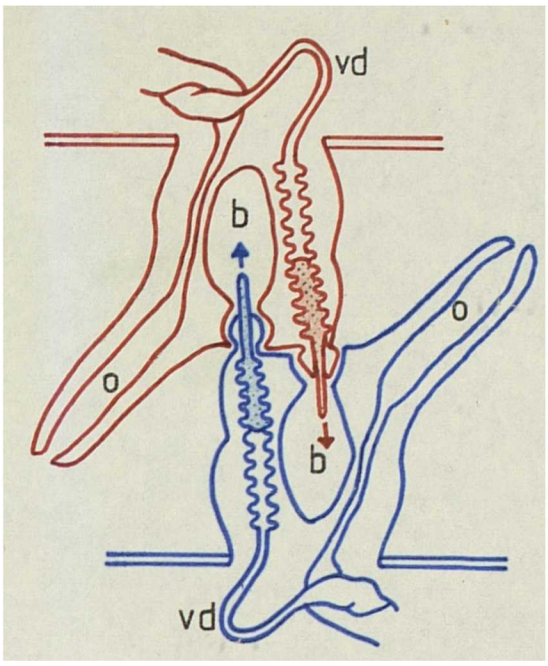

d.

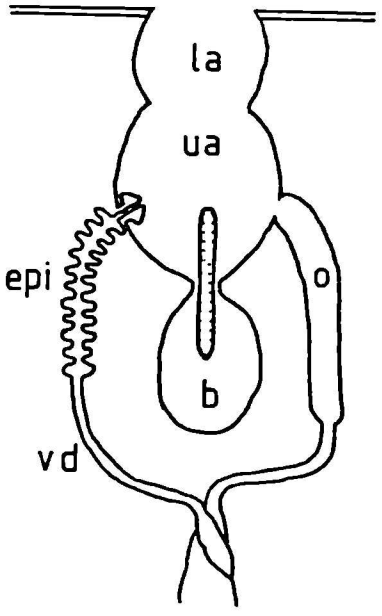

e.

Fig. 431 (cont.)